Transient Shear Flow Rheology of Concentrated Long Glass Fiber Suspensions in a Sliding Plate Rheometer

Neeraj Agarwal

Thesis submitted to the faculty of the Virginia Polytechnic Institute and State University in partial fulfillment of the requirements for the degree of

Master of Science

In

Chemical Engineering

Advisory Committee:

Dr. Donald G, Baird, Committee Chair

Dr. Richey M. Davis

Dr. Peter Wapperom

August 14, 2009

Blacksburg, VA

Keywords: Sliding plate rheometer, long glass fiber suspension, transient viscosity growth at startup of shear flow

Transient Shear Flow Rheology of Concentrated Long Glass Fiber Suspensions in a Sliding Plate Rheometer

Neeraj Agarwal

ABSTRACT

Transient viscosity growth measurements at the startup of shear flow were performed on long glass fiber-filled polypropylene. Samples were prepared with fibers pre-oriented either in 1-direction, 3-direction or random in 1-3 plane, where the 1-direction is the direction of shear motion, the 2-direction is perpendicular to the shear plane and the 3-direction is the neutral direction. A sliding plate rheometer incorporating a shear stress transducer was constructed in the lab. It was shown that this device works well for the tested materials including a Newtonian oil, a low density polyethylene (LDPE) and short glass fiber-filled polypropylene. The transient viscosity growth behavior for long glass fiber suspensions was subsequently investigated. The results suggested that both, fiber length and fiber concentration have pronounced effect on the steady state suspension viscosity. It was also observed that the transient behavior of the pre-oriented samples was highly dependent on the initial orientation state of the fibers.

Acknowledgements

I would like to express my appreciation to Dr. Donald G. Baird for his support and guidance throughout the completion of this work. In addition, I wish to extend special thanks to my committee members Dr. Peter Wapperom and Dr. Richey Davis for their insight suggestions during the progression of this work.

I would also like to recognize the following people for their additional support:

- My Family: My grandparents, Ayodhaya and Yashodhara Agarwal, and parents, Pawan and Meena Agarwal, for their everlasting love and blind faith in my abilities. Ranu and Dheeru for always cheering me up.
- My friends: Neha, my biggest motivation and support, whose generous encouragement and selfless patience sustained me throughout this research. Nimisha, Rahul, Anchal, Vikas and many other close friends in Virginia Tech and in India who always treated me with great affection.
- Aaron Eberle, for initiating the construction of Sliding Plate Rheometer which eventually shaped the nature of the present work. His extended guidance at each and every stage of this research is highly appreciated.
- Lab Mates: Kevin, for helping me complete the Modeling chapter and for performing the fiber length distribution (FLD) analysis for me. Syed, for being a motivator and a guide. Mike, for being a good friend. Chris, for training me on RMS-800. Gregorio, Chen, Myoungbae and other past members of polymer processing lab for their help and support.
- Mike Vaught in Chemical Engineering work shop, without his machining experience and craftsmanship, successful construction of the Sliding Plate Rheometer was never possible.

- Diane Cannaday, Riley Chan, Tina Kirk and other chemical engineering staff members who made this work easier for me.

Original Contribution

- In order to perform transient simple shear experiments on the long glass fiber suspensions a sliding plate rheometer incorporating a shear stress transducer was constructed. It was shown that this device works well for the tested materials including a Newtonian oil, a low density polyethylene (LDPE) and short glass fiber-filled polypropylene. It was argued that the fabricated sliding plate rheometer overcomes the problems associated with conventional rheometers when charactering the transient rheological behavior of long glass fiber suspensions.

- The constructed sliding plate rheometer, due to its rectilinear geometry, facilitated the possibility of making samples which had fiber pre-oriented in a specific direction. Shear viscosity growth behavior at the startup of shear flow for these pre-oriented samples showed that the transient behavior is highly dependent on the initial orientation of fibers.

Format of Thesis

This thesis is written in journal format. Chapter 4 is a self contained paper that is to be submitted for journal publication. This paper separately describes the introduction, experiments, results and discussion, and conclusions. With the exception of chapter 1 and 2, the figures and tables are presented after the reference section of each chapter.

Attribution

A few colleagues and coworkers aided in the writing and research behind the chapter 4 of this thesis. A brief description of their background and their contributions are included here.

Dr. Donald G. Baird- Ph.D. **(**Harry C. Wyatt Professor of Chemical Engineering, Virginia Tech) is the primary Advisor and Committee Chair. Dr. Baird provided with his guidance and support throughout the completion of this work. He also contributed to this chapter in terms of discussing the Results and Discussion section and helping the author in reaching the logical conclusions.

Aaron P. R. Eberle- Ph.D. (Department of Chemical Engineering, Virginia Tech) currently a Postdoctoral Researcher in the Department of Chemical Engineering, University of Delaware, was a student in the author's group and contributed to this chapter in terms of initiating the construction of Sliding Plate Rheometer which eventually shaped the nature of the present work.

Table of Contents

List of Figures

List of Tables

1.0 Introduction

Long glass fiber composites exist in many forms. Among them the best known materials are Glass Mat Thermoplastics (GMTs), containing continuous or discontinuous glass fibers. The GMT materials have been in use for many decades and are proven in challenging applications, such as car underbody shields, front-end mounting units and seat shells.[1] They are usually moulded using compression molding process and give good mechanical strength in all direction because of their web-like structure. However, the requirement to design more intricate parts has shifted the focus to the materials, such as fiber filled granulates which can be easily processed in conventional equipments, e.g. extruder and injection molder. Fair dispersion of fiber in every section of the designed part allows stresses to be distributed throughout the part and results in a fiber composites that exhibit a unique balance of high performance properties.[2] For this reason fiber filled composites are progressively replacing the conventional materials in various industries, such as automobile and transportation as they offer light weight material, low production cost and improved mechanical properties.[3]

Length of the fibers in these granulates is one of the major factors that determines the mechanical properties in the final part. It is well known that maximizing the fiber length contributes significantly to the composite strength.[2,4,5] Comparison between long fiber composites (LFC) and short fiber composite (SFC), listed in Table 1.1[6] shows improvements in stiffness, strength, and toughness for LFCs. Furthermore, considerable increase in fatigue endurance, creep and impact strength is also observed for composites containing large aspect ratio fibers.[7, 8]

Apart from fiber length, physical properties of fiber filled polymers also depend on the concentration, type, size and most importantly orientation of reinforced fibers.[9,10] During the processing, fibers change their orientation state within the matrix which influences their mechanical properties. [3, 11,12,13] A composite is much stiffer along the direction to which fibers are aligned, while it is more compliant in other directions.[13] This flow induced fiber orientation greatly emphasizes the importance of rheological properties in determining the mechanical properties of the fiber composite. A better understanding of the flow characteristics could be instrumental in optimizing the processing conditions for fiber composites in order to obtain desired mechanical properties.[14,15,16] Hence, a study of rheological behavior of long fiber suspensions and its connection to fiber orientation as determined in simple flow is of significant relevance.

Table 1.1 Comparison between physical properties of Long- and Short-Fiber Reinforced Nylon 6,6 Composites[6]

Property	**Units**	**35% Long Glass**	**35% Short Glass**	**50% Long Glass**	**50% Short Glass**
Tensile strength	MPa	206	199	254	221
Tensile modulus	GPa	10	9.7	18	17
Flexural strength	MPa	321	274	405	321
Flexural modulus	GPa	10	9.6	16	15
Compressive strength	MPa	261	214	273	219
Shear Strength	MPa	93	87	103	92

1.1 Rheology

Rheology of long fiber suspensions is quite complex because of various factors such as fiber-matrix interaction, fiber-fiber interaction, fiber migration and fiber breakage during processing.[3] These factors become more prominent in high concentration regimes for which the volume fraction of fibers $\varphi \geq a_r^{-1}$, where a_r is aspect ratio of the fiber. As fibers flow in close proximity

to each other, the possibility of encountering enhanced hydrodynamic forces, friction and other mechanical interactions between fibers increases.[9] These complexities make study of the rheological properties of concentrated long fiber suspensions more challenging.

Fiber flexibility is another factor that plays an important role in determining the rheological behavior of long fiber composites. Because the fiber length in these materials is more than a critical value they, unlike short fibers, do not remain straight and change their curvature under flow deformations. Typically, for glass fibers this critical value is assumed to be 1 mm. Flexibility of the fiber varies with the intrinsic properties of the fiber, its aspect ratio and strength of the flow field.[12] If the fibers are flexible enough then bending forces acting on fibers through velocity field can influence the orientation state of the fibers,[11] which in turn can influence the macroscopic properties of the fluid. As a result, fiber flexibility has shown to be responsible for a considerable increase in suspension viscosity.[16,17,18]

There exist only a limited literature devoted to experimental studies of the rheology of long fiber composites due to the complex nature of these materials and the difficulties that are encountered during their rheological characterization. Forgacs and Mason[19] investigated the role of fiber length on rotation period of fibers in dilute fiber suspensions. They found that as the apparent aspect ratio decreased due to bending of fibers, it shortened the period of rotation. Tchen[20] showed that curvature of fibers greatly influences the drag applied on it while moving in a viscous medium.

Many experimental results have emphasized the role of flexibility on fluid viscosity. Nawab and Mason[21] in their study of thread like particles in castor oil, found the viscosity becomes more and more shear dependent with increase in fiber length. They expected this

behavior was due to elastic deformation of fibers. Blakeney[22] showed that even a 'slight curvature' of fibers has a pronounced effect on the viscosity. Kitano el.al.[23, 24] and Goto et.al.[25] illustrated the effect of fiber stiffness on the suspension rheology. They showed that more flexible fibers had a more pronounced effect on rheological properties.

Becraft and Metzner[26] concentrated their efforts on the effect of volume fraction on suspension rheology. They showed a significant increase in viscosity with increased fiber loading at low shear rates, but only a small increase in viscosity at high shear rates. Thomasset et.al.[27] in a similar study on polypropylene based long fiber suspensions observed an increase in shear viscosity with the increased fiber content and fiber length, however, this viscosity rise was very small which they attributed to high shear rates and fiber breakage during the processing. Non- Newtonian fluid characteristics, such as shear thinning were also observed.

In a recent study, Keshtkar et.al.[28] investigated the effect of two fiber flexibility parameters, stiffness and aspect ratio, in semi-dilute and semi-concentrated regimes. They found a significant increase in steady-state shear viscosity in the semi-concentrated regime compared to the semi-dilute regime. Viscosity of these suspensions also increased considerably with fiber flexibility. They found that in both the regimes, the addition of fibers results in significant normal forces under shear flow, and as the fiber content increases, the first normal force increases with it. Keshtkar and co-workers are also among the very few authors to observe transient stress growth behavior for long fiber composites. Stress growth experiments were carried out in the forward as well as in the reverse flow directions, and shear stress overshoots were observed at the start of the forward flow which they attributed to the fiber orientation under flow. They also found that the width and magnitude of the overshoot increased with increasing fiber flexibility.

Traditionally, capillary and rotational rheometers have been used to characterize the rheological behavior of concentrated long fiber composites. However, there are certain limitations associated with these rheometers which makes them undesirable to perform rheological measurement on fiber suspensions. Rotational rheometers which are generally used at low shear rates employ two geometries, cone-and-plate (CPR) and plate-and-plate (PPR). Viscosity measurement are made utilizing the entire sample area of the sample which makes results susceptible to edge phenomena, e.g free boundary effects, flow instabilities and thermal oxidation.[29] This may severely affect the outcome for fiber filled systems and may also reduce the maximum shear rate that can be achieved.[30] In the case of PPR the shear rate varies from center to the outer boundary which results in an inhomogeneous shear field. Since the rate of rotation of fibers depends on shear rate it is quite possible that this could result in increased fiber-fiber interaction giving rise to unnecessary stress overshoots.[31] In general, CPR provides a homogeneous shear field but the gap between plates varies from center to the outer edge, this can disrupt the fiber packing and may impart an unwanted flow history on sample as it is squeezed to required gap dimensions.[31, 32] Boundary interactions may also severely affect the rheology if the gap between plates is small compared to fiber characteristic length.

Capillary rheometers, on the other hand are mostly used to investigate the deformation behavior of long fiber filled suspensions at very high shear rates that are out of reach of rotational devices. But like rotational rheometers they too present certain limitations. Studies[33] have shown that, in laminar flow, migration of fibers may occur across the streamlines, away from the capillary wall. This can reduce the fiber concentration at the boundaries of the capillary resulting in a stress response similar to pure matrix. Additionally, there is considerable fiber

breakage that occurs during the extrusion of fibers through the capillary.[26,27] At this point there is no way to account for effect of fiber migration and fiber breakage on the rheological results.

Few attempts have been made to overcome some of the problems encountered with conventional rheometers. Jones and Roberts[34] utilized a linear oscillator to perform an experimental investigation of the dynamic behavior of an aligned continuous fiber suspension. They measured both longitudinal as well as transverse viscosity of unidirectional fiber suspension. Shuler and Advani[35] developed an experimental approach to utilize squeeze flow in order to more accurately resemble the real processing of composite sheet laminates. In another experimental investigation, Laun[36] utilized a sandwich rheometer to obtain creep curves on fiber filled low density polyethylene (LDPE) having different initial fiber orientation. Ericsson et.al.[29] employed a similar device called sliding plate rheometer (SPR) incorporating a shear stress transducer (SST) to characterize the shear response of concentrated planar fiber suspension. This new rheometer was proven to be very useful to overcome the limitations posed by capillary and rotational rheometers. Unlike conventional rheometers localized measurements could be carried out in SPR, which eliminates typical problems arising from edge effects, oxidative degradation and sample size.[29] Moreover, rectilinear homogeneous flow fields and sufficient gap size restrict unwanted fiber-fiber and fiber-wall interactions. This geometry also facilitates a setting where fibers can be aligned in any preferential direction, which is not a possibility for the rotational rheometers.

A sliding plate rheometer incorporating a wall shear stress transducer was first developed by Giacomin et al.[30,37] In various publications by Dealy and co-workers,[38, 39, 40] it has proven itself as a trustworthy tool to measure rheological properties of polymer melts. Given the

advantages it has over conventional rheometers it is decided to explore SPR to perform transient shear experiments on concentrated long glass fiber composites.

1.2 Research Objectives

The goal of this research is to develop a mean to obtain the transient rheological behavior of long glass fiber suspensions in concentrated regime as a function of fiber concentration, fiber aspect ratio and intitial fiber orientation, and to find a connection between the rheology and fiber orientation evolution in the system. The present work covers the rheological part of this goal, and the connection between the rheology and fiber evolution would be explored in the future. Objectives required to accomplish the set goals are stated below:

- Analyze and develop a rheometer to characterize the rheological behavior of concentrated long glass fiber composites that can produce unbiased and reproducible results.
- Characterize the transient rheological behavior of long glass fiber composite in simple shear experiments to investigate the role of fiber concentration, fiber aspect ratio and initial fiber orientation.

1.3 References

1. High performance at medium fibre length in long glass fibre polypropylene. *Plastics, Additives and Compounding* **2000,** 2, (12), 14-21.

2. Lee, S., *Handbook of composite reinforcements*. Wiley-VCH: 1992.

3. Sepehr, M.; Ausias, G.; Carreau, P., Rheological properties of short fiber filled polypropylene in transient shear flow. *Journal of Non-Newtonian Fluid Mechanics* **2004,** 123, (1), 19-32.

4. Nguyen, B.; Bapanapalli, S.; Holbery, J.; Smith, M.; Kunc, V.; Frame, B.; Phelps, J.; Tucker III, C., Fiber Length and Orientation in Long-Fiber Injection-Molded Thermoplastics--Part I: Modeling of Microstructure and Elastic Properties. *Journal of Composite Materials* **2008,** 42, (10), 1003.

5. Bartus, S.; Vaidya, U., Performance of long fiber reinforced thermoplastics subjected to transverse intermediate velocity blunt object impact. *Composite Structures* **2005,** 67, (3), 263-277.

6. Yang, J. M., Modeling and Characterization of 2-D and 3-D Textile Structural Composites, Ph.D. dissertation, University of Delware, Newark **1986**.

7. Silverman, E., Effect of glass fiber length on the creep and impact resistance of reinforced thermoplastics. *Polymer Composites* **1987,** 8, (1).

8. McAllister, L.; Lachman, W.; Kelly, A.; Mileiko, S., Handbook of Composites. *Vol. IV" Fabrication of Composites", edited by A. Kelly (North Holland, 1983) pp*, 109-75.

9. Guo, R.; Azaiez, J.; Bellehumeur, C., Rheology of fiber filled polymer melts: Role of fiber-fiber interactions and polymer-fiber coupling. *Polymer Engineering & Science* **2005,** 45, (3).

10. Tang, W.; Advani, S.; Source, C., Dynamic Simulation of Carbon Nanotubes in Simple Shear Flow. *Computer Modeling in Engineering and Sciences* **2008,** 25, (3), 149.

11. Strautins, U.; Latz, A., Flow-driven orientation dynamics of semiflexible fiber systems. *Rheologica Acta* **2007,** 46, (8), 1057-1064.

12. Wang, G.; Yu, W.; Zhou, C., Optimization of the rod chain model to simulate the motions of a long flexible fiber in simple shear flows. *European Journal of Mechanics/B Fluids* **2006,** 25, (3), 337-347.

13. Folgar, F.; Tucker III, C., Orientation behavior of fibers in concentrated suspensions. *Journal of reinforced plastics and composites* **1984,** 3, (2), 98.

14. Ganani, E.; Powell, R., Rheological properties of rodlike particles in a Newtonian and a non-Newtonian fluid. *Journal of Rheology* **1986,** 30, 995.

15. Switzer III, L.; Klingenberg, D., Rheology of sheared flexible fiber suspensions via fiber-level simulations. *Journal of Rheology* **2003,** 47, 759.

16. Joung, C.; Phan-Thien, N.; Fan, X., Direct simulation of flexible fibers. *Journal of Non-Newtonian Fluid Mechanics* **2001,** 99, (1), 1-36.

17. Joung, C.; Phan-Thien, N.; Fan, X., Viscosity of curved fibers in suspension. *Journal of Non-Newtonian Fluid Mechanics* **2002,** 102, (1), 1-17.

18. Bapanapalli, S.; Nguyen, B., Prediction of elastic properties for curved fiber polymer composites. *Polymer Composites* **2008,** 29, (5), 544-550.

19. Forgacs, O.; Mason, S., Particle motions in sheared suspensions IX. Spin and deformation of threadlike particles. *Journal of Colloid Science* **1959,** 14, 457-472.

20. Tchen, C.-M., Motion of Small Particles in Skew Shape Suspended in a Viscous Liquid. *Journal of Applied Physics* **1954,** 25, (4), 463-473.

21. Nawab, M.; Mason, S., Viscosity of Dilute Suspensions of Thread-like Particles. *The Journal of Physical Chemistry* **1958,** 62, (10), 1248-1253.

22. Blakeney, W., The viscosity of suspensions of straight, rigid rods. *Journal of Colloid and Interface Science* **1966,** 22, 324.

23. Kitano, T.; Kataoka, T.; Nagatsuka, Y., Dynamic flow properties of vinylon fibre and glass fiber reinforced polyethylene melts. *Rheologica Acta* **1984,** 23, (4), 408-416.

24. Kitano, T.; Kataoka, T.; Nagatsuka, Y., Shear flow rheological properties of vinylon-and glass-fiber reinforced polyethylene melts. *Rheologica Acta* **1984,** 23, (1), 20-30.

25. Goto, S.; Nagazono, H.; Kato, H., The flow behavior of fiber suspensions in Newtonian fluids and polymer solutions. *Rheologica Acta* **1986,** 25, (2), 119-129.

26. Becraft, M.; Metzner, A., The rheology, fiber orientation, and processing behavior of fiber-filled fluids. *Journal of Rheology* **1992,** 36, 143.

27. Thomasset, J.; Carreau, P.; Sanschagrin, B.; Ausias, G., Rheological properties of long glass fiber filled polypropylene. *Journal of Non-Newtonian Fluid Mechanics* **2005,** 125, (1), 25-3

28. Keshtkar, M.; Heuzey, M.; Carreau, P., Rheological behavior of fiber-filled model suspensions: Effect of fiber flexibility. *Journal of Rheology* **2009,** 53, 631.

29. Anders Ericsson, K.; Toll, S.; Månson, J., Sliding plate rheometry of planar oriented concentrated fiber suspension. *Rheologica Acta* **1997,** 36, (4), 397-405.

30. Giacomin, A. A sliding plate melt rheometer incorporating a shear stress transducer. McGill University, 1987.

31. Eberle, A.; Baird, D.; Wapperom, P., Rheology of Non-Newtonian Fluids Containing Glass Fibers: A Review of Experimental Literature. *Ind. Eng. Chem. Res* **2008,** 47, (10), 3470-3488.

32. Cross, M.; Kaye, A., Techniques for the viscometry of suspensions. *Polymer Engineering & Science* **1986,** 26, (2).

33. Mondy, L.; Geller, A.; Rader, D.; Ingber, M., Boundary element method calculations of the mobility of nonspherical particles—II. Branched chains and flakes. *Journal of Aerosol Science* **1996,** 27, (4), 537-546.

34. Jones, R. S.; Roberts, R. W., Anisotropic shear flow in continuous fibre composites. *Composites* **1994,** 25, (3), 171-176.

35. Shuler, S.; Advani, S., Transverse squeeze flow of concentrated aligned fibers in viscous fluids. *Journal of Non-Newtonian Fluid Mechanics* **1996,** 65, (1), 47-74.

36. Laun, H., Orientation effects and rheology of short glass fiber-reinforced thermoplastics. *Colloid & Polymer Science* **1984,** 262, (4), 257-269.

37. Giacomin, A.; Samurkas, T.; Dealy, J., A novel sliding plate rheometer for molten plastics. *Polymer Engineering and Science* **1989,** 29, (8), 499-504.

38. Dealy, J.; Soong, S., A parallel plate melt rheometer incorporating a shear stress transducer. *Journal of Rheology* **1984,** 28, 355.

39. Park, H.; Lim, S.; Smillo, F.; Dealy, J.; Robertson, C., Wall slip and spurt flow of polybutadiene. *Journal of Rheology* **2008,** 52, 1201.

40. Koran, F.; Dealy, J., A high pressure sliding plate rheometer for polymer melts. *Journal of Rheology* **1999,** 43, 1279.

2.0 Literature Review

The chapter provides the review of the literature relevant to this research. The first section assesses the reasons behind surface modifications of fibers in a composite. It is followed by a review of rheological behavior of long fiber composites and previous rheological work that has been done in the area. In the end, there is a brief discussion on the modeling of the evolution of fiber orientation in flexible fiber suspensions.

2.1 Surface Modifications of Fibers

Fiber-fiber interaction and matrix-fiber interaction play an important role in determining the rheological characteristics of a fiber suspension.[1,2,3,4] Many approaches such as fiber-matrix interface treatment [5] and matrix modification [6] are taken to minimize the erosive contacts between fibers and to improve the matrix-fiber interaction. Among these methods, control of fiber-matrix interface adhesion by treating it with a chemical agent is the most promising approach to ensure better impact strength for the glass fiber composite.[5] Typically, saline based coupling agents are used for coating the fiber surface because they improve the surface interaction between the fiber and the matrix and thus promote better adhesion.[7]

One way to check the compatibility between fiber and matrix is to measure the degree of wetting or in other words the contact angle. Neumann and Good [8] proposed that if the contact angle; i.e the angle between liquid-air interface and solid-liquid interface, is less than 90^{o} then the fiber surface is wettable otherwise it is non-wettable. Well wetted fibers are usually recommended as they guarantee better adhesion between fiber and polymer matrix.

2.2 Rheology

In the following chapter experimental literature relevant to the rheological behavior of Newtonian and non-Newtonian fluids containing long fibers will be discussed. But, before reviewing the rheology it is vital to have a clear understanding of fiber suspensions, the rheometers used to characterize their rheology and basic characteristics of fiber filled systems. For this reason, in subsection § 2.2.1 fiber suspension are classified by their concentration and length. It is followed by the discussion on different rheometers (§ 2.2.2) that have been used to obtain rheological measurements in long fiber suspensions. In the end, § 2.2.3, different non-Newtonian fluid characteristics, e.g. shear thinning and Weissenberg effect, exhibited by fiber suspensions are discussed.

2.2.1 Classifying Fiber Suspension

2.2.1.1 Classifying Fiber Suspension by Concentration

The rheological behavior of fiber suspensions is highly dependent on fiber concentration and aspect ratio of fibers within the suspension. The major factor determining this dependence is the 'entanglement' constraint that fibers cannot pass through each other. Following the theory of Doi and Edwards[9], consider a solution of rod-like macromolecules having n rods per unit volume. If each rod has length L and diameter d then the volume fraction φ is defined as,

$$\varphi = \frac{\pi n L d^2}{4} \tag{2.1}$$

If $a_r = L/d$, be the aspect ratio of the rod then,

$$\varphi = \frac{\pi n L^3}{4 {a_r}^2} \tag{2.2}$$

Based on the 'entanglement' constraint, the concentration of fiber suspension can be divided into three regimes.

(a) Dilute Regime. The dilute regime is described as the regime which has a sufficiently low concentration of fibers so that a fiber is free to rotate without encountering other fibers. Theoretically, it is possible only if the average distance between two fibers is greater than L. This constraint can be mathematically represented as $n < 1/L^3$. Using *Eq. 2.2* it can be related to the volume fraction by $4\varphi < \pi a_r^{-2}$ which is roughly $\varphi < a_r^{-2}$.

(b) Semi-dilute Regime. The semi-dilute regime is described such that the free rotation of each fiber is restricted by other fibers. However, actual collision or contact is still rare. The interaction between fibers is achieved by keeping $n > 1/L^3$ while the upper limit in randomly oriented fiber suspension is subjected to the constraint that the average spacing between the fibers $S_m >> d$, or in other words $n << 1/dL^2$.[10] For the suspensions in which fibers are completely aligned, the average spacing is of the order of $S_m \cong (nL)^{-1/2}$, [11] and the upper limit can be represented as $n << 1/d^2L$. Both these lower and upper limits in the semi-dilute regime can be related to volume fraction by $a_r^{-2} < \varphi << a_r^{-1}$.

(c) Concentrated Regime. The concentrated regime is described such that the dynamic properties of the rods can be severely affected by fiber-fiber interactions and can lead to solid-like behavior.[12] It happens if the average spacing between fibers is of the order *d*. This limit can be represented as $n \geq 1/dL^2$ or $\varphi \geq a_r^{-1}$. As a note, glass fiber composites used for industrial applications typically have fiber concentration in the concentrated regime.

2.2.1.2 Classifying Fiber Suspensions by Length

As described later, fiber length plays a major role in determining the rheological behavior of fiber suspensions. For a suspension containing a distribution of fiber lengths, the probability

distribution function *p(l)* is defined such that the probability of a fiber having its length in the range of *l* and *l+dl* is *p(l)dl*. From this distribution function, the two most common length averages, namely number average (L_n) and weight average (L_w) are defined as:

$$L_n = \int_0^\infty p(l) l \, dl \tag{2.3}$$

$$L_w = \frac{\int_0^\infty p(l) l^2 \, dl}{\int_0^\infty p(l) l \, dl} \tag{2.4}$$

Both these averages are basically moments of fiber length distributions, and are defined in a similar manner as molecular weight distributions are defined. For discrete data same averages can be calculated as,

$$L_n = \frac{\sum_i N_i L_i}{\sum_i N_i} \tag{2.5}$$

$$L_w = \frac{\sum_i N_i {L_i}^2}{\sum_i N_i L_i} \tag{2.6}$$

The ratio of L_w to L_n is called polydispersity index, and it indicates the degree of scatter or broadness of fiber length distributions about the mean. The majority of literature refers to fiber number average to define the aspect ratio and concentration regimes.

In general, fiber filled systems are categorized either as long or short glass fiber suspensions depending on the length of fibers used in the system. What differentiate long fibers from short fibers is somewhat ambiguous as no precise definition is available in the literature. Usually, short glass fibers are assumed to be small enough that the fiber remains straight and their curvature does not change during the flow, whereas long glass fibers are more flexible and their curvature cannot be neglected. Forgacs and Mason[13] developed a criterion for fiber

flexibility. They observed that as the fiber stiffness decreases or aspect ratio increases, the fibers tend to bend during flow. They also estimated the critical stress required to bend the fibers as,

$$(\dot{\gamma}\eta_m)_{Crictical} = \frac{E_b(l\,n(2a_r) - 1.75)}{2{a_r}^4} \tag{2.7}$$

where η_m is the viscosity of suspending matrix and E_b is the bending modulus of the rod. The authors found good agreement between the equation and experimental results for different type of fibers. Stress imposed by the suspending fluid on the fibers is another important factor that affects the fiber flexibility. To incorporate the relative importance of hydrodynamic forces on a fiber, Switzer and Klingenberg[14] proposed the following equation to define effective stiffness (S^{eff})

$$S_{eff} = \frac{E_Y \pi d^4}{64\eta_m \dot{\gamma} L^4} \tag{2.8}$$

where E_Y is Young modulus of the fiber. As S_{eff} approaches zero, fibers behave like completely flexible threads; while if S_{eff} approaches infinity, the fibers behave like rigid rods and retain their shape during flow. Both *Eq. 2.7* and *Eq. 2.8*, can be used to define the 'criterion for flexibility' for any fiber suspension. However, in concentrated fiber regimes enhanced friction and other mechanical interactions between fibers introduce additional complexity and this makes it very difficult to set any mathematical boundaries that separates short from long fiber suspensions. Regardless, for glass fiber suspension, fiber length of 1 mm has typically been used as the boundary between long and short fiber composites.

2.2.2 Rheometry

Rheology of long fiber suspensions is very difficult to characterize due to the size of the fibers. Conventional devices such as rotational and capillary rheometers have been most

commonly used to investigate these composites. It is important to note that these rheometers have small flow field dimensions compared to the length of fibers.[15] This geometric restriction may highly influence the rheology of the suspension. In addition, there are other limitations posed by these devices, which have motivated researchers to look into unconventional rheological devices. The following section covers few of these conventional and unconventional devices utilized to study long fiber suspensions. In the end, a rheometer that could help in overcoming most of the limitations posed by other rheometers is discussed.

2.2.2.1 Rotational Rheometers

Rotational rheometers are generally used to characterize the rheology of fiber suspension at low shear rates. These rheometers employ two geometries: cone-and-plate (CPR) and parallel-plate (PPR). Both CPR and PPR fixtures have plate diameters ranges from 25 - 50 mm.

For the CPR usually two measurements, torque $\tau(t)$ required to rotate the upper disk and total normal force $F(t)$ on the plate to maintain the desired gap, are made. From these measurements various material functions are calculated. Since the shear rate $\dot{\gamma}$ is constant in the fluid, the viscosity becomes an explicit function of the applied torque. The equations to solve various material functions can be found elsewhere.[16]

Similar to CPR, in a parallel-plate system, the same two quantities, $\tau(t)$ and $F(t)$, are measured as a function of time. But because of the inhomogeneity of the shear rate, the viscosity is not an explicit function of the applied torque and is given by, [16]

$$\eta(t) = \frac{\tau(t)/2\pi R^3}{\dot{\gamma}_R}\left[3 + \frac{d\ln\left(\frac{\tau(t)}{2\pi R^3}\right)}{d\ln\dot{\gamma}_R}\right] \tag{2.9}$$

where R is the radius of plate and $\dot{\gamma}_R$ is the shear rate at R.

Both the CPR and the PPR are among the most common devices used to investigate the rheological behavior of fiber suspension, but there are certain restrictions arising from their geometry, flow fields and size which make them inherently inaccurate while characterizing the behavior of long fiber suspensions. The gap in the CPR varies from center to the edge of the plate. This can disrupt the fiber packing and can impart an undesirable flow history when a sample is squeezed to the required gap dimension.[17,18] For the PPR where the flow field is non-homogeneous, shear rate is a function of R. For sufficiently long fiber suspension where fiber rotation is a function of shear rate, it is speculated that this may result in excessive fiber-fiber interaction giving rise to stress overshoot.[17] Moreover, in both parallel-plate and cone-and-plate geometry viscosity is measured using the whole sample area as it is a function of torque required to rotate the upper plate. This makes the measurements highly vulnerable to edge phenomena, e.g., flow instabilities and thermal oxidation.[19] It also restricts the maximum shear rate that can be achieved using these devices.[20]

Boundary interactions may also take place if the gap is small compared to the fiber characteristic length. For a fiber suspension, the characteristic length may vary from the length of the fiber to its diameter depending on the orientation of fibers in the composite. For example, if a fiber is oriented perpendicular to the plates its characteristic length would be equal to the length of fiber, while for a fiber that is oriented in the flow direction has a characteristic length equal to the diameter of the fiber.[21] Time and again it has been suggested in the literature that to minimize the boundary effects, the gap should be greater than three times the characteristic length.[22,23,24] Eberle[25] showed the effect of boundary interaction due to gap size, where he found that

rheological results did not depend on the gap height when the gap size was more than two times the length of the fibers.

Curvilinear streamlines may be another factor that may lead to inaccurate results for rotational rheometers. Under deformation fibers try to align themselves parallel to the streamlines, but it seems highly unlikely for long fibers to align themselves with curvilinear streamlines. Moreover, the small flow field dimensions compared to length of the fibers also limits the rheometer's accuracy.

2.2.2.2 Capillary Rheometer

Like rotational rheometers, the capillary rheometer is another shear flow device that is commonly used to study the deformation behavior of fiber suspensions, though at high shear rates. Basically, the device consists of a barrel for melting the polymer and a plunger that pushes this polymer through a capillary. Data obtained from the device consist of the pressure difference across the capillary and the volumetric flow rate of the polymer through capillary. Various corrections are employed to correct the data collected from the rheometer to obtain meaningful rheological results.

Investigating the deformation behavior of long fiber suspension using capillary rheometer presents a few severe problems. Mondy et al. [26] studied the rheology of fibers suspended in a Newtonian medium and found shear-induced fiber migration away from the capillary wall. In laminar flow through capillary, fibers can migrate away from the high shear regions, i.e. the wall, to balance the shear rate gradients. This migration may decrease the concentration of fibers in the wall regions which could result in erroneous stress response at the wall. Another major difficulty in using the capillary rheometer is the fiber breakage during the flow in capillary. Thomasset et al.[27] reported significant breakage of fibers during the processing in a capillary rheometer. They

observed reduction of fiber length from 5.1 mm at the capillary entrance to 4.0 and 2.4 mm after extrusion through the capillary of 30 and 60 mm, respectively. Becraft and Metzner[28] in their study of long fiber suspensions also showed considerable fiber breakage. They found that this breakage doesn't depend on the extrusion rate.

2.2.2.3 Squeeze Flow Rheometer

Limitations presented by standard rheometers have motivated researchers to look into unconventional rheological devices to characterize the behavior of long fiber suspensions. One of such device is the squeeze flow rheometer. It employs two impermeable parallel surfaces to squeeze the polymer sample held between them. The time dependent planar flow of viscous fluids between the two plates is used to study the viscosity of the material. With the lower plate fixed, either a constant force or constant closure rate is applied on the upper surface. If a constant force is applied, measurement of the resulting displacement between the two plates is used to calculate rheological properties. If a constant closure rate is applied, measurement of the resulting force is used.

The advantages of the squeeze flow rheometer include mechanical simplicity, the very high shear rates that can be achieved and the ease with which the high viscosity materials can be tested.[29] But above all it gives a better understanding of the squeeze flow behavior of fiber reinforced thermoplastic composites, which is important considering it resembles the actual processing of GMT composites at the industrial scale.

Shuler and Advani[30] incorporated a squeeze flow rheometer to examine the effect of unidirectional long fiber composites on the processing characteristics of thermoplastic composites. In order to get meaningful rheological data from the rheometer they made a few assumptions: The material is incompressible; the squeeze flow is very slow (creeping flow);

there is no flow in the direction along which the fibers are initially oriented and no-slip condition applies on the platen surfaces. All these assumptions are reasonable under the test conditions used by the authors. They also assumed that the composite can be described by the three-parameter Carreau fluid model, and obtained the model parameters by comparing the experimental and theoretical platen loads for constant closure rate experiments.

The approach adopted by Shuler and Advani to calculate the shear viscosity in the direction transverse to the direction of aligned fibers, seems to work reasonably well as good agreement between experimental force and the calculated force on the upper plate was achieved. But, it is important to note that their basic assumption to describe the composite as a Carreau fluid may not hold true for all the suspensions. This presents a serious restriction with the squeeze flow rheometer for which it is vital to describe the fluid by a phenomenological model in order to solve the governing equations defining the flow of the composite, and consequently to solve the normal force on the upper surface. These are, however, overwhelming range of fiber suspensions where power-law behavior is observed. Also this rheometer, due to its large size, can be a useful tool to study the evolution of fiber orientation under the squeeze flow.

2.2.2.4 Extensional Rheometer

Unlike the rheometers discussed before which have been used to characterize the shear rheology of the materials, the extentional rheometer is utilized to obtain their elongational viscosity. Extensional behavior of fiber filled polymers has been studied by a few researchers including Batchelor,[11] Goddard,[31] Creasy et al.,[15] and the effect of fibers on the elongational viscosity is well documented.

An extensional rheometer usually consists of a hydraulic test machine to stretch a sample held between two grips. Using the computer the grip could be displaced at a determined speed or

it could be displaced to maintain constant stress on the sample.[15] As a result, two types of tests could be performed to determine elongational behavior of a specimen.

(a) Controlled elongation rate test. The elongation rate $\dot{\epsilon}$ can be defined in terms of changing length of the specimen *L(t)* as,

$$\dot{\epsilon} = \frac{1}{L}\frac{dL}{dt} \tag{2.10}$$

If deformation of the melt is homogeneous then elongational stress τ_E is defined as,

$$\tau_E = \frac{F(t)}{A_0 e^{-\dot{\epsilon}t}} \tag{2.11}$$

where *F(t)* is the force recorded by the load transducer and A_0 is the initial cross-section area of the sample. Elongational viscosity can be obtained from elongational stress and elongational rate,

$$\eta_E = \frac{\tau_E}{\dot{\epsilon}} \tag{2.12}$$

(b) Controlled elongational stress test. For a constant elongational stress τ_E, ϵ vs *t* data is collected. From this data, elongation rate can be determined to obtain the elongation viscosity using Eq. 2.12.

One of the major assumptions in order to get rheological data from elongational rheometers is that the homogeneous deformation is achieved during the extension of the specimen. But in case of long fiber composites, homogeneity is limited due to the distribution of fibers in the sample and the phase change across its length.[15] To secure the ends of the specimen from the high loads encountered during the extension at high temperature, a phase change from the melt in the gauge length to solid composite at each end is employed. This together with the distributed fiber length restricts the uniform strain rate throughout the gauge section, and consequently limits the accuracy of the results produced.

2.2.2.5 Sliding Plate Rheometer

Ideally it is desirable to perform the rheological measurements in a suitably large device so that the boundary and flow effects can be minimized.[21] Although the squeeze flow rheometer fulfils this criterion, a device which can characterize the rheology of LFC in a more fundamental flow, such as simple shear flow would be highly favored. Laun[32] and Ericsson et al.[19] employed one such device, the sliding plate rheometer, which generated rectilinear simple shear flow fields to study the rheology of long fiber suspensions. Ericsson and co-workers used a commercial version of the sliding plate rheometer that incorporates a shear stress transducer developed by Giacomin et al.[20,33] Such a rheometer offers many improvements over conventional rheometers in obtaining the rheological measurements. Detailed discussion on this device and its advantages over other rheometers can be found in Chapter 3.

2.2.2.6 Summary of Rheometers

As discussed in this section, the rheology of a fiber suspension could be highly influenced by the rheometers used to characterize it. The limitations associated with each rheometer are outlined and it is found that the rheological results are influenced by the rheometer geometry, size, flow field and their functioning. Despite these limitations, some of these rheometers have been widely used by researchers to characterize the rheology of fiber suspensions due to their easy availability. However, results from these rheometers cannot be used quantitatively to assess the rheological behavior of long fiber suspensions, but they can surely be used to make qualitatively assessments.[17]

2.2.3 Characteristics of long glass fiber suspensions

Various nonlinear characteristics exhibited by fiber filled Newtonian and non-Newtonian fluids which are attributed to fiber-fiber interaction, fiber-fluid interaction, nature of the matrix and fiber flexibility are discussed in this section. Although, the origin for few of the characteristics is still unknown but considerable efforts have been made by researchers to theorize them.

2.2.3.1 Weissenberg Effect

The Weissenberg effect or rod-climbing is a phenomenon that occurs when a spinning rod is placed into a viscoelastic fluid. Instead of being pushed away, the fluid climbs up the rod. Usually, this effect is attributed to the presence of normal stresses within the polymer. Taylor[34] indirectly predicted that the similar phenomenon would occur in systems filled with fibers. Later, it was confirmed by a few researchers[35-37] who observed the rod-climbing effect in both Newtonian as well as non-Newtonian fiber suspensions. Zirnsak et al[38] attributed the required normal stress, and therefore rod-climbing behavior, to the mechanical contacts between fibers.

2.2.3.2 Shear Thinning

Adding fibers to a Newtonian or a non-Newtonian fluid can significantly alter its shear thinning behavior.[14, 28, 39-41] For both short and long fiber suspensions, shear thinning behavior has been reported in literature. Goto et al.[40] who studied the rheological behavior of nylon, glass and vinylon fibers in glycerin, observed that the shear thinning behavior became more prominent as the fiber aspect ratio was increased. Ganani and Powell[42] and Ericsson et al.[19] showed that the inception of shear thinning behavior is usually shifted towards lower shear rates with respect to pure matrix. In general, shear thinning behavior in fiber suspensions has been attributed to either the shear thinning nature of non-Newtonian solvents or the bending of the flexible fibers but its

origin is still unclear. Chaouche and Koch[41] in their study on short nylon fibers in various silicon oils suggested that the shear thinning behavior at small shear rates and low viscosity solvents is due to the adhesive contacts among fibers. However, for high shear rates they too attributed this behavior to fiber bending and solvent properties.

2.2.3.3 Yield Stress

Like the Weissenberg effect and shear thinning, the yield stress is another nonlinear rheological characteristic observed in fiber suspensions.[27, 43,44,45] Yield stress, i.e a stress below which the composite behaves like a solid, which is usually attributed to mechanical contacts between the fiber suspensions with yield values representing the interfiber failure of the network.[43] Bennington et al.[43] measured the yield stress of various pulp and synthetic fibers and found that it scales with fiber volume fraction. The scaling factor was consistent with the simple fiber network theory[14] proposed by Meyer and Wahren[46]. They observed that physical properties of fibers such as aspect ratio and elastic modulus also influence the yield stress, but this dependence was significantly dissimilar for both type of fibers. The pulp fiber suspensions showed an increase in the yield strength with a decrease in elastic modulus while synthetic fibers behaved in the opposite way. Kitano and Kataoka,[39] who worked on the suspensions of vinylon fibers in silicon oil, also noticed the dependence of yield stress on fiber aspect ratio, which they attributed to fiber flexibility and wall effects.

2.2.3.4 Stress Overshoot during transient flow

The transient shear response, i.e. the development of the stresses at the start up of the shearing flow, is very important in case of fiber filled systems. Many researchers[32,3,47,48,49] have shown the presence of the stress overshoot at the start up of the shear flow. Upon the inception of the flow, the shear stress grows, reaches a maximum value, and then decline to a steady state.

This stress overshoot is mainly caused by the presence of fibers in the system. Laun[32] and Powell [21] substantiated this claim by employing flow cessation experiments. They found that upon cessation of shearing flow, i.e. allowing the stress to relax completely did not bring the fluid back to its initial state. On resuming the shearing again in the same direction, the stress returned to the same value at which the flow was halted. This was because when the flow was stopped the microstructure of the fibers in the sample remained unchanged as the matrix relaxed. It confirmed that the stress overshoot is the result of fiber orientation and not of conformation of the fibers.

2.3 Rheological work

As mentioned previously, long glass fiber composites (LFCs) are widely used in industry as they offer cost effective, light weight and high performance materials. Physical properties such as elasticity modulus, strength, thermal expansion and thermal conductivity, depends on the concentration, type, size and orientation of reinforced fibers in polymer composites.[50,51] During processing, fiber-reinforced polymers are subjected to rigorous deformations which cause fibers to translate, bend and rotate with the flow of the fiber matrix.[52] This greatly influences the mechanical properties in different parts of the final product because of the close dependence of these properties on the orientation state of the fibers.[53,54] Similarly, rheological properties which are a function of the flow induced fiber configuration in the matrix also influence the physical properties of the fiber composite. This makes it important to study and understand the evolution of orientation state of fibers and how rheological properties have their effect on it. Moreover, a thorough knowledge of rheological behavior of fiber suspensions can be instrumental in designing and optimizing processing conditions for variety of industries to achieve LFCs having better mechanical properties.[42,14,55]

This present work deals with only the characterization of transient rheological properties for different initial fiber orientation. Evolution of the orientation state, during processing, is not discussed here and is left for future work.

Rheology of LFCs is very complex because various factors such as fiber-matrix interaction, fiber-fiber interaction, fiber-wall interaction, fiber breakage and migration affect flow induced fiber orientation in these suspensions.[3] In high concentration regimes fiber-matrix and fiber-fiber interaction becomes more important as the conformation of the polymer chains gets influenced by the orientation of neighboring fibers. Also, as fibers flow in close proximity with each other, there is an increased possibility of encountering enhanced hydrodynamic forces, friction and other mechanical interactions between fibers.[50] All these factors equally affect the rheology of short as well as long glass fiber reinforcements, but the property which differentiates long glass fibers from their short counterparts is 'flexibility'. For short fiber composites (SFCs), flexibility is not important as their length is small enough to assume that the fiber remains straight and their curvature does not change during flow. However, in case of long glass fibers where the average fiber length is more than 1mm, the curvature of fibers cannot be neglected because it considerably affects the composite properties and has been shown to be responsible for large increases in suspension viscosity.[56,55,57] If the fibers are flexible enough, then the bending forces acting on fibers through the velocity field can influence the orientation state of the fibers,[53] which in turn can influence the macroscopic properties of the composite.

The flexibility of a fiber varies with the intrinsic properties of the fiber, its aspect ratio and strength of the flow field.[52] As a result, the rheological properties of the LFCs are said to be affected by fiber properties, fiber interactions, suspending fluid properties and the flow field imposed.

There have been several theoretical attempts dedicated to the analysis and prediction of the evolution of fiber orientation and its effect on the rheology of LFCs, some of which are discussed in Subsection § 2.4. However, there exist only a limited literature devoted to experimental studies of long fiber suspensions due to the difficulties that are encountered during their rheological characterization. It is difficult to obtain the shear and extensional properties of long fiber reinforced composites using traditional rheological techniques. Arlov et al.[58] were among the first few authors to investigate the dynamics of flexible fibers. They classified the dynamics of flexible fibers into three modes. The different dynamics reflected the relative flexibility of fiber in different conditions.

Forgacs and Mason[13] investigated the role of fiber length on the rotation period of fibers in dilute suspensions and made comparison with the Jeffery's[59] model predictions. They observed that as fiber length or aspect ratio increased, fibers started to bend due to the axial forces imposed by shear flow. It shortened the apparent aspect ratio and, thus, the period of rotation for these fibers. Tchen[60] found that large curvature of the fibers greatly affects the drag applied on it while moving in a viscous medium.

Nawab and Mason[35] characterized the rheological behavior of dilute suspensions of thread like particles in castor oil, concluding that fiber length shows a pronounced effect on viscosity of the suspension. They found viscosity to be more and more shear dependent with an increase in fiber length, which they expected was due to elastic deformation of fibers. Fibers underwent increasing amount of bending as the aspect ratio was increased. A prominent Weissenberg effect was also noticed for higher aspect ratio suspensions. Blakeney[23] also showed that a very 'slight curvature' of the fiber has a pronounced effect on the viscosity.

Ganani and Powell[61] in their review concluded that the relative viscosity of a fiber suspension depends upon the following factors: volume fraction, aspect ratio, shear rate and particle flexibility. In addition, Keshtkar et al.[47] in their review cited the work of Kitano et al.[62, 63] and Goto et al[40], where they stressed the affect of a fiber's stiffness on the viscosity of a fiber suspension. Kitano et al.[62] took polyethylene based suspensions of vinylon and glass fibers, vinylon being more flexible, and showed that vinylon fiber suspensions had a more pronounced effect on rheological properties. Similarly, Goto and et al.[40] also studied the rheological behavior of different fiber types such as carbon, glass, vinylon and nylon fibers in Newtonian and viscoelastic suspending mediums. They too observed the prominent effect of fiber flexibility on the suspension rheology. However, results obtained by both Goto et al. as well as Kitano et al. were inconclusive because they used different fiber lengths depending on the fiber type.

There have been few experimental studies concentrated on the effect of fiber aspect ratio and volume fraction on flow characteristics of long fiber suspensions. Becraft and Metzner[28] studied the rheological behavior of glass fiber-filled high density polyethylene and isotactic polypropylenes suspensions. They used two different concentrations of fibers, 10 wt. % and 40 wt. %. Once these fiber suspensions were compounded, significant fiber breakage was observed, but the average fiber length still remained close to 1 mm. The fiber length also went down a little further due to some additional fiber breakage during the high shear rate experiments in the capillary rheometer. Authors of this paper observed Newtonian like behavior at low shear rates and shear thinning at high shear rates. Their results also showed a significant increase in viscosity with increased fiber loading at low shear rates and only a small change in viscosity at high shear rates.

Another experimental work concerning the rheological properties of LFCs was carried out by Thomasset et al.[27] They used polypropylene (PP) based long fiber suspensions having different fiber lengths and concentration. Fiber weight fraction in their samples varied from 20 to 40 %, and fiber length varied from 10 to 20 mm. A comparison between LFCs and SFCs was also made. An injection molder was used to disperse the fibers adequately in the suspension, but it also significantly reduced the fiber size. They found that steady-shear viscosity increases were very small with fiber length, which they attributed to excessive fiber breakage during injection molding and then in the capillary rheometer. Viscosity of short-fiber filled PP was found to be lower than that of long fiber filled PP. This result contradicted the results of a similar study conducted by Gibson[64] where they observed that the viscosity increases were smaller with long fibers than with short fibers.

In a recent study, Keshtkar et al.[47] investigated the effect of fiber flexibility parameters (stiffness and aspect ratio) in semi-dilute and semi-concentrated regimes. They studied three fiber types, polyarylate, vinylon and nylon fibers, with two different fiber aspect ratios. A high viscosity silicon oil polydimethylsiloxane (PDMS), was used as the Newtonian suspending medium. They found a significant increase in steady-state shear viscosity in the semi-concentrated regime compared to the dilute regime. The viscosity of these suspensions also increased considerably with fiber flexibility. They also found that in both regimes, the addition of fibers results in significant normal forces under shear flow, and as the fiber content increases, the first normal force increases with it.

Keshtkar and co-workers are also among the very few authors to observe the transient shear growth behavior for long fiber composites. The significance of transient rheological experiments rests in the fact that processing time for these composites are usually short and

steady flow may only be achieved in limited regions if at all.[15] Stress growth experiments were carried out in the forward and reverse flow directions. Stress overshoots were observed at the start of the forward flow which they attributed to fiber orientation under flow. They also found that the width and magnitude of the overshoot increased with increasing fiber flexibility.

A few different shear and extensional rheometer studies have been used to characterize the rheological behavior of long fiber suspensions. Among them, the most common rheometers are the rotational rheometer and capillary rheometer. These conventional rheometers have been used for fiber composites having a range of concentrations and fiber lengths. However, their geometry, flow field, and functioning impose certain limitations when it comes to the rheology of long fiber filled suspensions, especially in the concentrated regime. In subsection § 2.2.2 these rheometers and the specific problems that are encountered while investigating the rheology of fiber suspensions are discussed in detail.

A few of the limitations which are mentioned in § 2.2.2 can be overlooked to some extent for the case of short fiber suspensions due to their small fiber size, but these inadequacies cannot be ignored for concentrated long glass fiber suspensions used in this study. This obviously presents a need for a novel device that could be used without encountering such problems. Also, it would be interesting to look at the rheology of fiber reinforced composites having some predefined initial fiber orientation because from early discussion we know that fiber orientation plays an important role in determining the rheological behavior of these composites. But again, due to non-rectangular geometries, it is nearby impossible to align fibers in any particular direction in conventional rheometes.

A few attempts have been made to overcome some of the problems encountered with conventional rheometers by designing more suitable devices to study long fiber suspensions. Jones and Roberts[65] performed an experimental investigation of the dynamic behavior of an oriented assembly of aligned continuous nylon fiber suspended in viscous suspension using a linear oscillator. The constructed instrument was tested using isotropic materials and gave data which were in good agreement with commercial rheometers. They used various volume fraction of fiber ranging from 30 % to 80% with Golden Syrup as the suspending fluid. Samples were prepared as 39 x 39 mm rectangular plates with the desired concentration of 39 mm nylon fibers aligned in one direction. In each experiment the sample was characterized both along and transverse to the fiber direction. They found a critical fiber concentration, above which longitudinal dynamic viscosity was less than the transverse dynamic viscosity whereas below this critical concentration longitudinal viscosity was greater than transverse viscosity.

Creasy and Advani[15] investigated the transient elongation behavior of a highly-aligned 60% fiber volume fraction long discontinuous fiber-filled polyether-ketone-ketone (PEKK). Samples were prepared, first by chopping the fibers and then combining them with matrix to produce a pre-impregnated 1.25 mm thick tape. These tapes were hand laid on top of each other and then consolidated under pressure at the processing temperature to produce panels measuring 2.5 x 42 cm with all fibers aligned in the long dimension. An electric tube furnace combined with a computer-controlled hydraulic test machine was used to produce transient elongation measurements. The sample was loaded between an unmovable grip and a movable grip that connects to the servo-hydraulic ram to displace the grip at any determined velocity as a function of time. They concluded that long fiber suspensions tested in elongation at controlled elongation rate displayed stress growth consistent with a non-linear viscoelastic fluid in a shear dominant

flow. Test in elongation at controlled stress confirmed that increasing stress produces a decreasing viscosity.

Shuler and Advani[30] developed an experimental approach to utilize squeeze flow in order to more accurately resemble the real processing of composite sheet laminates. It allowed them to characterize the transverse shear viscosity for a model composite material system composed of clay filled with either nylon or glass fiber and a commercially available carbon fiber reinforced polyether-ether-ketone (PEEK) thermoplastic (APC-2) laminate. Samples of dimensions 5 cm * 5 cm * 1 cm were prepared by aligning 5 cm long fibers perpendicular to the direction of squeeze motion. The anisotropic nature of the aligned fiber filled material system constrained the material to two-dimensional flow perpendicular to the fiber direction. Experiments with 20, 40, 50 and 60 vol. % fiber composites revealed that both the unfilled clay and the fiber filled composites could be described as shear thinning Carreau fluids. A non-linear increase in transverse shear viscosity was observed as fiber content was increased. Though both glass and nylon fibers were used for this experimental investigation, the role of fiber flexibility is inconclusive as different fiber diameters were used. However, for smaller diameter glass fiber clay composites enhanced transverse shear viscosities are reported. For APC-2, similar shear thinning behavior and enhanced shear viscosity with increase in fiber content were observed.

In another experimental investigation, Ericsson et al.[19] developed a sliding plate rheometer (SPR) incorporating a shear stress transducer (SST) to characterize the shear response of concentrated planer fiber suspension. This new rheometer was proven to be very useful to overcome the limitations posed by other conventional rheometers. Ericsson and co-workers are among very few authors who have incorporated a SPR to investigate the fiber suspension rheology. However, unlike the present work their results are limited to steady state viscosity, and

do not cover transient viscosity growth. For their work, they used three different grades of chopped glass fiber filled polypropylene. The material was in the form of pre-consolidated sheets with highly two-dimensional fiber orientation distribution. One fiber length, 12.7 mm, was available at two initial fiber volume fractions, 14 and 28 %, and the second fiber length, 25.4 mm, was available at an initial fiber volume of 14 %. Authors observed an increase in viscosity of 2-3 orders of magnitude at low shear rates as fiber volume fraction was increased to 28 %. At high, shear rates the increase was less than an order of magnitude. They also observed a shift in power law region towards lower shear rates compared to the neat melt. Effect of fiber aspect ratio was not pronounced; they found a very week influence of aspect ratio on the steady shear viscosity.

2.4 Modeling

The first theoretical work that is extensible to the theory of evolution of fiber orientation is the work by Jeffery.[59] Jeffery mathematically described the motion of a neutrally buoyant ellipsoidal particle immersed in an unbounded fluid subjected to Strokes' flow field. For non-dilute fiber suspensions Folgar and Tucker[54] extended Jeffery's work by introducing a phenomenological Brownian-motion-like term to account for fiber-fiber interactions influencing the degree of fiber alignment. To account for enhanced stresses as a result of inter-particle hydrodynamic interaction, theories of Dinh and Armstrong[66] and Shaqfeh and Fredrickson[67] are commonly used. Despite of many deficiencies of the Folgar-Tucker model due to being based on Strokes' flow for infinitely extended liquids and very crude treatment of fiber-fiber interaction, it has proved itself a very useful tool to calculate fiber orientation distribution in non-dilute rigid fiber suspensions.[53] However, it does not deal with suspensions of flexible fibers. An attempt to

simulate long glass fiber suspension using a modified version of the Folgar-Tucker model produced very little success.[68]

There is only a limited literature concerning the modeling of long fiber suspensions due to the difficulty associated with modeling the dynamics of flexible fiber systems. This difficulty originates from the fact that flexible fibers can no longer be assumed as rigid rods. To bring the effect of flexibility, particle-level simulations are commonly used. In these simulations, the equations of motion for each particle are solved numerically and thus the evolution of the particle's position and orientation is predicted. This method also allows various forms of interactions such as short range hydrodynamic interaction, long range hydrodynamic interaction and fiber-fiber interaction to be accounted for. But the computational resources required to solve the equations of particle motion limits the complexity of the physical model, and therefore its efficacy. Hinch[69] was among the first authors who studied the motion of flexible fiber in shear flow with the assumption of inextensibility and perfect flexibility. Goddard and Huang[70] included the idea of mobility into the Hinch equations for concentrated suspensions. They introduced a mobility tensor which restricted the motion of the fiber in the lateral direction. Yamamoto and Matsuoka[71] modeled flexible fibers as chains of rigid spheres that can bend and twist, and investigated the motion in shear flow. Joung et al.[55] modeled a flexible fiber as a chain of beads joined with connectors. They accounted for the interaction of fibers through both short and long range hydrodynamic interactions and predicted that a more flexible fiber inclusion will produce a more viscous suspension, which they found was consistent with the results of Goto et al.[40]

Switzer and Klingenberg[14] probed the effects of fiber interactions on the rheology of fiber suspensions in simple shear flow through modeling the fibers as linked, rigid spherocylinders

connected by ball and sockets. They considered the interaction between the fibers through short range hydrodynamic forces and interfiber static friction, and concluded that viscosity of fiber suspensions is strongly influenced by the fiber equilibrium shape, interfiber friction and fiber stiffness. Rajabian et al.[72] proposed another approach, where they developed a mesoscopic rheological model of semiflexible fiber suspension to account for the fiber-fiber and the fiber-polymer interactions. For the transient viscosity growth experiments in shear flow, they predicted bigger overshoots for the higher aspect ratio fiber suspensions.

In an attempt to formulate a continuum model similar to Folgar-Tucker model but still capturing the flexibility of the fiber, Strautins and Latz [53] modeled flexible fibers as two rods connected by a bead which allows pivoting, as shown in Fig. 2.1. The model, also referred to as Bead-Rod model, consists of two rigid segments with length l_B that are allowed to slightly pivot about the connecting bead, with some restorative bending rigidity. Both $\vec{p}$ and $\vec{q}$ are unit vectors that represent the orientation of the corresponding fiber segments, with respect to the center bead. Restrictions, associated in the mathematical development of this model, mandate the fiber be only semi-flexible and hence $\vec{q} \cong -\vec{p}$. Additional assumptions used in this development states that the fiber has negligible inertia, inferring that the center of mass of the fiber instantaneously adjusts to changes in solvent velocity, and that the fiber is neutrally buoyant within the suspending medium. Nonetheless, the kinematics and governing Smoluchowski equation are developed for the representative fiber and used to form the following model,

$$\frac{D\underline{\underline{A}}}{Dt} = \underline{\underline{A}}.\underline{\underline{\kappa}}^T + \underline{\underline{\kappa}}.\underline{\underline{A}} - \left[\left(\underline{\underline{\kappa}} + \underline{\underline{\kappa}}^T\right) : \underline{\underline{A}}\right]\underline{\underline{A}} + \frac{l_B}{2}\left[\vec{C}\vec{\mu} + \vec{\mu}\vec{C} - 2(\vec{\mu}.\vec{C})\underline{\underline{A}}\right] - 2k\left[\underline{\underline{B}} - \underline{\underline{A}}\, tr\left(\underline{\underline{B}}\right)\right] \quad (2.13)$$

$$\frac{D\underline{\underline{B}}}{Dt} = \underline{\underline{B}}.\underline{\underline{\kappa}}^T + \underline{\underline{\kappa}}.\underline{\underline{B}} - \left[\left(\underline{\underline{\kappa}} + \underline{\underline{\kappa}}^T\right) : \underline{\underline{A}}\right]\underline{\underline{B}} + \frac{l_B}{2}\left[\vec{C}\vec{\mu} + \vec{\mu}\vec{C} - 2(\vec{\mu}.\vec{C})\underline{\underline{B}}\right] - 2k\left[\underline{\underline{A}} - \underline{\underline{B}}\, tr\left(\underline{\underline{B}}\right)\right] \quad (2.14)$$

$$\frac{D\vec{C}}{Dt} = \underline{\underline{\kappa}}.\vec{C} - \left(\underline{\underline{A}} : \underline{\underline{\kappa}}\right)\vec{C} + \frac{l_B}{2}\left[\vec{\mu} - \vec{C}(\vec{\mu}.\vec{C})\right] - k\vec{C}\left[1 - tr\left(\underline{\underline{B}}\right)\right] \quad (2.15)$$

$$\vec{\mu} = \sum_{i=1}^{3}\left(\sum_{j=1}^{3}\sum_{k=1}^{3}\frac{\partial^2 v_i}{\partial x_i \partial x_k}A_{jk}\right)\vec{e_i} \quad (2.16)$$

Within this model, $\frac{D}{Dt}$ is the material derivative and $\underline{\underline{\kappa}}^T$ is the velocity gradient tensor. The two orientation tensors represent the second moment of the distribution function of the unit vectors, $\vec{p}$ and $\vec{q}$, in the following manner,

$$\underline{\underline{A}} = \int \vec{p}\,\vec{p}\,\psi(\vec{p},\vec{q})d\vec{p}\,d\vec{q} \quad (2.17)$$

$$\underline{\underline{B}} = \int \vec{p}\,\vec{q}\,\psi(\vec{p},\vec{q})d\vec{p}\,d\vec{q} \quad (2.18)$$

where $\psi(\vec{p},\vec{q})$ is the orientation distribution function for an arbitrary two-rod system satisfying the normality condition that $\int \psi(\vec{p},\vec{q})\,d\vec{p}\,d\vec{q} = 1$. As a direct consequence to the bending rigidity, encompassed within the model by the parameter k, the expectancy of a segment orientation (with respect to the orientation distribution function) may be non-zero in general and is accounted for in Eq. 2.15 by the following definition,

$$\vec{C} = \int \vec{p}\;\psi(\vec{p},\vec{q})d\vec{p}\,d\vec{q} \quad (2.19)$$

Lastly, Eq. 2.16 contributes second order derivatives of the velocity field that originate from a Taylor series approximation applied to the bead kinematics. In simple shear flow, for example, all components are zero.

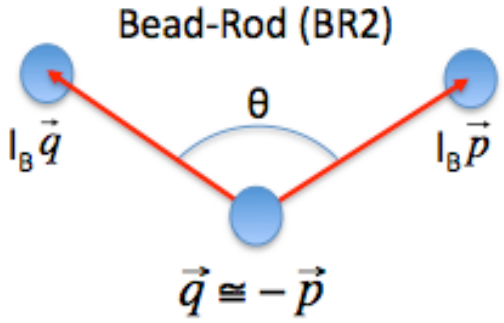

Figure 2.1. Bead Rod model, with segment length $l_{B,}$ allowing semi-flexibility. The segment orientations are denoted by unit vector $\vec{p}$ and $\vec{q}$, and are separated by an angle Θ.[53]

Simulations performed using Bead Rod model have shown some improvement in predicting the evolution of fiber orientation compared to modified Foglar-Tucker model. It should, however, be noted that parameters available within this model should be more precisely determined, and/or fit, in order to get better results. It is, therefore, decided to obtain these parameters from more fundamental flow such as simple shear flow experiments. Transient shear flow experiments discussed in Chapter 4 may be used to fit the model parameters more precisely, and it will become the emphasis of our future work.

2.5 References

1. Petrich, M.; Koch, D., Interactions between contacting fibers. *Physics of Fluids* **1998,** 10, 2111.

2. Sundararajakumar, R.; Koch, D., Structure and properties of sheared fiber suspensions with mechanical contacts. *Journal of Non-Newtonian Fluid Mechanics* **1997,** 73, (3), 205-239.

3. Sepehr, M.; Ausias, G.; Carreau, P., Rheological properties of short fiber filled polypropylene in transient shear flow. *Journal of Non-Newtonian Fluid Mechanics* **2004,** 123, (1), 19-32.

4. Mary, B.; Dubois, C.; Carreau, P.; Brousseau, P., Rheological properties of suspensions of polyethylene-coated aluminum nanoparticles. *Rheologica Acta* **2006,** 45, (5), 561-573.

5. Park, R.; Jang, J., Effect of surface treatment on the mechanical properties of glass fiber/vinylester composites. *Journal of Applied Polymer Science* **2004,** 91, (6).

6. Collings, T., The use of resin hybrids to control moisture absorption in fibre-reinforced plastics. *Composites* **1991,** 22, (5), 369-372.

7. De, S.; White, J., *Short fibre-polymer composites*. CRC: 1996.

8. Neumann, A.; Good, R., Techniques of measuring contact angles. *Surface and colloid science* **1979,** 11, 31-91.

9. Doi, M.; Edwards, S., *The theory of polymer dynamics*. Oxford University Press, USA: 1986.

10. Doi, M.; Edwards, S., Dynamics of rod-like macromolecules in concentrated solution. Part 2. *Journal of the Chemical Society, Faraday Transactions 2* **1978,** 74, 918-932.

11. Batchelor, G., K. 1971 The stress generated in a non-dilute suspension of elongated particles by pure straining motion. *J. Fluid Mech* 46, 813.

12. Doi, M.; Kuzuu, N., Nonlinear elasticity of rodlike macromolecules in condensed state. *Journal of Polymer Science: Polymer Physics Edition* **1980,** 18, (3).

13. Forgacs, O.; Mason, S., Particle motions in sheared suspensions IX. Spin and deformation of threadlike particles. *Journal of Colloid Science* **1959,** 14, 457-472.

14. Switzer III, L.; Klingenberg, D., Rheology of sheared flexible fiber suspensions via fiber-level simulations. *Journal of Rheology* **2003,** 47, 759.

15. Creasy, T.; Advani, S.; Okine, R., Transient rheological behavior of a long discontinuous fiber-melt system. *Journal of Rheology* **1996,** 40, 497.

16. Bird, R.; Armstrong, R.; Hassager, O., Dynamics of polymeric liquids, Vol. 1, Fluid mechanics. *John Wiley & Sons, New York* **1987**.

17. Eberle, A.; Baird, D.; Wapperom, P., Rheology of Non-Newtonian Fluids Containing Glass Fibers: A Review of Experimental Literature. *Ind. Eng. Chem. Res* **2008,** 47, (10), 3470-3488.

18. Cross, M.; Kaye, A., Techniques for the viscometry of suspensions. *Polymer Engineering & Science* **1986,** 26, (2).

19. Anders Ericsson, K.; Toll, S.; Månson, J., Sliding plate rheometry of planar oriented concentrated fiber suspension. *Rheologica Acta* **1997,** 36, (4), 397-405.

20. Giacomin, A. A sliding plate melt rheometer incorporating a shear stress transducer. McGill University, 1987.

21. Powell, R., Rheology of suspensions of rodlike particles. *Journal of Statistical Physics* **1991,** 62, (5), 1073-1094.

22. Sepehr, M.; Carreau, P.; Moan, M.; Ausias, G., Rheological properties of short fiber model suspensions. *Journal of Rheology* **2004,** 48, 1023.

23. Blakeney, W., The viscosity of suspensions of straight, rigid rods. *Journal of Colloid and Interface Science* **1966,** 22, 324.

24. Attanasio, A.; Bernini, U.; Galloppo, P.; Segre, G., Significance of viscosity measurements in macroscopic suspensions of elongated particles. *Journal of Rheology* **1972,** 16, 147.

25. Eberle, A. The Dynamic Behavior of a Concentrated Composite Fluid Containing Non-Brownian Glass Fibers in Rheometrical Flows. Ph.D. Thesis, Virginia Tech, 2008.

26. Mondy, L.; Geller, A.; Rader, D.; Ingber, M., Boundary element method calculations of the mobility of nonspherical particles—II. Branched chains and flakes. *Journal of Aerosol Science* **1996,** 27, (4), 537-546.

27. Thomasset, J.; Carreau, P.; Sanschagrin, B.; Ausias, G., Rheological properties of long glass fiber filled polypropylene. *Journal of Non-Newtonian Fluid Mechanics* **2005,** 125, (1), 25-3

28. Becraft, M.; Metzner, A., The rheology, fiber orientation, and processing behavior of fiber-filled fluids. *Journal of Rheology* **1992,** 36, 143.

29. Leider, P.; Bird, R., Squeezing flow between parallel disks. I. Theoretical analysis. *Industrial & Engineering Chemistry Fundamentals* **1974,** 13, (4), 336-341.

30. Shuler, S.; Advani, S., Transverse squeeze flow of concentrated aligned fibers in viscous fluids. *Journal of Non-Newtonian Fluid Mechanics* **1996,** 65, (1), 47-74.

31. Goddard, J. D., The stress field of slender particles oriented by a non-Newtonian extensional flow. *Journal of Fluid Mechanics Digital Archive* **1976,** 78, (01), 177-206.

32. Laun, H., Orientation effects and rheology of short glass fiber-reinforced thermoplastics. *Colloid & Polymer Science* **1984,** 262, (4), 257-269.

33. Giacomin, A.; Samurkas, T.; Dealy, J., A novel sliding plate rheometer for molten plastics. *Polymer Engineering and Science* **1989,** 29, (8), 499-504.

34. Taylor, G. I., Proceedings Second International Congress on Rheology. **1954**, 1.

35. Nawab, M.; Mason, S., Viscosity of Dilute Suspensions of Thread-like Particles. *The Journal of Physical Chemistry* **1958,** 62, (10), 1248-1253.

36. Chan, Y.; White, J.; Oyanagi, Y., A fundamental study of the rheological properties of glass-fiber-reinforced polyethylene and polystyrene melts. *Journal of Rheology* **1978,** 22, 507.

37. Mewis, J.; Metzner, A. B., The rheological properties of suspensions of fibres in Newtonian fluids subjected to extensional deformations. *Journal of Fluid Mechanics Digital Archive* **1974,** 62, (03), 593-600.

38. Zirnsak, M.; Hur, D.; Boger, D., Normal stresses in fibre suspensions. *Journal of Non-Newtonian Fluid Mechanics* **1994,** 54, 153-193.

39. Kitano, T.; Kataoka, T., The rheology of suspensions of vinylon fibers in polymer liquids. I. Suspensions in silicone oil. *Rheologica Acta* **1981,** 20, (4), 390-402.

40. Goto, S.; Nagazono, H.; Kato, H., The flow behavior of fiber suspensions in Newtonian fluids and polymer solutions. *Rheologica Acta* **1986,** 25, (2), 119-129.

41. Chaouche, M.; Koch, D., Rheology of non-Brownian rigid fiber suspensions with adhesive contacts. *Journal of Rheology* **2001,** 45, 369.

42. Ganani, E.; Powell, R., Rheological properties of rodlike particles in a Newtonian and a non-Newtonian fluid. *Journal of Rheology* **1986,** 30, 995.

43. Bennington, C.; Kerekes, R.; Grace, J., The yield stress of fibre suspensions. *The Canadian Journal of Chemical Engineering* **1990,** 68, (5).

44. Onogi, S.; Mikami, Y.; Matsumoto, T., The rheology of suspensions of titanate fibers in polymer solution. *Polymer Engineering and Science* **1977,** 17, (1), 1-8.

45. White, J., 'A plastic-viscoelastic constitutive equation to represent the rheological behavior of concentrated suspensions of small particles in polymer melts. *J. Non-Newtonian Fluid Mech* **1979,** 5, 177–190.

46. Meyer, R.; Wahren, D., On the elastic properties of three-dimensional fibre networks. *Svensk Papperstidn* **1964,** 67, (10), 432-436.

47. Keshtkar, M.; Heuzey, M.; Carreau, P., Rheological behavior of fiber-filled model suspensions: Effect of fiber flexibility. *Journal of Rheology* **2009,** 53, 631.

48. Wang, J.; O'Gara, J.; Tucker III, C., An objective model for slow orientation kinetics in concentrated fiber suspensions: Theory and rheological evidence. *Journal of Rheology* **2008,** 52, 1179.

49. Eberle, A.; Baird, D.; Wapperom, P.; Vélez-García, G., Using transient shear rheology to determine material parameters in fiber suspension theory. *Journal of Rheology* **2009,** 53, 685.

50. Guo, R.; Azaiez, J.; Bellehumeur, C., Rheology of fiber filled polymer melts: Role of fiber-fiber interactions and polymer-fiber coupling. *Polymer Engineering & Science* **2005,** 45, (3).

51. Tang, W.; Advani, S.; Source, C., Dynamic Simulation of Carbon Nanotubes in Simple Shear Flow. *Computer Modeling in Engineering and Sciences* **2008,** 25, (3), 149.

52. Wang, G.; Yu, W.; Zhou, C., Optimization of the rod chain model to simulate the motions of a long flexible fiber in simple shear flows. *European Journal of Mechanics/B Fluids* **2006,** 25, (3), 337-347.

53. Strautins, U.; Latz, A., Flow-driven orientation dynamics of semiflexible fiber systems. *Rheologica Acta* **2007,** 46, (8), 1057-1064.

54. Folgar, F.; Tucker III, C., Orientation behavior of fibers in concentrated suspensions. *Journal of reinforced plastics and composites* **1984,** 3, (2), 98.

55. Joung, C.; Phan-Thien, N.; Fan, X., Direct simulation of flexible fibers. *Journal of Non-Newtonian Fluid Mechanics* **2001,** 99, (1), 1-36.

56. Bapanapalli, S.; Nguyen, B., Prediction of elastic properties for curved fiber polymer composites. *Polymer Composites* **2008,** 29, (5), 544-550.

57. Joung, C.; Phan-Thien, N.; Fan, X., Viscosity of curved fibers in suspension. *Journal of Non-Newtonian Fluid Mechanics* **2002,** 102, (1), 1-17.

58. Arlov, A.; Forgacs, O.; Mason, S., Particle motions in sheared suspensions IV. General behaviour of wood pulp fibres. *Svensk Papperstidn* **1958,** 61, (3), 61-67.

59. Jeffery, G., The motion of ellipsoidal particles immersed in a viscous fluid. *Proceedings of the Royal Society of London. Series A, Containing Papers of a Mathematical and Physical Character* **1922**, 161-179.

60. Tchen, C.-M., Motion of Small Particles in Skew Shape Suspended in a Viscous Liquid. *Journal of Applied Physics* **1954,** 25, (4), 463-473.

61. Ganani, E.; Powell, R., Suspensions of rodlike particles: literature review and data correlations. *Journal of Composite Materials* **1985,** 19, (3), 194.

62. Kitano, T.; Kataoka, T.; Nagatsuka, Y., Dynamic flow properties of vinylon fibre and glass fiber reinforced polyethylene melts. *Rheologica Acta* **1984,** 23, (4), 408-416.

63. Kitano, T.; Kataoka, T.; Nagatsuka, Y., Shear flow rheological properties of vinylon-and glass-fiber reinforced polyethylene melts. *Rheologica Acta* **1984,** 23, (1), 20-30.

64. Gibson, A., Rheology and packing effects in injection moulding of long-fibre reinforced materials. *Plastics and rubber processing and applications* **1985,** 5, (2), 95-100.

65. Jones, R. S.; Roberts, R. W., Anisotropic shear flow in continuous fibre composites. *Composites* **1994,** 25, (3), 171-176.

66. Dinh, S.; Armstrong, R., A rheological equation of state for semiconcentrated fiber suspensions. *Journal of Rheology* **1984,** 28, 207.

67. Shaqfeh, E.; Fredrickson, G., The hydrodynamic stress in a suspension of rods. *Physics of Fluids A: Fluid Dynamics* **1990,** 2, 7.

68. Phelps, J.; Tucker, C., An anisotropic rotary diffusion model for fiber orientation in short- and long-fiber thermoplastics. *Journal of Non-Newtonian Fluid Mechanics* **2009,** 156, (3), 165-176.

69. Hinch, E., The distortion of a flexible inextensible thread in a shearing flow. *Journal of Fluid Mechanics Digital Archive* **2006,** 74, (02), 317-333.

70. Goddard, J.; Huang, Y., On the Motion of Flexible Threads in a Stokes Shear Field. *J. Non-Newtonian Fluid Mech* **1983,** 13, 47-62.

71. Yamamoto, S.; Matsuoka, T., A method for dynamic simulation of rigid and flexible fibers in a flow field. *The Journal of Chemical Physics* **1993,** 98, 644.

72. Rajabian, M.; Dubois, C.; Grmela, M., Suspensions of semiflexible fibers in polymeric fluids: rheology and thermodynamics. *Rheologica Acta* **2005,** 44, (5), 521-535.

3.0 Sliding Plate Rheometer

A sliding plate rheometer usually consists of two parallel plates separated by a small gap. A simple shear flow is induced in the material kept between the two plates by linear motion of one plate parallel to another. A homogenous flow field insures that the deformation of the fluid is same at every point in the fluid, i.e. there is no shear rate difference within material.

Sliding plate rheometers are either stress-controlled or strain controlled. Classically, shear stress used to be inferred from a measure of total force on the apparent contact area of the sample. But, this method was subject to experimental errors due to free boundary effects. An uncontrollable flow induced by the stress-free condition at the sample boundaries caused large errors in the calculation of shear stress. To overcome these difficulties the use of a wall shear stress transducer, which measures shear stress locally in the region of controllable flow, was suggested.[1]

As discussed later in section § 3.5, a sliding plate rheometer overcomes most of the problems encountered by conventional rheometers during the characterization of rheological behavior of concentrated long fiber suspensions. Hence, it was decided to fabricate a sliding plate rheometer incorporating a wall shear stress transducer. The new device is based on a design initially developed by Giacomin[1,2] and later modified by Daley et al.[3] The following sections give an overview of the fabricated device, design considerations and its operation. Giacomin's Ph.D. thesis[1] has been taken as the primary reference to write this chapter.

3.1 Design

There have been many theoretical concerns which were considered before initiating the design of the sliding plate rheometer. It was imperative to look at various physical constrains

which might affect the proper functioning of the new device. In this section a few of these theoretical concerns are discussed. It is followed by a discussion on several design considerations that have been undertaken during the fabrication of the sliding plate rheometer and accompanying wall shear stress transducer, respectively. A detailed study of other theoretical and design considerations which have not been discussed in this chapter can be found elsewhere.[1]

3.1.1 Theoretical Considerations

This section talks about the two most important theoretical considerations undertaken before designing the sliding plate rheometer. The magnitude of their impact on the performance of the device is also discussed.

3.1.1.1 Viscous Heating. Under deformation, the sample undergoes a temperature rise due to viscous heating. As viscosity is a function of temperature, heat generated through viscous dissipation can alter the flow properties. The maximum temperature difference in the sample can be calculated using the energy equation,[4]

$$\Delta T = \frac{2\eta_s UL}{\rho_p c_p h^2} \tag{3.1}$$

where η_s is the suspension viscosity, U is velocity of the moving plate, L is the characteristic flow length, ρ_p is polymer density, c_p is the heat capacity of the polymer and h is the gap between two plates. Using Eq. 3.1, ΔT is found to be less than 1^0 C for the conditions we operated at. Therefore, it is concluded that viscous dissipation does not have any considerable effect on the viscosity of our materials.

3.1.1.2 Flow due to Gravity. Fig. 3.10 shows that the sliding plate rheometer is mounted vertically to measure the shear rheology of the samples. This could lead to the flow of the fluid due to gravity. However, if the gap size is small enough and viscosity of the fluid is large enough, this flow can be prevented. The maximum velocity, U_{max}, of a Newtonian fluid in a narrow slit caused by gravity is given as,[5]

$$U_{max} = \frac{\rho_p g h^2}{8\eta_s} \tag{3.2}$$

where ρ_p is the density of the fluid, h is the gap distance between the two plates, η_s is the suspension viscosity and g is the acceleration due to gravity. U_{max} for the polypropylene suspension used in the study is less than 0.3 mm/min, which is negligible compared to the minimum speed of the moving plate in this study. Moreover, for a sufficiently viscous fluid, which was the case for the present study, flow due to gravity is nullified by the surface tension.[1]

3.1.2 Design of sliding plate rheometer (SPR)

A new sliding plate rheometer has been fabricated based on the design originally developed by Giacomin et al.[1-2] Fig. 3.1, 3.2 and 3.3 depict an exploded isometric view, a cross-sectional drawing and the assembled drawing of the SPR, respectively. As shown in 3.3, the entire rheometer is housed in a steel structure with holes at the side to allow better heat transfer. A precision bearing table configured within the framework serves as the base for the movable plate of the rheometer. It is connected to an electromagnetic drive system, Instron Model 4204, which moves it at a constant speed or at a constant load. The stationary plate which serves as the housing for a wall shear stress transducer can be bolted into the main frame. 0.5 mm thick brass shims can be inserted into the structure to vary the gap size between the two plates from 0.5 to 3 mm. The rheometer is mounted vertically on Instron and is completely enclosed in an Oven. This

oven incorporates a fan to help keeping the temperature constant though out the oven. A few design considerations that are undertaken during the fabrication of the SPR are discussed below.

3.1.2.1 Material of Construction. The entire rheometer including the shear stress transducer was constructed from stainless steel, which provides the desired structural strength and can sustain large temperature variations. Moreover, constructing the whole device using one material also eliminated any possibility of thermal stresses due to joining materials of different linear expansion coefficients.

3.1.2.2 Effect of thermal expansion. Under high temperatures, thermal expansion can change the gap size between two plates. However, for a stainless steel structure and for brass shims the thermal expansion coefficient is too small. The percentage change in the gap size due to thermal expansion is less than 0.5 % for a 250^0 C temperature change, which can be neglected without any difficulty.

3.1.2.3 Temperature Control. The rheometer is encapsulated in a forced convection oven manufactured by Russells Technical Products (Model RB-2-340). The need of forced convection arises due to the high thermal mass of the shear fixtures and significant heat loss through the drive shafts. It takes too much time to reach thermal equilibrium if only natural convection is relied upon.

It was determined that in 2 hours under forced convection heating, the rheometer reaches the equilibrium temperature close to 200^0 C. However, what is more important is the time to bring the temperature back to equilibrium in case there is a small drop in temperature due to activities such as sample insertion. It takes on average around 2-3 minutes to place the sample in the rheometer before the test can be performed. A considerable amount of heat is lost during this

period due to the exposure to room temperature. Giacomin[1] observed that, for similar circumstances, the time required for the plate temperature to get back to the set point is roughly double of the time taken during sample insertion. The large thermal mass of the fixtures also proves useful as temperature variations are not too big for the small exposure times.

3.1.3 Design of wall shear stress transducer (SST)

A wall shear stress transducer has been fabricated to measure the shear stress locally in a sample. This eliminates any error arising due to uncontrollable flow at shear-free boundaries. One of the other advantages of having a local shear stress transducer is that it prevents problems due to oxidative degradation which are confined to the sample edges for a long period of time.[6] This allows a user to keep the sample inside the oven for more time to bring the temperature to equilibrium, and it also eliminates the need for nitrogen blanketing.

Fig. 3.4 shows a complete assembly diagram of the wall shear stress transducer. US Patent 5,094,100[3] by Dealy and co-workers has been used as a key reference to design this transducer. It is comprised of a rigid lever, a diaphragm, an upper housing and a lower housing, shown in Fig. 3.5 to 3.8, respectively. The rigid lever which has two ends, an active end and a reactive end, is completely surrounded by the upper and lower housing without touching them. A diaphragm connects the middle portion of the lever to the housing, thus suspending it at the center of the transducer. This diaphragm comprises of an outer ring secured to the housing, an inner ring securing the middle portion of the lever and an ‘elastic element’ connecting both the rings. The whole transducer is mounted in the stationary plate of the rheometer and the active face of the rigid lever is positioned flush with the surface on which the shear stress is to be

applied. A small gap is left between the active face and the housing, allowing small deflection of the face in response to shear force.

When a shear stress is applied on the active face, a torsional force bends the elastic element of the diaphragm making the active end of the lever to move in the direction of the stress. This causes the reactive end of the lever to deflect in the opposite direction. A capacitance probe is mounted close to the reactive end of the lever to measure this deflection. When the transducer is properly designed, the deflection of the reactive end, d_r, is proportional to the shear stress,

$$d_r = \frac{\sigma A L_a L_r}{K} \tag{3.3}$$

where σ is the shear stress applied on the active surface, A is the area of active surface, L_a is length of the active arm, L_r is the length of the reactive arm and K is the torsional modulus of elastic member. A few of the considerations that have been undertaken during the design of the SST are discussed below.

3.1.3.1 Effect of gap around the active surface. There is a narrow gap (0.5 mm) around the active face of the lever that allows a little amount of polymer to penetrate inside it. It may affect the dynamic response of the transducer. However, it has been found that the polymer inside the gap only dampens the dynamic response and doesn't make any quantifiable effects on the steady state measurements.[3] Dealy and co-workers in their various publications[7, 8, 9] have shown that this gap has negligible effect on the transducer data, and SST reliably indicates the true shear stress. Dealy et al.[8] cited the work of Bergem,[10] who showed that when the bulk polymer go past an adsorbed layer, even a large groove in the wall has little effect on the flow. In the light of this evidence, it has been assumed that the gap would have little to no effect on the SPR results.

Furthermore, the edge of the active arm has been sharpened, as shown in Fig. 3.5, to increase the effective gap for the damping motion and to minimize the squeezing flow of the polymer in the beam-housing gap.[1,3,11]

3.1.3.2 Lever. When designing the lever for the shear stress transducer, its length and shape are the two main design considerations that are undertaken. It is imperative to have a small gap around the active face to minimize its effect on fluid flow. It can be achieved by keeping d_a small. Since $d_a = d_r L_a / L_r$, it is desirable to have the ratio L_a/L_r to be small. However, it contradicts the criterion for maximum sensitivity for which $L_a = L_r$ is advantageous. In order to keep gap size small and still achieve better sensitivity it is decided to keep the ratio L_a/L_r close to 2.5.

Mechanical vibrations while using the SPR are another cause of concern as this may result in a noisy transducer response. These vibrations are more evident when a forced convection oven encapsulates the entire rheometer. To reduce the effect of these vibrations, the center of gravity of the lever should be on the axis of lever at the location that is mounted to the diaphragm.[3] This could be achieved by designing a lever with a thick active arm and a thinner and larger reactive arm as shown in Fig. 3.5.

3.1.3.3 Diaphragm. The elastic element or the torsional arm of the diaphragm plays an important role in determining the sensitivity of the transducer. It is advantageous to have a highly sensitive diaphragm to achieve better level of accuracy. This can be achieved by reducing the cross-sectional area of the torsional arm, which in turn decreases the value of torsional modulus K. However, other constraints such as beam-housing gap size, viscosity of the polymer and structural strength of the transducer restrict the cross-sectional area of the arm to go below a

certain point. Two diaphragms with different torsional arm cross-section area are designed and shown in Fig. 3.9.

3.1.3.4 Capacitance probe. To measure the displacement of the reactive end, a threaded capacitance probe from Capacitec (Model HPT-75G-E-L2-2-B-D), shown in Fig. 3.4, is chosen. It can be used over a wide temperature range as the dielectric constant of the air doesn't vary too much even with large changes in temperature.[12] It is an offset independent probe for which voltage varies linearly with displacement and thus, there is no need to recalibrate the probe if offset position, i.e. distance between the active area of the probe and the undeflected target, changes. Moreover, the threaded surface of the probe helps in securing the probe in such a way that it doesn't move from its position, either laterally or longitudinally, during the test.

With maximum active end displacement of 0.5 mm, a measuring range of 1.0 mm is required for the capacitance probe. However, in order for the SST to perform better, it was decided to keep the measuring range less than 0.5 mm. With this displacement magnitude, a capacitance probe was required which can accurately measure the displacements up to 1 micron. The capacitance probe used for this work can precisely measure the deflection of 0.5 microns.

3.2 Operation of sliding plate rheometer

This section gives the operating procedure of the newly built SPR. This operating procedure has been refined time and again after various trials, and it is found that following this procedure produces consistent and reproducible results.

3.2.1 Preparation of the sample

The first step before performing the test is to prepare a polymer sample. A fixture of dimensions 150 x 50 mm is used to compression mold the sample of the same length and width. However, the sample's thickness may vary depending on the gap between the two plates of the rheometer. Generally, the thickness of the sample is kept 15-20 % thicker than the gap size. This way it can be squeezed a little while inserting it between the two plates, assuring better polymer-plate adhesion and no-slip while shearing the sample.

3.2.2 Heating the rheometer

If the rheometer is not at the desired temperature, it is heated in a forced convection oven until the thermal equilibrium is reached. During this period the stationary plate is positioned away from the rheometer to allow better heat transfer. It is found that 2 hours of heating is sufficient to bring the equilibrium temperature to 200^0 C. Once the desired temperature is reached, a static calibration can be performed before inserting the sample. However, the calibration step can be skipped if the calibration for the same temperature has been done before.

3.2.3 Inserting the Sample

Precaution must be taken when inserting a sample in the rheometer. It is advisable to wear an elbow length gloves when working at high temperature. When the rheometer is at thermal equilibrium, the prepared sample is carefully placed on the moving plate in such a way that when the stationary plate is fastened back, the active face of SST touches the top portion of the sample center line, still avoiding the ends. Fig. 3.11 illustrates the sample insertion process. The oven is then closed for 5 minutes. Once the thermal equilibrium is reached again, the stationary plate is fastened against the moving plate by hand tightening the bolts. The squeeze flow during the insertion ensures good contact between the sample and plates. The oven is once

again closed for 12 minutes to preheat the rheometer. During this time, a weight of 200 grams is hung on the calibration hook which will be removed before the start of the test. Also the bolts are re-tightened using a hex key after 5 minutes of closing the oven.

3.2.4 Performing a Test

Only simple shear tests are performed on the designed rheometer. The Instron is programmed to move the movable plate at desired constant speed *U*. Applied shear rate can be calculated using

$$\dot{\gamma} = \frac{U}{h} \tag{3.4}$$

where *h* is the gap height between the two plates. As the sample is sheared, the active face of the SST lever deflects with it. As a result, the reactive end of the lever also deflects, but in the opposite direction, causing the voltage in the capacitance probe to vary. This change in voltage is proportional to the displacement of the reactive end with 0.1 mm displacement of the reactive end corresponds to 1 V change in capacitance probe. Signals from the capacitance probe are amplified in a signal amplifier (Capacitec 4100-SL-BNC Amplifier Card) and are sent to a computer using a Data Acquisition Card (National Instruments USB-6008). The computer converts these voltage signals into time versus shear stress data.

3.2.5 Cleaning the Rheometer

Once the test is performed, the oven door is left open for one hour and thirty minutes to let the rheometer cool down. Metal surfaces are then cleaned and the sample is scraped off using brass tools. One advantage of cooling the rheometer before taking out the sample is that the sample can then be preserved to be used for further investigations. Another important thing to remember

when cleaning the rheometer is that there should be no polymer left in the narrow gap around the active face of the SST lever. If some polymer still remains in the gap, the SST should be disassembled and the sample should be taken out before the start of another test.

3.3 Limitations with SPR

There are various limitations concerning the operating variables of the fabricated SPR. Most of these limitations originate from the Instron, sample size or capacitance probe used.

3.3.1 Temperature

Tests can be performed over the wide range of temperatures in the designed SPR because stainless steel can sustain very high temperatures. However, the capacitance probe limits the maximum temperature to 225 ^{o}C.

3.3.2 Shear Rate

The instron limits the minimum and maximum shear rates that can be achieved for the constructed device. The minimum and maximum head speeds for the Instron are 0.0009 and 8.5 mm/s, respectively. It bounds the shear rates between 0.0003 s^{-1} and 17 s^{-1}. SST sensitivity puts a further limit on the minimum shear rate. For the most sensitive transducer used in this study, the minimum shear rate that can be achieved without compromising the accuracy of the device is 0.05 s^{-1}. The maximum shear rate is restricted due to the gap size between the two plates. In order to avoid the wall effects, the gap between two plates is kept at 1.5 mm. This limits the maximum shear rate to 5.6 s^{-1}.

3.3.3 Strain

The length of the sample in the direction of shear and the gap size *(h)* determine the maximum strain that can be obtained from the SPR. As strain $\gamma = D_{max}/h$, where D_{max} is effective length of the sample in the direction of shear motion, it is desirable to have bigger sample and small gap between the plates to maximize the strain. However, the minimum gap size for the fiber filled samples is 1.5 mm and D_{max} for the samples used in this study is 105 mm. This limits the maximum strain that can be achieved to 70 strain units.

3.4 Calibration

The shear stress transducer calibration is a signal output per unit shear stress acting on the active face. As shown in Fig. 3.4 the threaded end of a hook, specifically designed for this purpose, passes through a hole in the upper housing and is threaded to a small hole in the cantilever. This configuration allows weights to be hung directly from the lever at the desired temperature. The hole in the lever is at the same distance from the diaphragm as the active face is from the diaphragm, or, in other words, the force exerted by a weight on the lever is equivalent to applying the same force on the active face of the lever. Series of weights can be hung on the lever to plot the transducer output verses equivalent shear force on active face. Fig. 3.12 shows one such calibration curve for the less sensitive transducer at 150^0 C.

The static calibration procedure discussed above provides a useful mean to perform day to day calibration checks. However, these curves are not so accurate with change in temperature. It is found that calibration using a fluid of known viscosity is a better method to check the calibration. Although tedious, this method gives more accurate calibration results. Fig. 3.13 shows a viscosity growth curve for polydimethylsiloxane (PDMS) of known viscosity at 30 ^{o}C and at a shear rate of 0.2 s^{-1}. The graph illustrates a comparison between viscosity growth tests

performed in the SPR and in a standard cone and plate rheometer, Rheometrics Mechanical Spectrometer (RMS-800). It can be seen that not only the same steady state has been reached in both rheometers, but the stress evolution at the start up of the flow follows the same trend.

Similar comparisons are made for a commercial low density polyethylene (LDPE), Equistar NA 952, which has no processing aids or slip/antiblock agents that might obscure its true melt flow behavior. Viscosity growth curves at shear rates 0.1and 0.5 s^{-1} are shown in Fig. 3.14 and 3.15, respectively. These curves are obtained at the temperature of 150 ^{o}C. The curve at 0.1 s^{-1} is used to obtain the calibration data, and then the same calibration data was used to obtain the other curve. Good agreement between the results from the SPR and the RMS-800 ensures the validity of the newly designed SPR.

3.5 Advantages of sliding plate rheometer when characterizing the rheology of long fiber suspensions

In the previous section it was illustrated that the fabricated device is capable of producing accurate results for Newtonian silicon oils and viscoelastic fluids. Still, it is yet to be emphasized that why SPR is a better device than the ones conventionally used to perform the rheological characterization of concentrated long fiber suspensions. In subsection § 2.2.2 some of these conventional rheometers are discussed with an emphasis on the problems arising due to their geometry, size, flow field and functioning when used to measure the rheological behavior of long fiber suspensions. This presents a need for a rheometer which is sufficiently large[13] and can overcome the limitations imposed by other rheometers.

Unlike conventional rheometers, the SPR has dimensions which are much larger than the physical size of the fibers used in the suspensions. Moreover, the SPR allows localized

shear stress measurements to be carried out, which eliminates typical problems arising from edge effects and oxidative degradation. Rectilinear homogeneous flow fields and sufficient gap size prevent any unwanted fiber-fiber and fiber-wall interaction. The rectangular geometry also facilitates a setting where fibers can be aligned in a preferential direction.

3.6 References

1. Giacomin, A. A sliding plate melt rheometer incorporating a shear stress transducer. McGill University, 1987.

2. Giacomin, A.; Samurkas, T.; Dealy, J., A novel sliding plate rheometer for molten plastics. *Polymer Engineering and Science* **1989,** 29, (8), 499-504.

3. Dealy, J.; Doshi, S.; Bubic, F. Method and apparatus for measuring shear stress, U.S. Patent 5,094,100. 1992.

4. Anders Ericsson, K.; Toll, S.; Månson, J., Sliding plate rheometry of planar oriented concentrated fiber suspension. *Rheologica Acta* **1997,** 36, (4), 397-405.

5. Bird, R.; Stewart, W.; Lightfoot, E., Transport Phenomena. 2002. *John Wiley and Sons Inc*.

6. Szczesniak, A.; Loh, J.; Manell, W., Effect of moisture transfer on dynamic viscoelastic properties of wheat flour/water systems. *J. Rheol.* **1983,** 27, 537.

7. Dealy, J.; Soong, S., A parallel plate melt rheometer incorporating a shear stress transducer. *Journal of Rheology* **1984,** 28, 355.

8. Park, H.; Lim, S.; Smillo, F.; Dealy, J.; Robertson, C., Wall slip and spurt flow of polybutadiene. *Journal of Rheology* **2008,** 52, 1201.

9. Koran, F.; Dealy, J., A high pressure sliding plate rheometer for polymer melts. *Journal of Rheology* **1999,** 43, 1279.

10. Bergem, N., Visualization studies of polymer melt flow anomalies in extrusion. In *Proc. Int. Congr. Rheol., 7th*, Gothenburg, Sweden, 1976; pp 50–54.

11. Soong, S. A parallel plate viscoelastometer for molten polymers. McGill University, 1983.

12. Bell, D., Temperature coefficient of capacitance and of inductance. *Electron. Techn.* **1960,** 37, 342-345.

13. Powell, R., Rheology of suspensions of rodlike particles. *Journal of Statistical Physics* **1991,** 62, (5), 1073-1094.

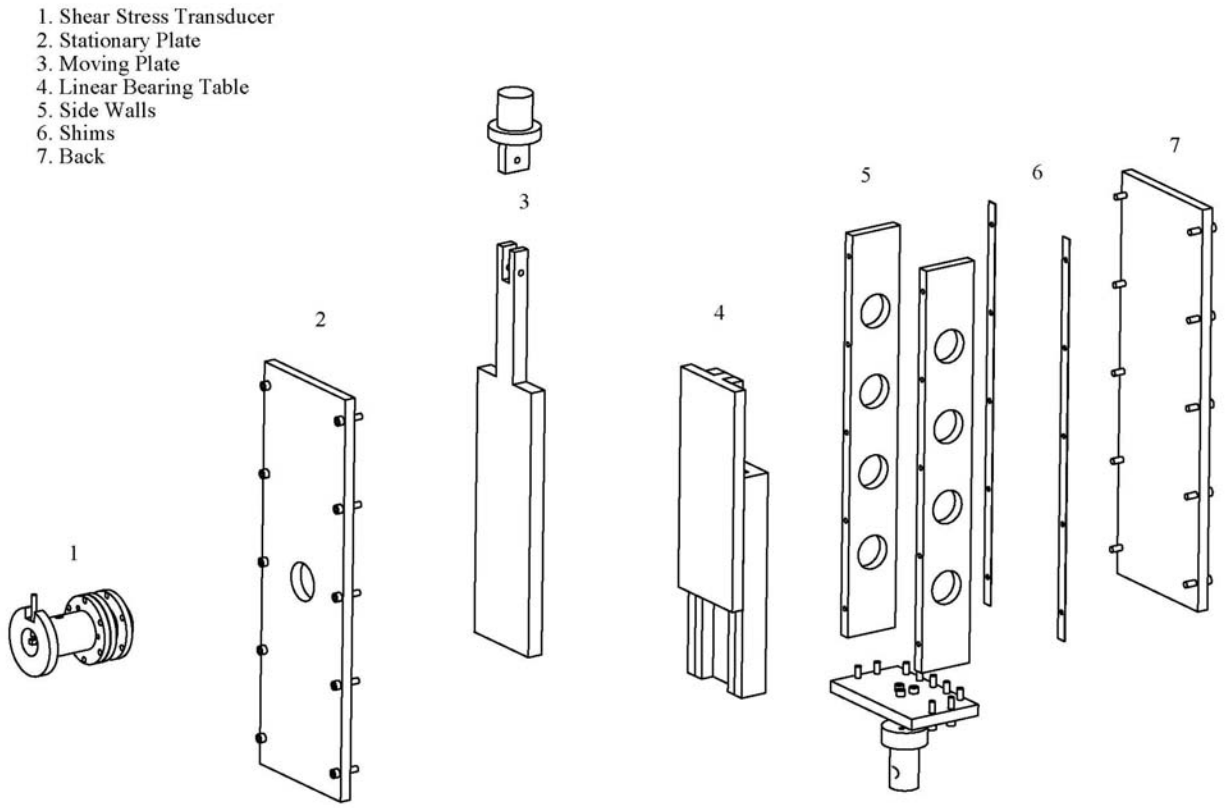

Figure 3.1. Exploded view of the Sliding Plate Rheometer.

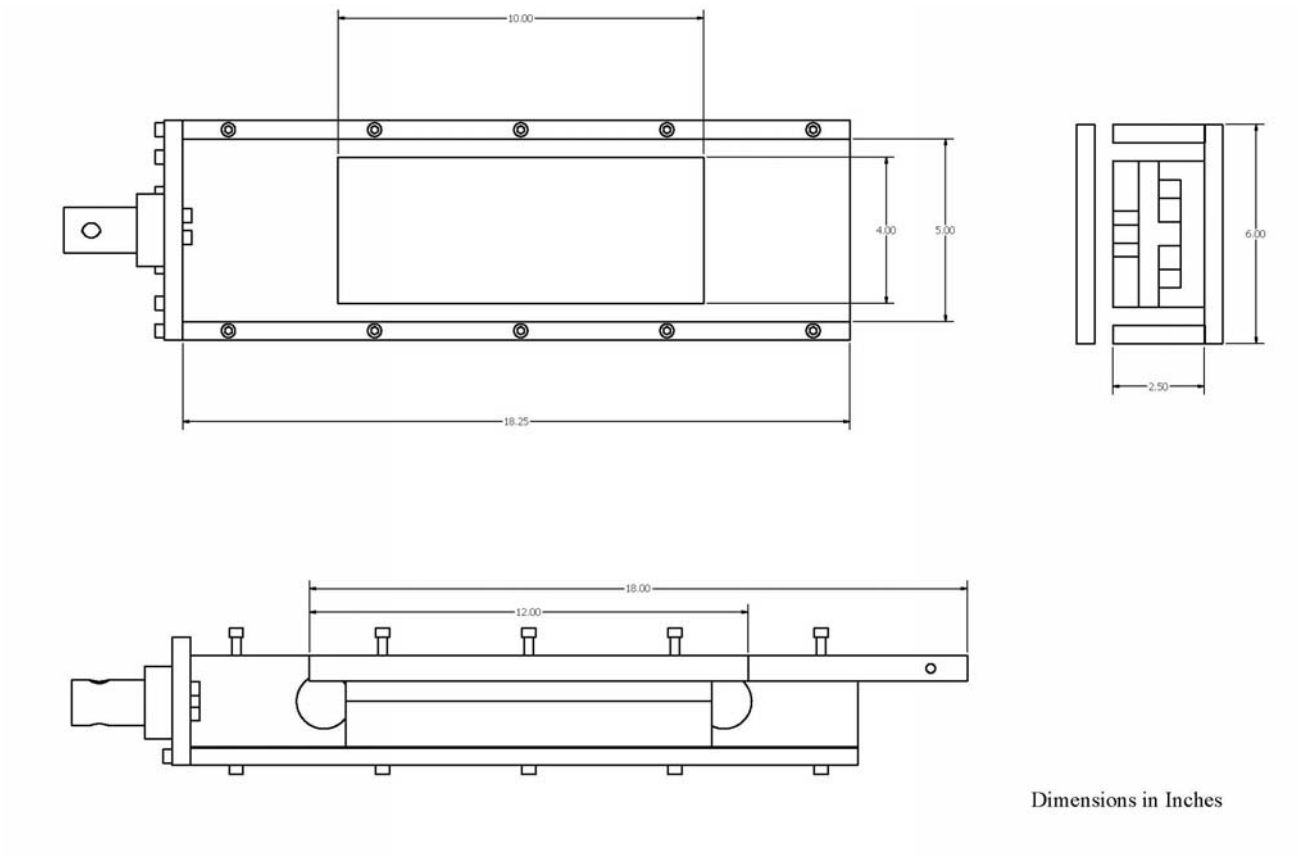

Figure 3.2. Engineering drawing of the Sliding Plate Rheometer.

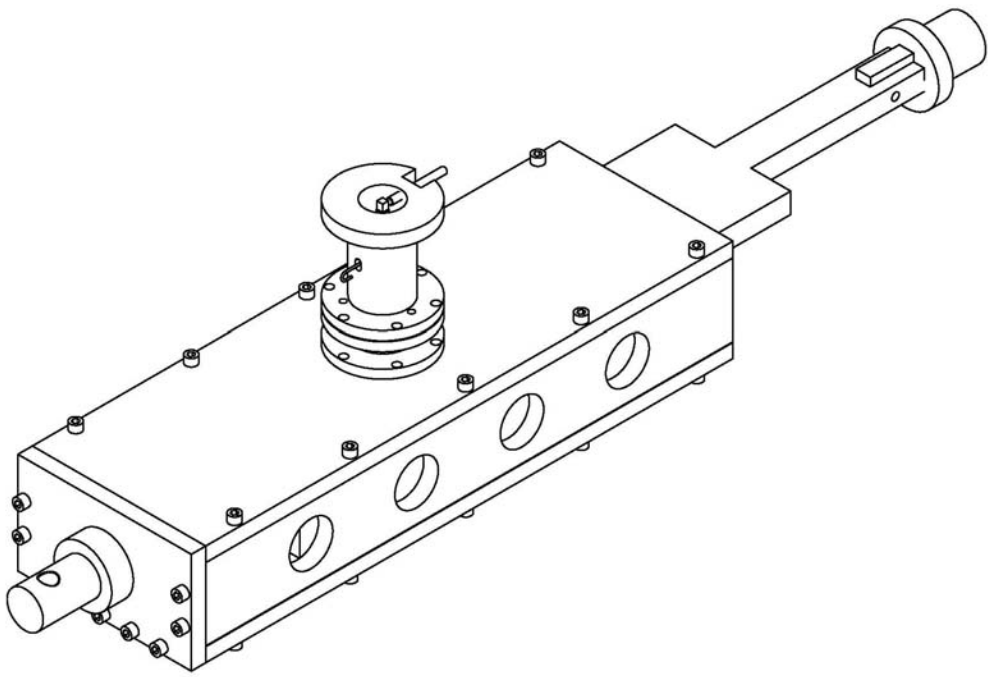

Figure 3.3. Assembled drawing of the Sliding Plate Rheometer.

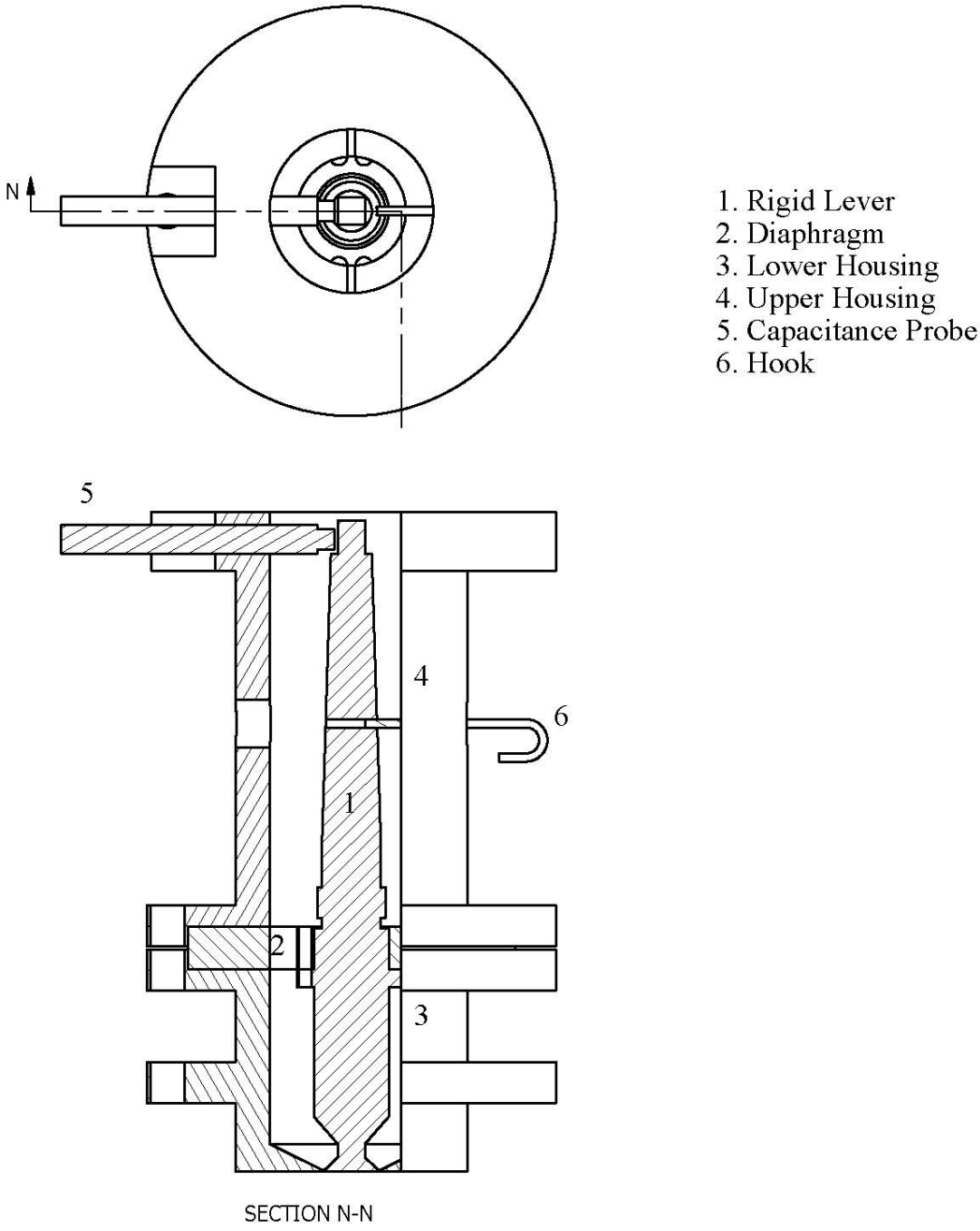

Figure 3.4. One-quarter cross-sectional drawing of the Shear Stress Transducer with a capacitance probe.

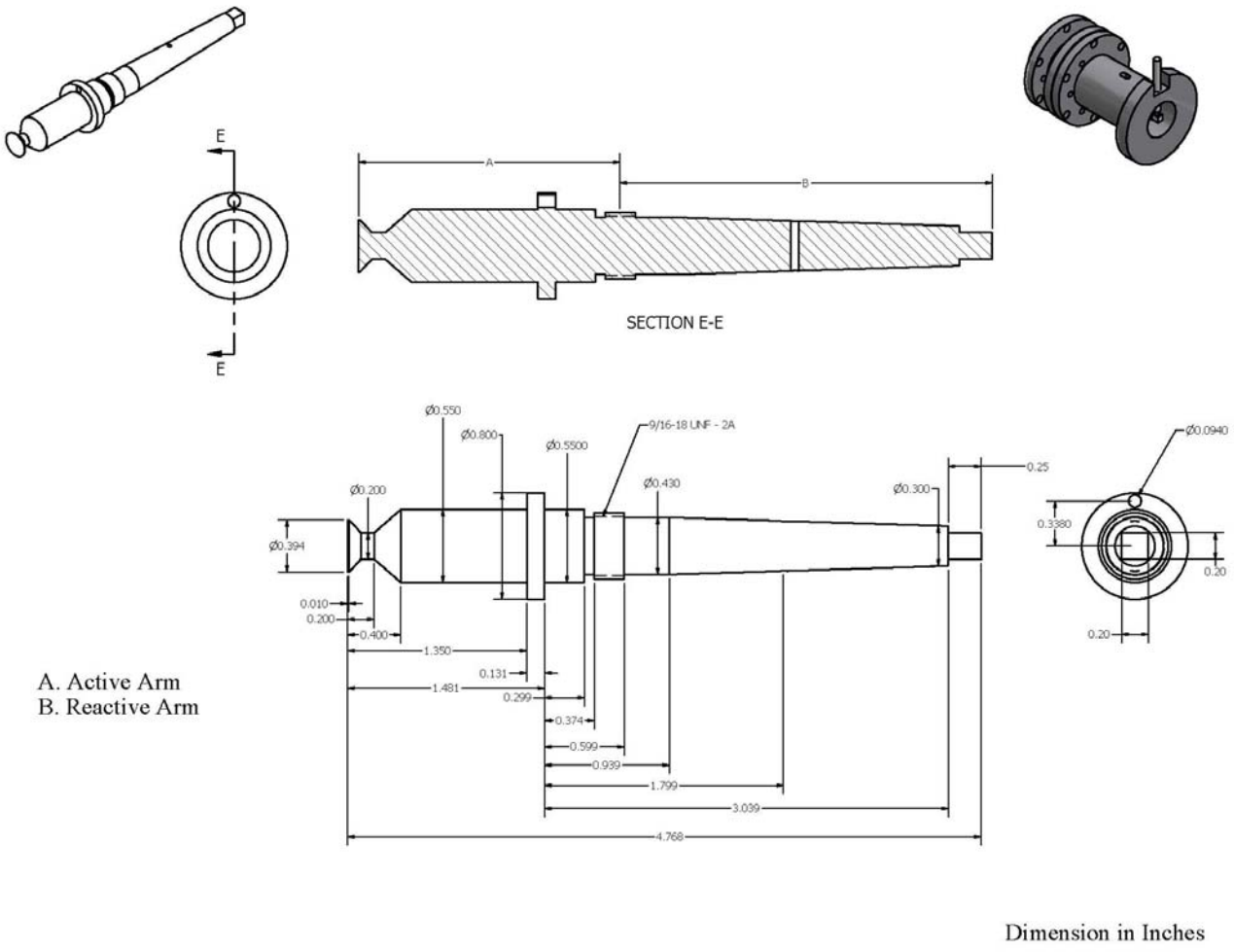

Figure 3.5. Engineering drawing of the Rigid Lever in Shear Stress Transducer.

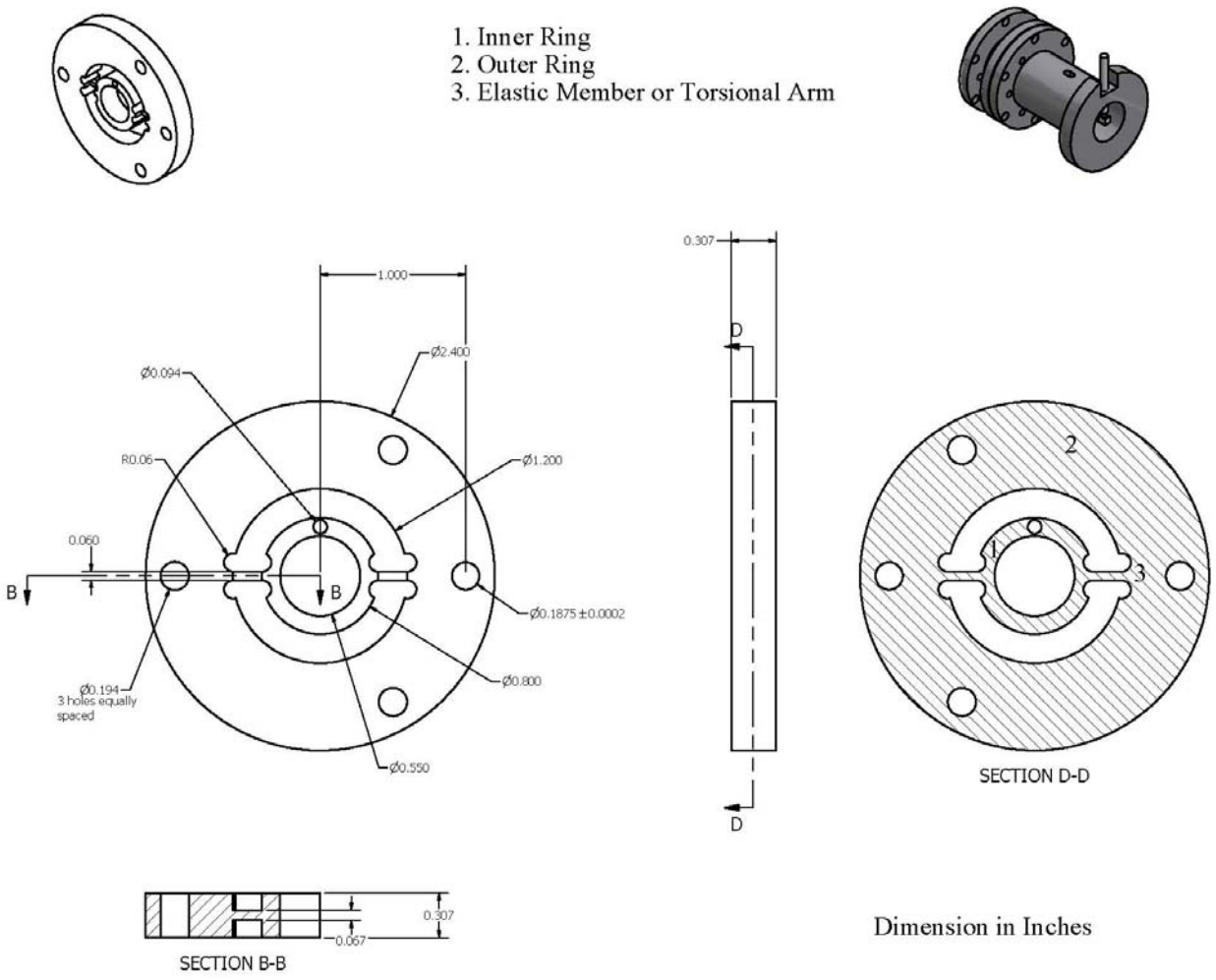

Figure 3.6. Engineering drawing of the Diaphragm in Shear Stress Transducer.

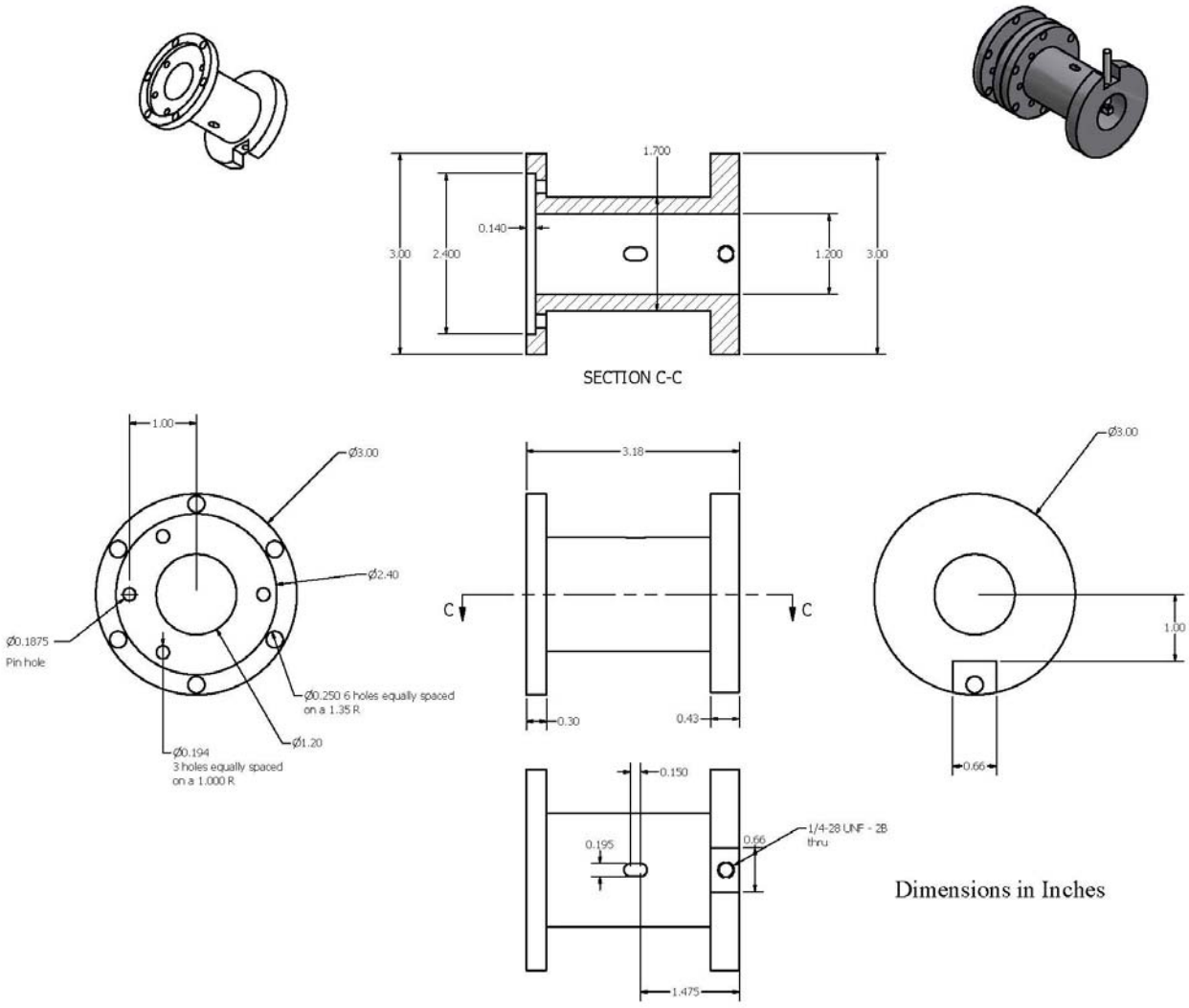

Figure 3.7. Engineering drawing of the Upper Housing in Shear Stress Transducer.

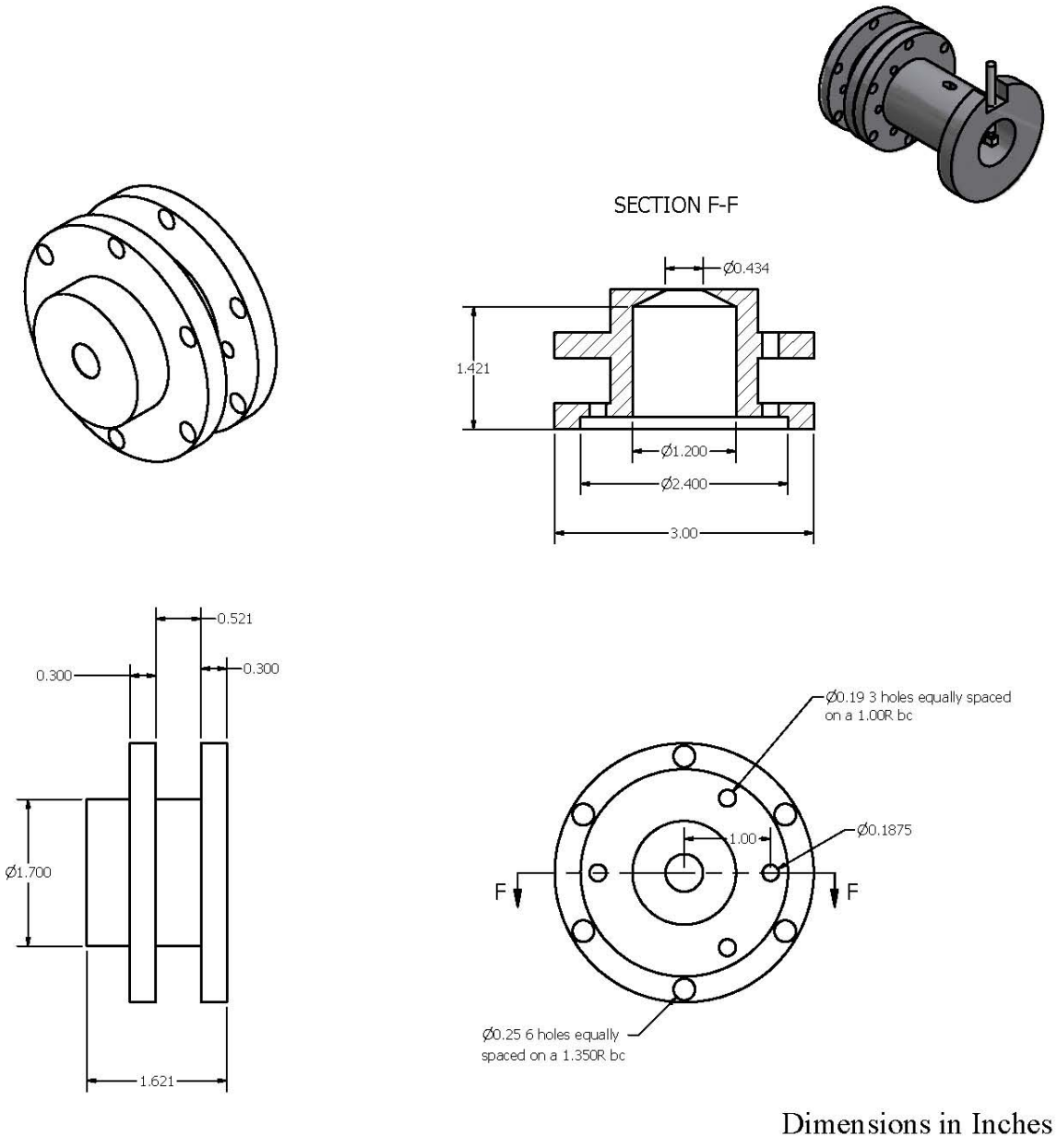

Figure 3.8. Engineering drawing of the Lower Housing in Shear Stress Transducer.

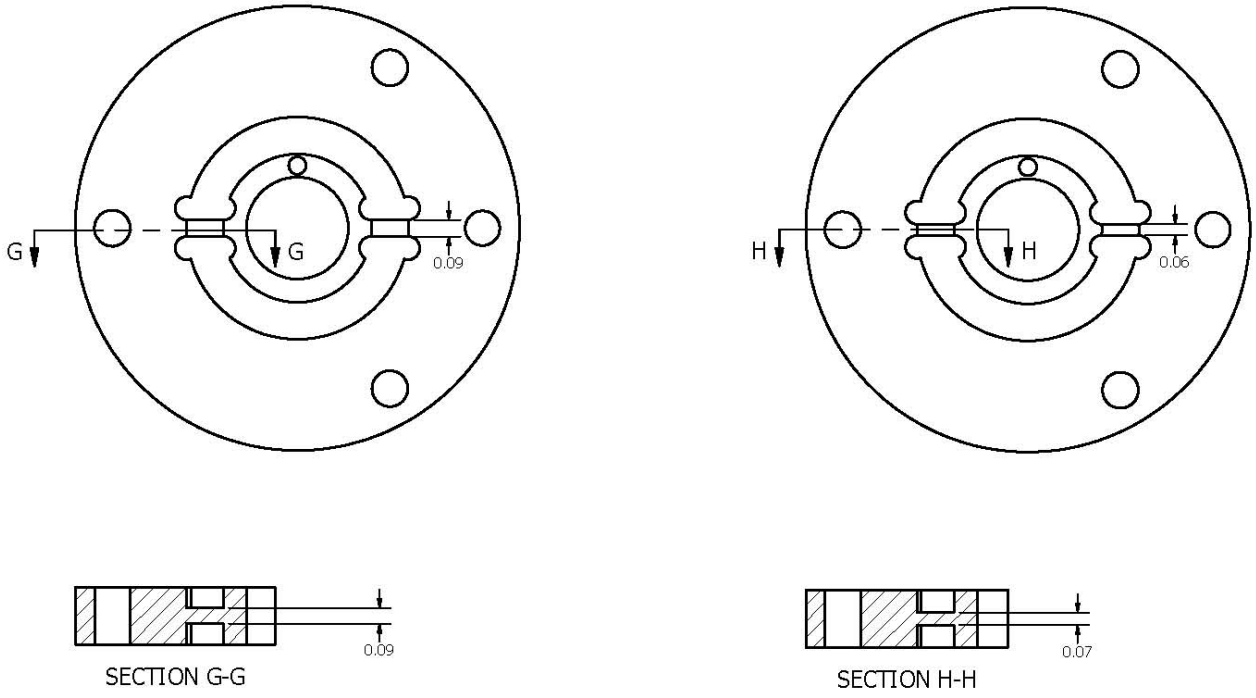

Figure 3.9. Engineering drawing of the two diaphragms with different torsional arm cross-sectional area.

Figure 3.10. Vertically mounted sliding plate rheometer.

Figure 3.11. Author inserting a polymer sample in the sliding plate rheometer.

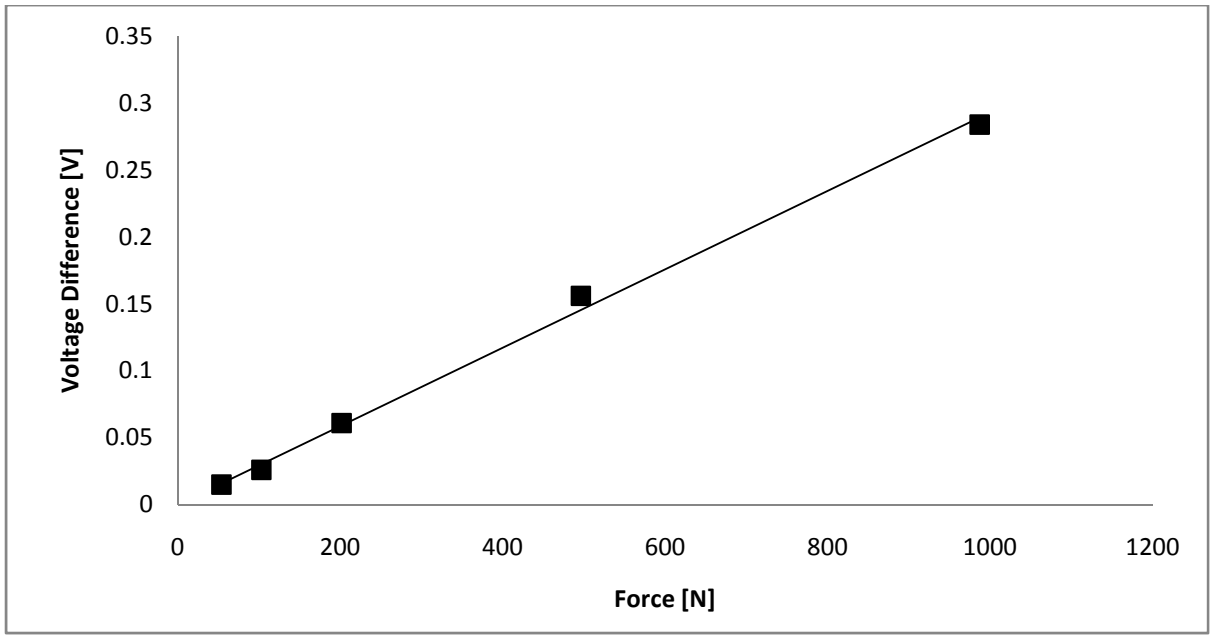

Figure 3.12. Calibration curve for less sensitive transducer.

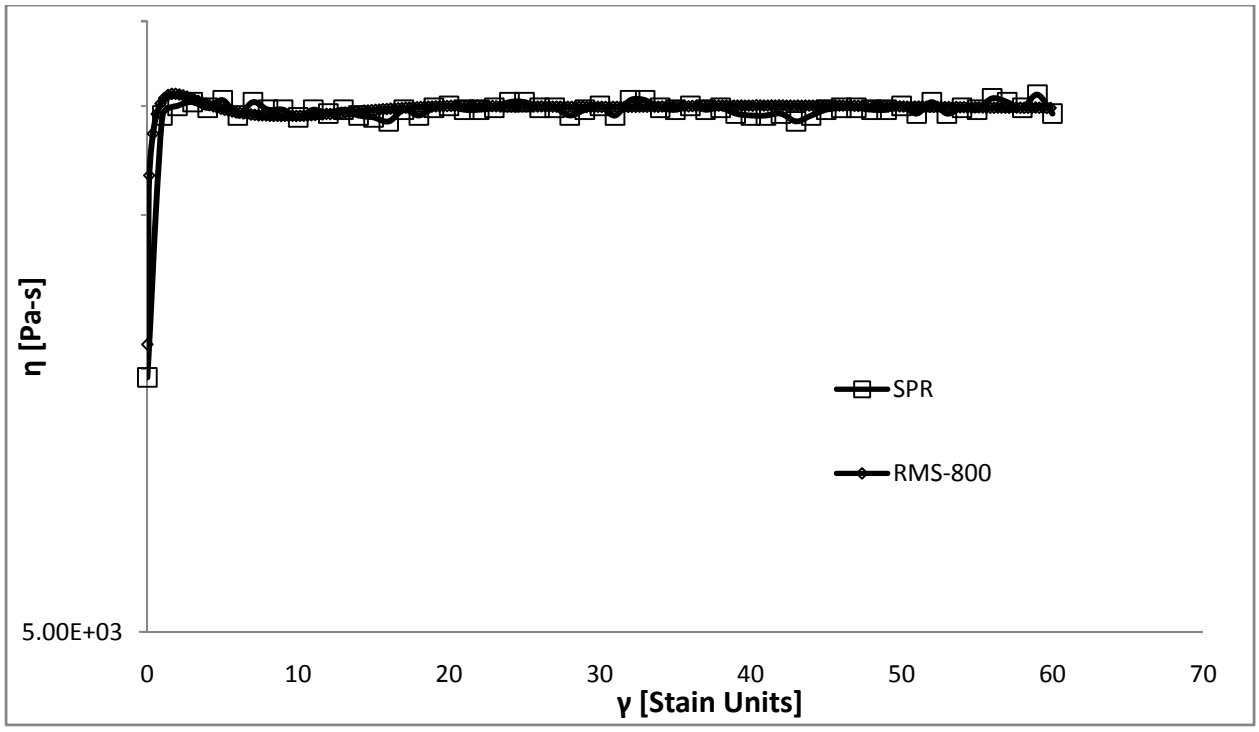

Figure 3.13. Comparison between shear viscosity growth curves obtained from the SPR and the RMS-800 for polydimethylsiloxane (PDMS), at a shear rate of 0.2 s^{-1}.

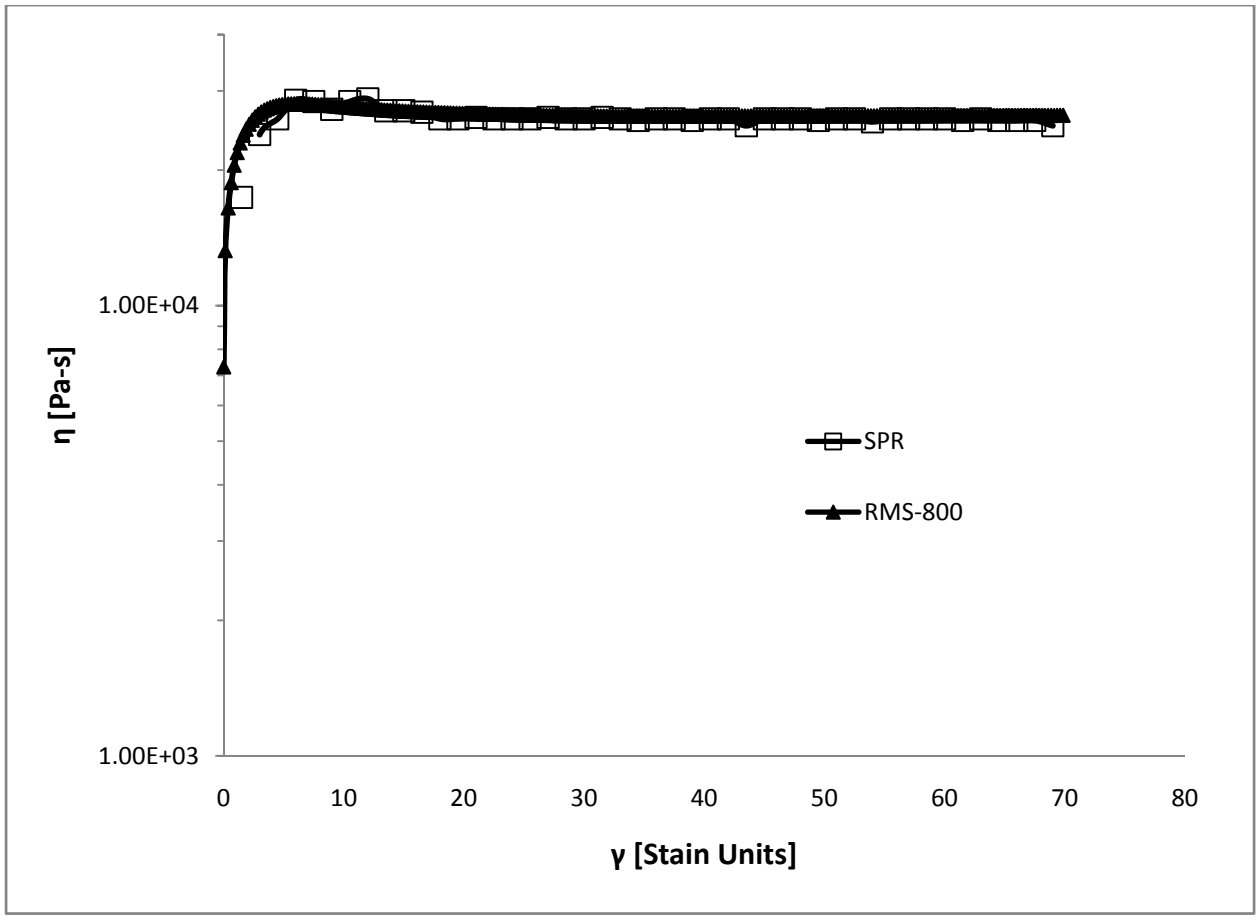

Figure 3.14. Comparison between shear viscosity growth curves obtained from the SPR and the RMS-800 for NA-952, at a shear rate of 0.1 s^{-1}.

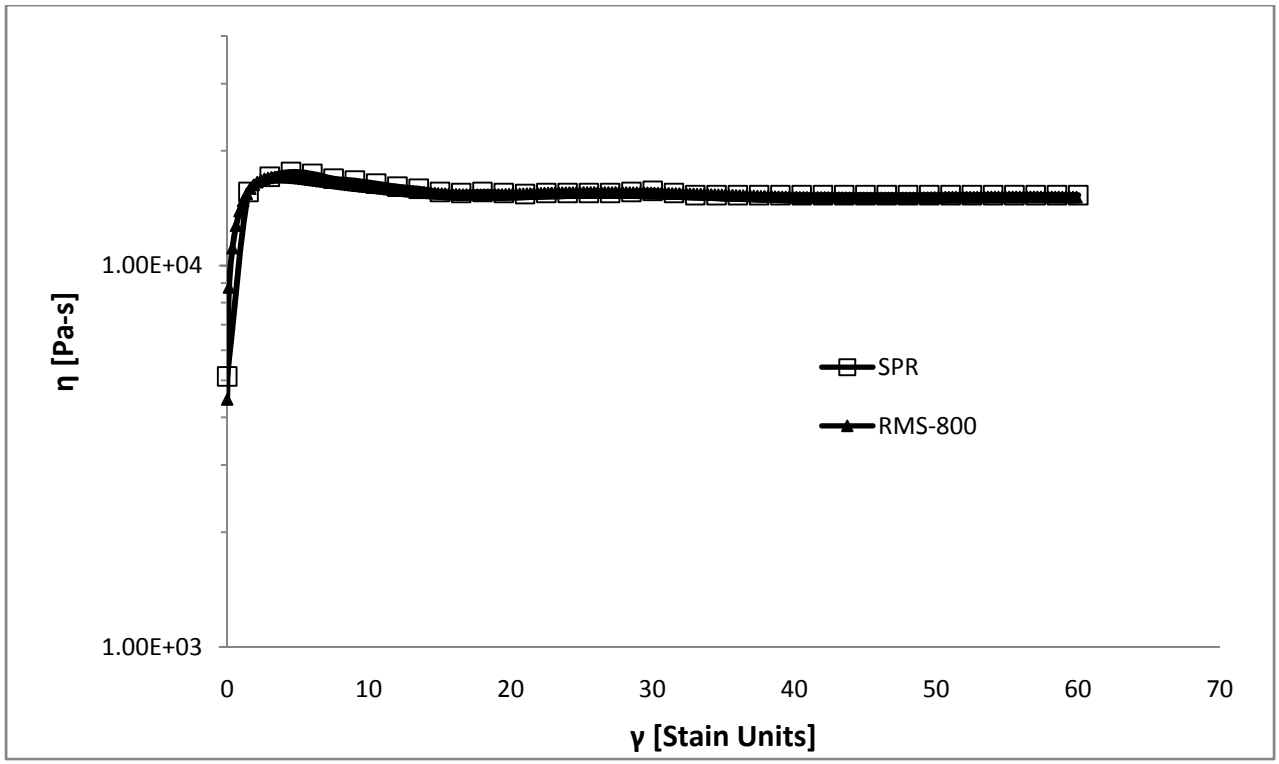

Figure 3.15 Comparison between shear viscosity growth curves obtained from the SPR and the RMS-800 for NA-952, at a shear rate of 0.5 s^{-1}.

4.0 Transient Shear Flow Rheology of Concentrated Long Glass Fiber Suspensions in a Sliding Plate Rheometer

Neeraj Agarwal, Donald G. Baird*, Aaron P. R. Eberle

Department of Chemical Engineering

* Author to whom correspondence should be addressed; email: dbaird@vt.edu

4.1 Abstract

Transient viscosity growth measurements at the startup of shear flow were performed on long glass fiber-filled polypropylene. Samples were prepared with fibers pre-oriented either in 1-direction, 3-direction or random in 1-3 plane, where the 1-direction is the direction of shear motion, the 2-direction is perpendicular to the shear plane and the 3-direction is the neutral direction. A sliding plate rheometer incorporating a shear stress transducer was constructed in the lab. It was shown that this device works well for the tested materials including a Newtonian oil, a low density polyethylene (LDPE) and short glass fiber-filled polypropylene. The transient viscosity growth behavior for long glass fiber suspensions was subsequently investigated. The results suggested that both, fiber length and fiber concentration have pronounced effect on the steady state suspension viscosity. It was also observed that the transient behavior of the pre-oriented samples was highly dependent on the initial orientation state of the fibers.

4.2 Introduction

Long glass fiber composites exist in many forms. Among them the best known materials are Glass Mat Thermoplastics (GMTs), containing continuous or discontinuous glass fibers. The GMT materials have been in use for many decades and are proven in challenging applications,

such as car underbody shields, front-end mounting units and seat shells.[1] They are usually moulded using compression molding process and give good mechanical strength in all direction because of their web-like structure. However, the requirement to design more intricate parts has shifted the focus to the materials, such as fiber-filled granulates which can be easily processed in conventional equipments, e.g. extruder and injection molder. Fair dispersion of fiber in every section of the designed part allows stresses to be distributed throughout the part and results in a fiber composites that exhibit a unique balance of high performance properties.[2] For this reason fiber-filled composites are progressively replacing the conventional materials in various industries, such as automobile, building construction and transportation as they offer light weight material, low production cost and improved mechanical properties.[3]

Length of the fibers in these granulates is one of the major factors that determines the mechanical properties in the final part. It is well known that maximizing the fiber length contributes significantly to the composite strength.[2,4,5] Comparison between long fiber composites (LFC) and short fiber composite (SFC) shows improvements in stiffness, strength, and toughness for LFCs.[6] Furthermore, considerable increase in fatigue endurance, creep and impact strength is also observed for composites containing large aspect ratio fibers.[7,8]

Apart from fiber length, physical properties of fiber-filled polymers also depend on the concentration, type, size and most importantly orientation of reinforced fibers.[9,10] During the processing, fibers change their orientation state within the matrix which influences their mechanical properties. [3,11,12,13] A composite is much stiffer along the direction to which fibers are aligned, while it is more compliant in other directions.[13] This flow induced fiber orientation greatly emphasizes the importance of rheological properties in determining the mechanical properties of the fiber composite. A better understanding of the flow characteristics could be

instrumental in optimizing the processing conditions for fiber composites in order to obtain desired mechanical properties.[14,15,16] Hence, a study of rheological behavior of long fiber suspensions and its connection to fiber orientation as determined in simple flow is of significant relevance.

Rheology of long fiber suspensions is quite complex because of various factors such as fiber-matrix interaction, fiber-fiber interaction, fiber migration and fiber breakage during processing.[3] These factors become more prominent in high concentration regimes for which the volume fraction of fibers $\varphi \geq a_r^{-1}$, where a_r is aspect ratio of the fiber. As fibers flow in close proximity to each other, the possibility of encountering enhanced hydrodynamic forces, friction and other mechanical interactions between fibers increases.[9] These complexities make study of the rheological properties of concentrated long fiber suspensions more challenging.

Fiber flexibility is another factor that plays an important role in determining the rheological behavior of long fiber composites. Because the fiber length in these materials is more than a critical value they, unlike short fibers, do not remain straight and change their curvature under flow deformations. Typically, for glass fibers this critical value is assumed to be 1 mm. Flexibility of the fiber varies with the intrinsic properties of the fiber, its aspect ratio and strength of the flow field.[12] If the fibers are flexible enough then bending forces acting on fibers through velocity field can influence the orientation state of the fibers,[11] which in turn can influence the macroscopic properties of the fluid. As a result, fiber flexibility has shown to be responsible for a considerable increase in suspension viscosity.[16,17,18]

There exist only a limited literature devoted to experimental studies of the rheology of long fiber composites due to the complex nature of these materials and the difficulties that are

encountered during their rheological characterization. Forgacs and Mason[19] investigated the role of fiber length on rotation period of fibers in dilute fiber suspensions. They found that as the apparent aspect ratio decreased due to bending of fibers, it shortened the period of rotation. Tchen[20] showed that curvature of fibers greatly influences the drag applied on it while moving in a viscous medium.

Many experimental results have emphasized the role of flexibility on fluid viscosity. Nawab and Mason[21] in their study of thread like particles in castor oil, found the viscosity becomes more and more shear dependent with increase in fiber length. They expected this behavior was due to elastic deformation of fibers. Blakeney[22] showed that even a 'slight curvature' of fibers has a pronounced effect on the viscosity. Kitano el.al.[23, 24] and Goto et.al.[25] illustrated the effect of fiber stiffness on the suspension rheology. They showed that more flexible fibers had a more pronounced effect on rheological properties.

Becraft and Metzner[26] concentrated their efforts on the effect of fiber volume fraction on suspension rheology. They showed a significant increase in viscosity with increased fiber loading at low shear rates, but only a small increase in viscosity at high shear rates. Thomasset et.al.[27] in a similar study on polypropylene based long fiber suspensions observed an increase in shear viscosity with the increased fiber content and fiber length, however, this viscosity rise was very small which they attributed to high shear rates and fiber breakage during the processing. Non- Newtonian fluid characteristics, such as shear thinning were also observed.

In a recent study, Keshtkar et.al.[28] investigated the effect of two fiber flexibility parameters, stiffness and aspect ratio, in semi-dilute and semi-concentrated regimes. They found a significant increase in steady-state shear viscosity in the semi-concentrated regime compared to

the semi-dilute regime. Viscosity of these suspensions also increased considerably with fiber flexibility. They found that in both the regimes, the addition of fibers results in significant normal forces under shear flow, and as the fiber content increases, the first normal force increases with it. Keshtkar and co-workers are also among the very few authors to observe transient stress growth behavior for long fiber composites. Stress growth experiments were carried out in the forward as well as in the reverse flow directions and shear stress overshoots were observed at the start of the forward flow which they attributed to the fiber orientation under flow. They also found that the width and magnitude of the overshoot increased with increasing fiber flexibility.

Traditionally, capillary and rotational rheometers have been used to characterize the rheological behavior of concentrated long fiber composites. However, there are certain limitations associated with these rheometers which makes them undesirable to perform rheological measurement on fiber suspensions. Rotational rheometers which are generally used at low shear rates employ two geometries, cone-and-plate (CPR) and plate-and-plate (PPR). Viscosity measurement are made utilizing the entire sample area of the sample which makes results susceptible to edge phenomena, e.g free boundary effects, flow instabilities and thermal oxidation.[29] This may severely affect the outcome for fiber-filled systems and may also reduce the maximum shear rate that can be achieved.[30] In the case of PPR the shear rate varies from center to the outer boundary which results in an inhomogeneous shear field. Since the rate of rotation of fibers depends on shear rate it is quite possible that this could result in increased fiber-fiber interaction giving rise to unnecessary stress overshoots.[31] In general, CPR provides a homogeneous shear field but the gap between plates varies from center to the outer edge, this can disrupt the fiber packing and may impart an unwanted flow history on sample as it is squeezed to

required gap dimensions.[31,32] Boundary interactions may also severely affect the rheology if the gap between plates is small compared to fiber characteristic length.

Capillary rheometers, on the other hand are mostly used to investigate the deformation behavior of long fiber-filled suspensions at very high shear rates that are out of reach of rotational devices. But like rotational rheometers they too present certain limitations. Studies[33] have shown that, in laminar flow, migration of fibers may occur across the streamlines, away from the capillary wall. This can reduce the fiber concentration at the boundaries of the capillary resulting in a stress response similar to pure matrix. Additionally, there is considerable fiber breakage that occurs during the extrusion of fibers through the capillary.[26,27] At this point there is no way to account for effect of fiber migration and fiber breakage on the rheological results.

Few attempts have been made to overcome some of the problems encountered with conventional rheometers. Jones and Roberts[34] utilized a linear oscillator to perform an experimental investigation of the dynamic behavior of an aligned continuous fiber suspension. They measured both longitudinal as well as transverse viscosity of unidirectional fiber suspension. Shuler and Advani[35] developed an experimental approach to utilize squeeze flow in order to more accurately resemble the real processing of composite sheet laminates.

A sliding plate rheometer (SPR) incorporating a shear stress transducer (SST) is another device which has proven itself as a very useful tool to overcome the limitations posed by capillary and rotational rheometers. It was first developed by Giacomin et al.[30,36] Later, in the various publications by Dealy and co-workers,[37,38,39] it has proven itself as a trustworthy tool to measure rheological properties of polymer melts. Laun[40] utilized a similar device called sandwich rheometer to obtain creep curves for fiber-filled polymer samples, having different

initial fiber orientation. Ericsson et.al.[29] were the first authors who employed SPR to characterize the shear response of concentrated planar long fiber suspensions.

The SPR, unlike conventional rheometers, has dimensions which are much larger than the physical size of the fibers used in the long fiber suspensions. SST allows localized shear stress measurements to be carried out, which eliminates typical problems arising from edge effects and oxidative degradation.[29] Rectilinear homogeneous flow fields and sufficient gap size prevent any unwanted fiber-fiber and fiber-wall interaction. The rectangular geometry also facilitates a setting where fibers can be aligned in a preferential direction. After a careful consideration of its advantages it was decided to construct a SPR in the lab in order to characterize the rheological behavior of concentrated long glass fiber suspensions. The new fabricated device is based on a design initially developed by Giacomin et al.[30,36] and later modified by Daley et al.[41]

The goal of this research is to develop a mean to obtain the transient rheological behavior of long glass fiber suspensions in concentrated regime as a function of fiber concentration, fiber aspect ratio and intitial fiber orientation. Transient experiments are of interest due to the connection between fiber orientation and transient stresses. Researchers[42,3, 43] have tried to determine the parameters for models predicting the fiber evolution and stress generated during flow, by fitting model predictions to transient rheological experiments in simple shear flow. However, most of the modeling work is performed for short fiber-filled suspensions. There is only a limited literature concerning the modeling of long fibers suspensions due to the difficulty associated with modeling the dynamics of flexible fiber systems. To bring the effect of flexibility, many authors[44,45,46,16,15] have used particle-level simulations. But these models are usually computation intensive and resources required to solve the equations of particle motion

limits the complexity of the physical model. In an attempt to formulate a continuum model capturing the flexibility of the fiber, Strautins and Latz [11] modeled fibers as two rods connected by a bead which allows pivoting. The model is also referred to as Bead-Rod model. By adopting a similar approach as for short fiber-filled suspensions, the simple shear flow experiments performed in this study can be utilized to obtain parameters for models, such as Bead-Rod model, by fitting the model predictions to the transient shear rheological experiments. However, this model fitting is out of scope of this work.

4.3 Experimental

4.3.1 Materials

Two different fiber-filled systems were used for this study. First, a 30 wt % chopped short glass fiber-filled propylene (SGF-30), provided by RTP Company under the commercial name RTP 105, was used to examine the performance of fabricated sliding plate rheometer (SPR) with fiber-filled systems. SGF-30 was processed by passing it through the extruder section of an Arburg Allrounder 221-55-250 injection molder at 200 rpm. The extrudate was collected and pelletized. The pellets were then compression molded in an appropriate mold for rheological testing. To characterize the fiber length of the glass fibers, pyrolysis was perfomed on the extrudate at 500 ^{o}C to separate the fibers from the matrix. An image analysis code was written in MATLAB to measure number average (L_N) and weight average length (L_W) of 1500 randomly chosen fibers. The L_N and L_W were found to be 0.350 and 0.403 mm, respectively.

Five different samples of long glass fibers in polypropylene with two different fiber lengths and three different fiber concentrations were used to study the effect of fiber concentration and fiber aspect ratio. The long fibers in the materials provided by SABIC

Innovative Plastic had initial concentration of 30 wt %. Table 4.1 lists all five long fiber composites used in this study. Different concentrations were accomplished by compounding the correct amount of long fiber granules with pure matrix in the extruder section of the injection molder at 200 rpm. Processing though the injection molder ensured adequate dispersion of fibers and the extrudate was collected from the nozzle of the extruder in the form of long stands. The initial fiber length was reduced severely during the processing and it was found that after extrusion the materials containing 13 mm long fibers had L_N and L_W as 4.22 and 7.48 mm, respectively, while for materials containing 8 mm long fibers L_N and L_W were reduced to 3.32 and 5.33 mm, respectively. To obtain these average lengths, around 1800 fibers were inspected employing the image analysis code. Precautions were taken to minimize the degree of thermo-oxidative degradation of polypropylene matrix by drying the materials at 90 ^oC for at least 4 hours in a vacuum oven before extruding them.

After the extrusion process, long glass fiber samples, having different initial fiber orientation in the shear plane, were prepared. These samples had fibers initially oriented either in 1-direction, 3-direction or random in 1-3 plane, and are referred to as D1, D3 and DX samples, respectively in the paper. Fig. 4.3 designates the 1 and 3 directions with respect to the direction of shearing motion. To fabricate these pre-oriented samples, extruded material was collected in the form of long strands where fibers were mostly orientation along the direction of the strand. These strands were then cut into either 150, 50 or 15 mm long pieces. The D1 samples were prepared by laying the 150 mm pieces parallel to each other in the long direction of a 150 x 50 mm mold and then compression mold them. Similarly, D3 samples were prepared by laying 50 mm pieces of the strands in the other direction of the mold. The samples having fiber oriented randomly in 1-3 plane are fabricated by randomly distributing the 15 mm pieces of the extruded

stands in the mold and then compression mold them. During the compression molding process a minimum pressure was applied to make sure that the initial fiber orientation is not disrupted. All the samples thus prepared, had the dimensions of 150 x 50 x 1.70 mm. However, the thickness varied between 1.6 mm to 1.8 mm. Tests on the long glass fiber-filled suspensions were performed at 185 ^{o}C

To check that the fibers are oriented in the desired direction, a sample where fibers are pre-oriented in the 3-direction was cut along the 1-2 plane and the cut surface was metallographically polished. The polished plane was then viewed under the microscope and the produced image can be seen in Fig. 4.1. Here the fibers are shown in white and the surrounding matrix is in black. This figure qualitatively verifies that the fibers do orient themselves along the direction of the strands and they, subsequently, can be arranged in a preferential direction in a rectangular geometry.

Table 4.1 Materials used in the study

Material	SGF-30	LGF13-10	LGF13-20	LGF13-25	LGF8-10	LGF8-20
Fiber wt. %	30	10	20	25	10	20
Fiber vol. %	17.6	3.8	8.2	10.6	3.8	8.2
Fiber length before extrusion (mm)	-	13	13	13	10	10
Fiber diameter (microns)	13	17	17	17	17	17

4.3.2 Rheological Measurements

Rheological measurements were performed using two different rheometers: a Rheometrics Mechanical Spectrometer (RMS-800) with cone-and-plate fixture and a sliding plate rheometer. The results from the RMS-800 were mostly used for the comparison purpose in order to validate the performance of the sliding plate rheometer. A 25 mm cone and plate fixture with cone angle of 0.1 radians was used to perform experiments on pure resins. Rheological measurements on the

SGF-30 were performed on a 50 mm cone and plate fixture having a same cone angle of 0.1 radians. Donut shaped samples, shown in Fig. 4.2 as proposed by Eberle et al.,[47] were used to eliminate the interaction of fibers with the plate walls near the center of the plates where the rheometer gap is small compared to fiber length. For such samples, sample disks were pre-formed using compression molding and a 25.4 mm diameter hole was drilled through the center. A detailed discussion on the donut sample design and testing can be found elsewhere.[47] After each experiment the void space at the center was measured to account for sample loading as the gap was adjusted to proper dimensions. The hole diameter varied slightly, 24.0 $\pm$ 0.4 mm, and was accounted for when calculating the stresses for each run. The shear viscosity $\eta(t)$ was calculated as a function of torque $T(t)$ required to rotate the upper disk from the following equation,[48]

$$\eta(t) = \frac{3T(t)}{2\pi R^3 \dot{\gamma}} ({R_o}^3 - {R_i}^3)^{-1} \quad (1)$$

where R_o and R_i are the outer and inner radii of the final sample, respectively. The experimental reproducibility of the viscosity measurements was found to be within $\pm$ 5%.

The sliding plate rheometer used in this work was fabricated based on the design initially developed by Giacomin[30] and later modified by Dealy et al.[41] Fig. 4.3 shows a schematic diagram of the shear stress transducer including the bottom moving plate and the inserted polymer sample. The apparatus is encased in a forced convection oven (Russells Technical Products, Model RB-2-340) and is mounted vertically in an electromagnetic drive system, an Instron-4204. The Intron can be programmed to drive the moving plate (A) at a desired speed. Once the plate is set into motion, the melt (B), which is kept between the moving and the

stationary plate (C) is sheared homogeneously. The resulting shear stress is measured using a shear stress transducer (SST) flush mounted to the stationary plate. The rigid lever (D) in the shear stress transducer which is suspended by a diaphragm (E) deflects in the direction of the motion of the stationary plate, i.e. direction 1, due to the applied shear stress. It causes other end of the lever to deflect in the opposite direction. This deflection is measured using a capacitance probe, Capacitec, Model HPT-75G-E-L2-2-B-D (F). The signals from the probe are amplified in a signal amplifier (Capacitec 4100-SL-BNC Amplifier Card) and then sent to a computer using a Data Acquisition Card (National Instruments USB-6008). The device is calibrated to convert the resulting deflection reading into the applied shear stress. The calibration is performed using the static calibration procedure[30] and by using a fluid of known viscosity. A detailed discussion of the calibration procedure adopted for the constructed device can be found elsewhere.[49] The face of the lever, which is in contact with the melt, has a small gap (0.5 mm) around it to allow the lever to deflect in response to a shear force. This allows a little amount of polymer to penetrate into this gap. Dealy and co-workers, in their various publications,[37-39] have shown that the gap doesn't have any significant effect on SPR data, and the device records the true wall shear stress. Two different diaphragms were constructed with different sensitivities to allow a range of materials to be tested on the SPR.

The SPR was primarily used to perform transient shear experiments on concentrated long glass fiber-filled polypropylene. But, it was imperative to first test the device using standard materials and compare the results with a commercial instrument. Two materials, a high viscosity silicon oil, polydimethylsiloxane (PDMS), and a low density polyethylene (LDPE) with no processing aids or antiblock agents that might obscure its true melt flow behavior[50] provided by Equistar under the commercial name Petrothene NA-952, were used as the test materials.

Samples with approximately 150 x 50 x 1.70 mm dimensions were prepared using compression molding. The gap between the stationary and moving plate of the SPR was kept at 1.5 mm. Samples were squeezed down to the gap size during the insertion process which allowed better wall-matrix contact and they were then sheared along the 1-direction. Excellent agreement between results from the SPR and the RMS-800 ensured that the contructed device is capable of producing reliable and reproducible results. Tests for both long- as well as short-fiber-filled systems were performed at the gap size of 1.5 mm. The ratio of the gap to fiber diameter was 88 which was large enough to avoid any gap effects for fibers oriented in the shear plane.

4.3.3 Sliding Plate Rheometer Considerations

Various theoretical and design considerations were undertaken while fabricating the SPR. A detailed study of these considerations can be found elsewhere.[30, 49] Among them the most important consideration is the effect of fibers on the transducer performance. It is important that the fibers do not hinder the motion of the rigid lever inside the transducer in order for it to work properly. To evaluate the performance of the SPR with fiber-filled systems, SGF-30 was used. Samples that were prepared had short fibers randomly oriented in the 1-3 plane. Results obtained from the SPR were then compared with the results obtained from the RMS-800. Donut shaped samples that were used for the cone-and-plate fixture also had fibers randomly oriented in the plane of the disk. As both the samples had similar initial fiber orientation, it was expected that similar results would be obtained from both the devices if fibers did not significantly alter the performance of the SST. A comparison between the shear viscosity growth behavior following the startup of shear flow experiment was made for both the rheometers. Tests were performed at 180 ^{o}C at three different shear rates of 0.5, 1.0 and 1.5 s^{-1} and are shown in Fig. 4.4, 4.5 and 4.6, respectively. It can be seen that both the devices exhibit transient growth behavior which is in

good agreement with each other. Not only the steady state values match well but the height and the width of the overshoot at the start up of the flow practically superimpose. In order to check the reproducibility of these results same experiments were performed twice in the SPR and it was found that the results are reproducible within an error of $\pm$ 5%.

From these results it is clear that the fabricated SPR is capable of producing unbiased and reproducible results for concentrated fiber-filled systems and the fibers inside the matrix do not influence the performance of the device.

4.3.3.1 Flow due to gravity. The sliding plate rheometer was mounted vertically to measure the shear rheology of the samples. This could lead to the flow of the fluid due to gravity. However, if the gap size is small enough and viscosity of the fluid is large enough, this flow can be prevented. The maximum velocity, U_{max}, of a Newtonian fluid in a narrow slit caused by gravity is given as[51]

$$U_{max} = \frac{\rho_p g h^2}{8\,\eta_s} \qquad (2)$$

where ρ_p is the density of the fluid, h is the gap distance between the two plates, η_s is the suspension viscosity and g is the acceleration due to gravity. U_{max} for the polypropylene suspension used in the study is less than 0.3 mm/min, which is negligible compared to the minimum speed of the moving plate in this study. Moreover, for a sufficiently viscous fluid, which was the case for the present study, flow due to gravity is nullified by the surface tension.[30]

4.4 Results and Discussion

Transient viscosity growth measurements following the startup of simple shear flow were investigated for different fiber orientation, fiber concentration and fiber length in the shear rate

range of 0.4 to 4.0 s^{-1}. Consequently, the effects fiber orientation, shear rate, fiber concentration and fiber aspect ratio were observed.

4.4.1 Influence of initial fiber orientation. In order to see the effect of fiber orientation on the stresses produced following the startup of shear experiments, samples with preferential initial fiber orientation were prepared. To ensure that the initial orientation does not change during the sample insertion process, un-sheared samples were cooled down to room temperature and observed visually. No significant change in the dimensions was found, which lead us to the conclusion that there was only a little, if any, change in the initial orientation during sample insertion. Also, it should be noted that the actual viscosity growth curves obtained for long glass fiber materials using the SPR were a little wavy and were smoothed down by taking the average values over a certain stain period. Due to this smoothing of the curves, there is an error of less than 15% associated with them, which we believe is acceptable for the case of long fiber-filled suspensions.

Shear viscosity growth behavior for LGF13-10 and LGF13-20 is presented in Fig. 4.7. Tests were run up to 70 stain units as the maximum strain was restricted due to the sample size. However, steady state has been reached in all the cases. Different transient behavior is observed for different initially oriented samples, but eventually the steady state viscosity for DX samples lies between the steady state viscosities of limiting cases of D1 and D3.

Transient behavior at the inception of the flow for all three orientations can be explained by how the fibers try to orient themselves when a shear flow is imposed. In the concentrated regime, where the fiber-fiber interaction is the dominant mechanism while hydrodynamic interactions are of secondary importance,[15] an improved rate of fiber-fiber contact increases the

projection of the fibers in the direction of velocity gradient.[52] This fiber flipping is enhanced more due to the higher number of contacts in the large aspect ratio fibers. As a result, these fibers try to align themselves in the direction of the flow. For the sample where the fibers are oriented randomly, large overshoots in the viscosity at the inception of the flow were observed. It is believed to be due to higher degree of fiber-fiber collision for randomly oriented fibers, and then resulting evolution of fiber orientation in shear direction. However, for the samples where the fibers were oriented perpendicular to the direction of the flow, a very small overshoot, if at all, was observed. The reason is, as all the fibers were already aligned in the same direction, fiber contacts would be fairly reduced and there would be less flipping for the fibers. It is hypothesized that fiber oriented in the 3-direction only move along the shear direction with a very little change in fiber orientation which is why viscosity overshoots are not as prominent as in case of DX samples.

The most interesting transient behavior was observed for the sample where fibers were initially oriented in the 1-direction. As soon as the sample was sheared it reached a steady state (primary steady state) but after a certain time the viscosity started decreasing, and it eventually reached a different steady state (secondary steady state). The primary steady state is easy to explain because the fibers were already aligned in 1-direaction so there was no gradient to change their orientation. But the reason for sudden decline in viscosity and then reaching a secondary steady state is not quite obvious. Our hypothesis is that after a certain time, fibers stop providing any resistance to the shear motion or in other words fibers position themselves in a way so that mechanical contacts between fibers are minimized and, therefore, the stress contribution due to fiber interaction becomes negligible and viscosity eventually tries to approach the suspending fluid viscosity. Another plausible reason for this sudden decline in

viscosity could be the migration of the fibers away from the shear stress transducer which may result in a shear response similar to the pure matrix.

4.4.2 Influence of shear rate. Suspensions with different fiber pre-orientation showed prominent shear shinning behavior at all concentrations as shown in Fig. 4.8-4.16. However, suspensions where fibers were oriented in the 1-direction did not reach a steady state at high shear rates within 70 strain units limit. Many researchers[15, 25, 53-55] have shown theoretically as well as experimentally that adding fibers can significantly alter the shear thinning behavior of the suspension. For the long fiber suspension this shear thinning behavior is usually attributed to the entanglements of fibers. Chaouche and Koch[54] suggested that the shear thinning behavior is due to flow-induced flocculation of the fibers, where flocs are held together by adhesive forces. According to them at low shear rates large clusters of fibers are formed due to adhesive contacts between fibers which results in higher viscosity. These structures can then easily be destroyed by increasing the shear rate,[28] which results in a drop in viscosity, or the shear thinning behavior.

Concentration of fibers also had a considerable effect on shear thinning behavior. Fig. 4.17, which presents shear thinning behavior at different fiber concentrations for DX samples, shows that as the fiber loading is increased, shear thinning behavior becomes more prominent. Compared to the neat matrix, a 4-5 times increase in viscosity can be seen at low shear rates, while at high shear rates the suspension viscosity is somewhat comparable to the matrix viscosity. One possible contributor of this enhanced shear thinning behavior could be the increased fiber-fiber interaction for highly concentrated suspensions at low shear rates, while when the shear rate is increased it imparted high degree of fiber orientation,[9] effectively decreasing the viscosity to that of the matrix viscosity.

For the samples oriented in the 1-direction, it is found that the primary steady state stays for a shorter strain period as the shear rate is increased. This suggests that the resistance due to fibers in the matrix is lost even sooner for high shear rates compared to low shear rates.

4.4.3 Influence of fiber concentration. Previous work on long fiber suspensions has shown that adding fibers to a suspending fluid increases the shear viscosity of the suspension[24,14, 26-27, 29,28] Fig. 4.18 represents the viscosity growth curves at different concentrations for DX and D3 samples. A significant increase in viscosities with increase in concentration can be observed. Koch and co-workers[52, 54] attributed this behavior to increased fiber-fiber interaction. According to them, at high concentrations the rate of collisions among the fibers is expected to increase significantly which give rise to a mechanical contact contribution to the stress.

Large stress overshoots were observed for DX samples which is the result of fiber evolution in the direction of the shear flow. Both the magnitude and the width of the overshoot increased with higher fiber loading. It indicates that as fiber concentration and, therefore, the frequency of fiber contacts increases, orientation of fibers in the flow direction becomes slower. As a result, it can be concluded that the mechanical contacts between fibers play a major role in determining the dynamics of fiber evolution in concentrated regimes.

4.4.4. Influence of fiber aspect ratio. Fig 4.19 shows a comparison between viscosity growth behavior of DX samples for two different fiber aspect ratios at fiber concentration of 10 and 20 wt. %. From these plots, it is clear that as fiber aspect ratio increases the steady state suspension viscosity increases with it. These results are consistent with results of Keshtkar et al.,[28] who found that higher flexibility due to larger aspect ratio of fibers results in increased steady state viscosity. They explained this behavior by additional fiber-fiber interaction for higher aspect-

ratio particles and also in some cases, due to formation of a network. Switzer and Klingenberg,[15] who employed particle-level simulation to probe the effects of interactions between flexible fibers, also found that for the same fiber stiffness, suspension viscosity increases with fiber aspect ratio.

The transient behavior of the suspensions containing fibers of different aspect ratios also appears to be different. Fig. 4.19 shows that for the shorter fiber suspensions, it takes longer to reach the steady state or the width of the overshoot is wider compared to the longer fiber suspensions. These results contradict the results of Keshtkar et al.[28] who found that the time to reach steady state increases with fiber flexibility. This contradictory behavior indicates that shorter fibers may take a longer time to orient in the direction of the flow.

In Fig. 4.20 a comparison between viscosity growth behavior of D3 samples for two different aspect ratios is shown. Like DX samples, they too show increase in steady state viscosity with increasing fiber length. However, there is no significant difference in the time to reach maximum viscosity value, or the steady state value if the little overshoots are neglected. This behavior again indicates that the fibers in these samples do not try to align themselves in the direction of shear motion, and therefore show very small viscosity overshoots, it any, after reaching the maximum viscosity.

4.5 Conclusions

The rheological behavior of various concentrated long fiber suspensions at the startup of shear flow was investigated and the effect of initial fiber orientation, fiber length and fiber concentration in these suspensions was emphasized. A sliding plate rheometer incorporating a shear stress transducer was fabricated and its performance was validated using a concentrated

short glass fiber-filled polypropylene before performing transient shear experiments on long fiber suspensions.

The transient behavior for 3 different pre-oriented samples was found to be different which is explained by how the fiber orientation evolves in simple shear flow in different samples. The steady state viscosity for samples having random planar oriented in shear plane was found to be in between the limiting cases of samples having fiber pre-oriented in 1- and 3-directions.

Shear thinning behavior was observed for all the pre-oriented samples at all fiber concentrations. This behavior is related to the formation of fiber clusters at low shear rates held together by adhesive forces, resulting in high viscosity. It had also been noticed that the shear thinning behavior becomes more dominant with increase in fiber concentration.

A significant increase in viscosities at high fiber concentrations was observed. This behavior is attributed to the extra stress contribution due to increased mechanical contacts between fibers at high fiber concentrations. Also for sample pre-oriented randomly in shear plane, both the magnitude and the width of the overshoot increased with fiber loading.

Fiber aspect ratio in the long fiber suspension also showed a considerable effect on the steady state viscosity. As the fiber aspect ratio increased, the steady state suspension viscosity increased. Also, in the case of randomly oriented fiber suspensions it was observed that shorter fibers took longer to reach the steady state.

Acknowledgements

This work was financially supported by the National Science Foundation through Grant No. CMMI-0853537. We thank Sabic Innovative Plastics and RTP Company for supplying the materials used in this work.

4.6 References

1. High performance at medium fibre length in long glass fibre polypropylene. *Plastics, Additives and Compounding* **2000,** 2, (12), 14-21.

2. Lee, S., *Handbook of composite reinforcements*. Wiley-VCH: 1992.

3. Sepehr, M.; Ausias, G.; Carreau, P., Rheological properties of short fiber filled polypropylene in transient shear flow. *Journal of Non-Newtonian Fluid Mechanics* **2004,** 123, (1), 19-32.

4. Nguyen, B.; Bapanapalli, S.; Holbery, J.; Smith, M.; Kunc, V.; Frame, B.; Phelps, J.; Tucker III, C., Fiber Length and Orientation in Long-Fiber Injection-Molded Thermoplastics--Part I: Modeling of Microstructure and Elastic Properties. *Journal of Composite Materials* **2008,** 42, (10), 1003.

5. Bartus, S.; Vaidya, U., Performance of long fiber reinforced thermoplastics subjected to transverse intermediate velocity blunt object impact. *Composite Structures* **2005,** 67, (3), 263-277.

6. Yang, J. M., Modeling and Characterization of 2-D and 3-D Textile Structural Composites, Ph.D. dissertation, University of Delware, Newark **1986**.

7. Silverman, E., Effect of glass fiber length on the creep and impact resistance of reinforced thermoplastics. *Polymer Composites* **1987,** 8, (1).

8. McAllister, L.; Lachman, W.; Kelly, A.; Mileiko, S., Handbook of Composites. *Vol. IV" Fabrication of Composites", edited by A. Kelly (North Holland, 1983) pp*, 109-75.

9. Guo, R.; Azaiez, J.; Bellehumeur, C., Rheology of fiber filled polymer melts: Role of fiber-fiber interactions and polymer-fiber coupling. *Polymer Engineering & Science* **2005,** 45, (3).

10. Tang, W.; Advani, S.; Source, C., Dynamic Simulation of Carbon Nanotubes in Simple Shear Flow. *Computer Modeling in Engineering and Sciences* **2008,** 25, (3), 149.

11. Strautins, U.; Latz, A., Flow-driven orientation dynamics of semiflexible fiber systems. *Rheologica Acta* **2007,** 46, (8), 1057-1064.

12. Wang, G.; Yu, W.; Zhou, C., Optimization of the rod chain model to simulate the motions of a long flexible fiber in simple shear flows. *European Journal of Mechanics/B Fluids* **2006,** 25, (3), 337-347.

13. Folgar, F.; Tucker III, C., Orientation behavior of fibers in concentrated suspensions. *Journal of reinforced plastics and composites* **1984,** 3, (2), 98.

14. Ganani, E.; Powell, R., Rheological properties of rodlike particles in a Newtonian and a non-Newtonian fluid. *Journal of Rheology* **1986,** 30, 995.

15. Switzer III, L.; Klingenberg, D., Rheology of sheared flexible fiber suspensions via fiber-level simulations. *Journal of Rheology* **2003,** 47, 759.

16. Joung, C.; Phan-Thien, N.; Fan, X., Direct simulation of flexible fibers. *Journal of Non-Newtonian Fluid Mechanics* **2001,** 99, (1), 1-36.

17. Joung, C.; Phan-Thien, N.; Fan, X., Viscosity of curved fibers in suspension. *Journal of Non-Newtonian Fluid Mechanics* **2002,** 102, (1), 1-17.

18. Bapanapalli, S.; Nguyen, B., Prediction of elastic properties for curved fiber polymer composites. *Polymer Composites* **2008,** 29, (5), 544-550.

19. Forgacs, O.; Mason, S., Particle motions in sheared suspensions IX. Spin and deformation of threadlike particles. *Journal of Colloid Science* **1959,** 14, 457-472.

20. Tchen, C.-M., Motion of Small Particles in Skew Shape Suspended in a Viscous Liquid. *Journal of Applied Physics* **1954,** 25, (4), 463-473.

21. Nawab, M.; Mason, S., Viscosity of Dilute Suspensions of Thread-like Particles. *The Journal of Physical Chemistry* **1958,** 62, (10), 1248-1253.

22. Blakeney, W., The viscosity of suspensions of straight, rigid rods. *Journal of Colloid and Interface Science* **1966,** 22, 324.

23. Kitano, T.; Kataoka, T.; Nagatsuka, Y., Dynamic flow properties of vinylon fibre and glass fiber reinforced polyethylene melts. *Rheologica Acta* **1984,** 23, (4), 408-416.

24. Kitano, T.; Kataoka, T.; Nagatsuka, Y., Shear flow rheological properties of vinylon-and glass-fiber reinforced polyethylene melts. *Rheologica Acta* **1984,** 23, (1), 20-30.

25. Goto, S.; Nagazono, H.; Kato, H., The flow behavior of fiber suspensions in Newtonian fluids and polymer solutions. *Rheologica Acta* **1986,** 25, (2), 119-129.

26. Becraft, M.; Metzner, A., The rheology, fiber orientation, and processing behavior of fiber-filled fluids. *Journal of Rheology* **1992,** 36, 143.

27. Thomasset, J.; Carreau, P.; Sanschagrin, B.; Ausias, G., Rheological properties of long glass fiber filled polypropylene. *Journal of Non-Newtonian Fluid Mechanics* **2005,** 125, (1), 25-3

28. Keshtkar, M.; Heuzey, M.; Carreau, P., Rheological behavior of fiber-filled model suspensions: Effect of fiber flexibility. *Journal of Rheology* **2009,** 53, 631.

29. Anders Ericsson, K.; Toll, S.; Månson, J., Sliding plate rheometry of planar oriented concentrated fiber suspension. *Rheologica Acta* **1997,** 36, (4), 397-405.

30. Giacomin, A. A sliding plate melt rheometer incorporating a shear stress transducer. McGill University, 1987.

31. Eberle, A.; Baird, D.; Wapperom, P., Rheology of Non-Newtonian Fluids Containing Glass Fibers: A Review of Experimental Literature. *Ind. Eng. Chem. Res* **2008,** 47, (10), 3470-3488.

32. Cross, M.; Kaye, A., Techniques for the viscometry of suspensions. *Polymer Engineering & Science* **1986,** 26, (2).

33. Mondy, L.; Geller, A.; Rader, D.; Ingber, M., Boundary element method calculations of the mobility of nonspherical particles—II. Branched chains and flakes. *Journal of Aerosol Science* **1996,** 27, (4), 537-546.

34. Jones, R. S.; Roberts, R. W., Anisotropic shear flow in continuous fibre composites. *Composites* **1994,** 25, (3), 171-176.

35. Shuler, S.; Advani, S., Transverse squeeze flow of concentrated aligned fibers in viscous fluids. *Journal of Non-Newtonian Fluid Mechanics* **1996,** 65, (1), 47-74.

36. Giacomin, A.; Samurkas, T.; Dealy, J., A novel sliding plate rheometer for molten plastics. *Polymer Engineering and Science* **1989,** 29, (8), 499-504.

37. Dealy, J.; Soong, S., A parallel plate melt rheometer incorporating a shear stress transducer. *Journal of Rheology* **1984,** 28, 355.

38. Park, H.; Lim, S.; Smillo, F.; Dealy, J.; Robertson, C., Wall slip and spurt flow of polybutadiene. *Journal of Rheology* **2008,** 52, 1201.

39. Koran, F.; Dealy, J., A high pressure sliding plate rheometer for polymer melts. *Journal of Rheology* **1999,** 43, 1279.

40. Laun, H., Orientation effects and rheology of short glass fiber-reinforced thermoplastics. *Colloid & Polymer Science* **1984,** 262, (4), 257-269.

41. Dealy, J.; Doshi, S.; Bubic, F. Method and apparatus for measuring shear stress, U.S. Patent 5,094,100. 1992.

42. Eberle, A.; Baird, D.; Wapperom, P.; Vélez-García, G., Using transient shear rheology to determine material parameters in fiber suspension theory. *Journal of Rheology* **2009,** 53, 685.

43. Wang, J.; O'Gara, J.; Tucker III, C., An objective model for slow orientation kinetics in concentrated fiber suspensions: Theory and rheological evidence. *Journal of Rheology* **2008,** 52, 1179.

44. Hinch, E., The distortion of a flexible inextensible thread in a shearing flow. *Journal of Fluid Mechanics Digital Archive* **2006,** 74, (02), 317-333.

45. Goddard, J.; Huang, Y., On the Motion of Flexible Threads in a Stokes Shear Field. *J. Non-Newtonian Fluid Mech* **1983,** 13, 47-62.

46. Yamamoto, S.; Matsuoka, T., A method for dynamic simulation of rigid and flexible fibers in a flow field. *The Journal of Chemical Physics* **1993,** 98, 644.

47. Eberle, A. The Dynamic Behavior of a Concentrated Composite Fluid Containing Non-Brownian Glass Fibers in Rheometrical Flows. Ph.D. Thesis, Virginia Tech, 2008.

48. Macosko, C.; Larson, R., *Rheology: principles, measurements, and applications*. Wiley, New York, NY: 1994.

49. Agarwal, N. Transient Shear Flow Rheology of Concentrated Long Glass Fiber Suspensions in a Sliding Plate Rheometer. Master's Thesis, Virginia Tech, Blacksburg, 2009.

50. Doerpinghaus Jr, P. Flow behavior of sparsely branched metallocene-catalyzed polyethylenes. Ph.D. Thesis, Virginia Tech, 2002.

51. Bird, R.; Stewart, W.; Lightfoot, E., Transport Phenomena. 2002. *John Wiley and Sons Inc*.

52. Sundararajakumar, R.; Koch, D., Structure and properties of sheared fiber suspensions with mechanical contacts. *Journal of Non-Newtonian Fluid Mechanics* **1997,** 73, (3), 205-239.

53. Kitano, T.; Kataoka, T., The rheology of suspensions of vinylon fibers in polymer liquids. I. Suspensions in silicone oil. *Rheologica Acta* **1981,** 20, (4), 390-402.

54. Chaouche, M.; Koch, D., Rheology of non-Brownian rigid fiber suspensions with adhesive contacts. *Journal of Rheology* **2001,** 45, 369.

55. Ganani, E.; Powell, R., Suspensions of rodlike particles: literature review and data correlations. *Journal of Composite Materials* **1985,** 19, (3), 194.

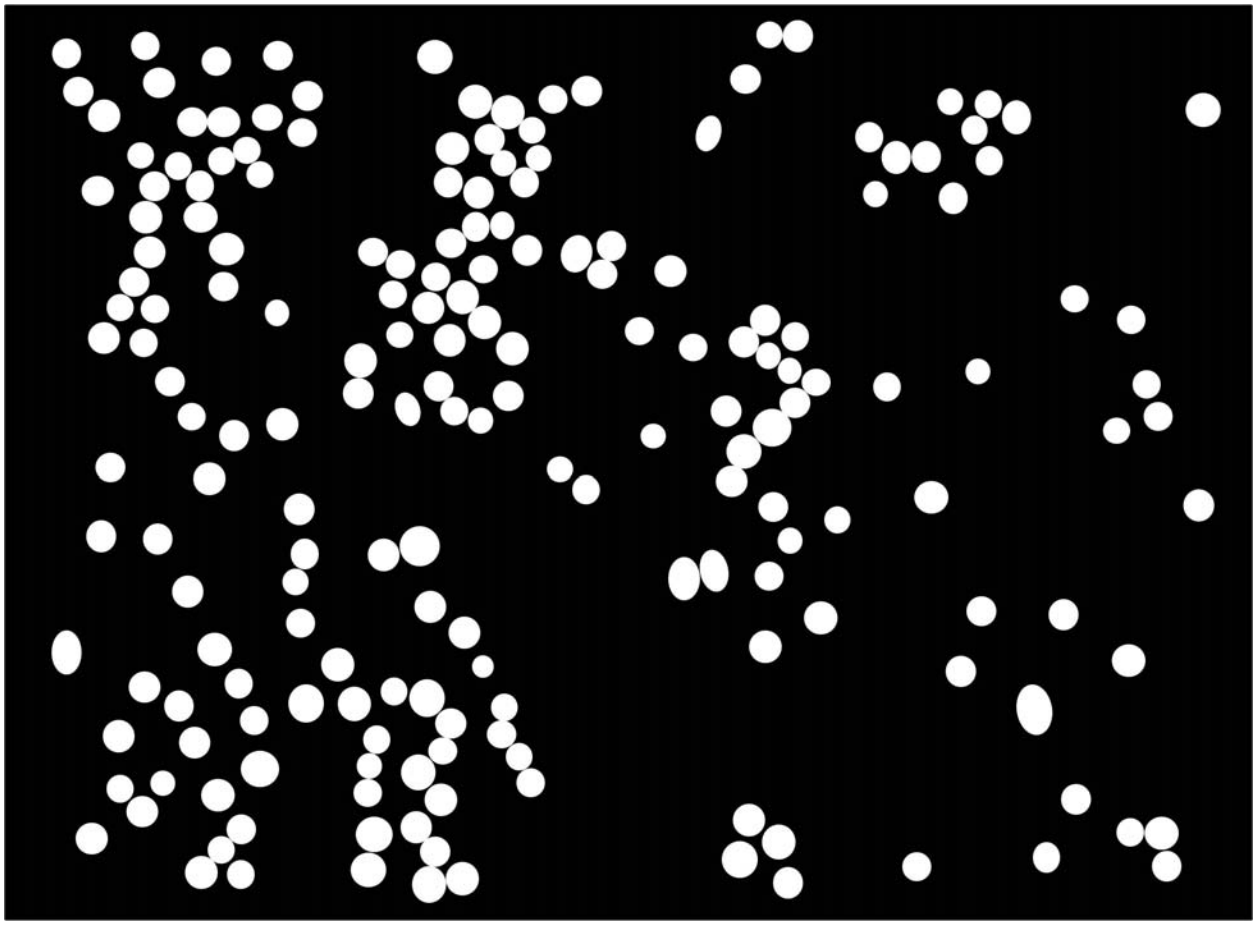

Figure 4.1. View of the 1-2 plane under microscope (Magnification: 300X) for a sample having fibers pre-oriented in 3-direction.

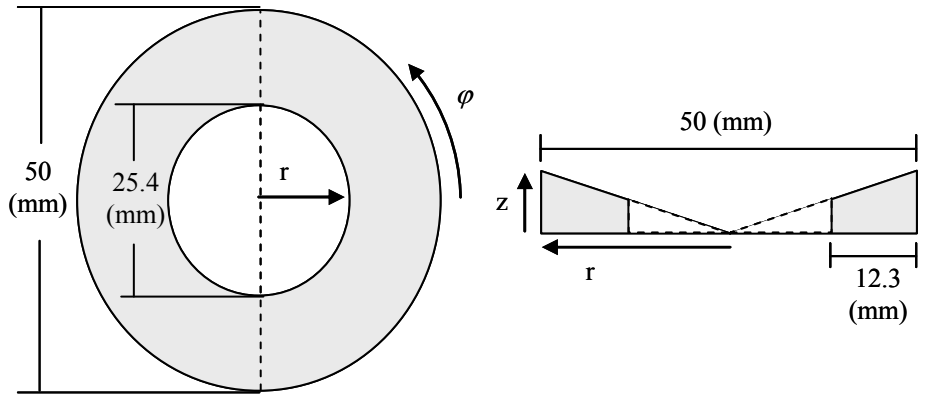

Figure 4.2. Schematic drawing and cross-sectional profile of the donut sample.[47]

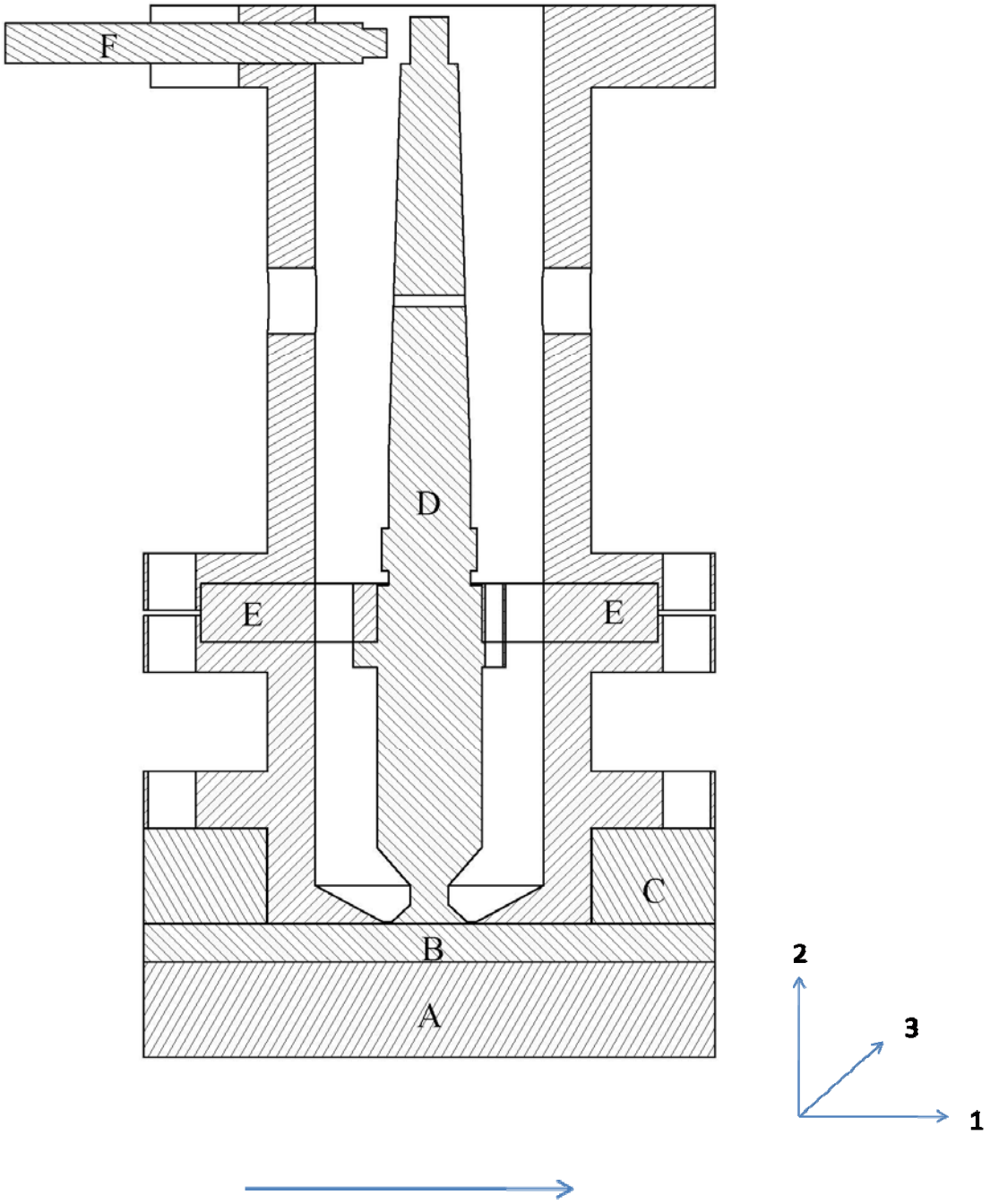

Figure 4.3. Schematic diagram of the shear stress transducer including the bottom moving plate (A) and the inserted polymer sample (B).

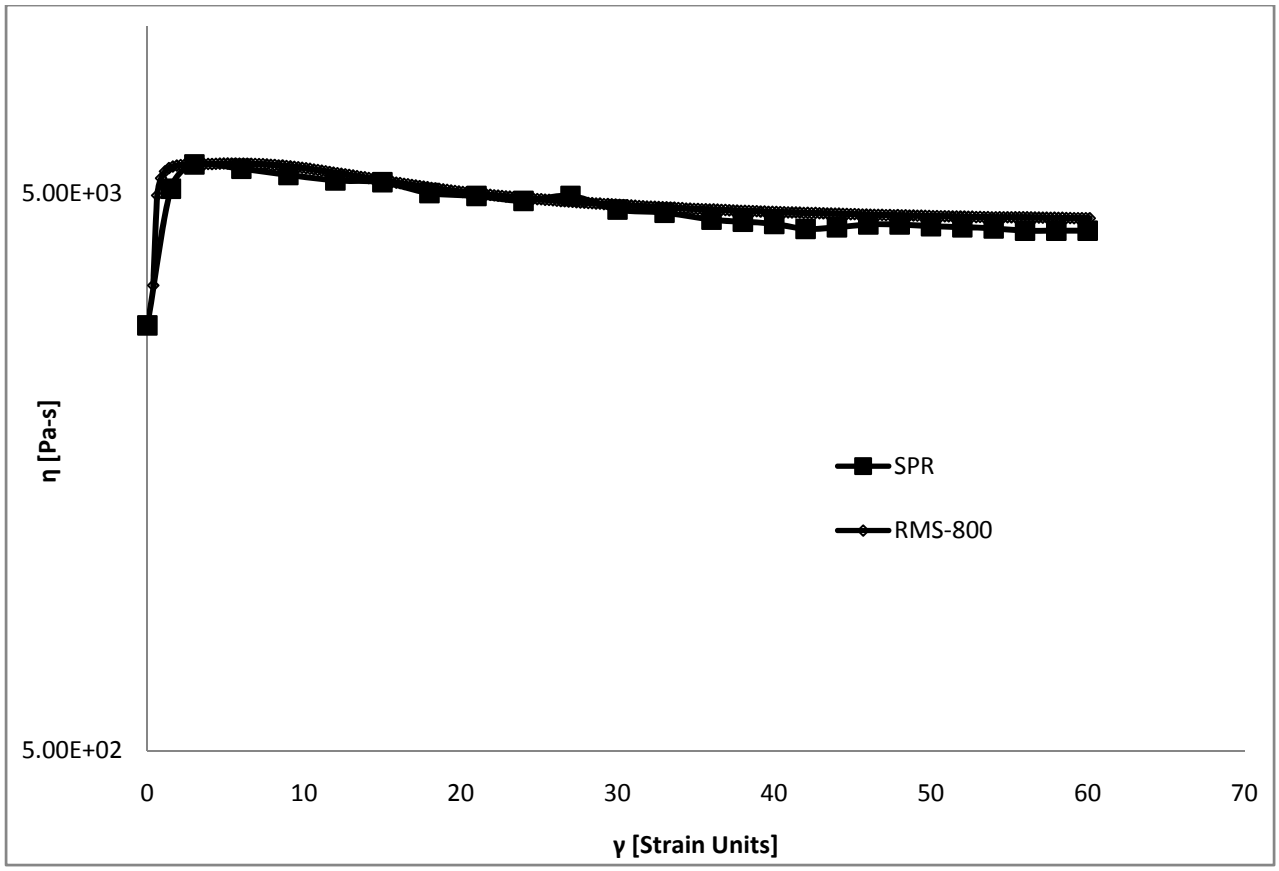

Figure 4.4. Comparison between shear viscosity growth curves obtained from the SPR and the RMS-800 for SGF-30, at a shear rate of 0.5 s^{-1}.

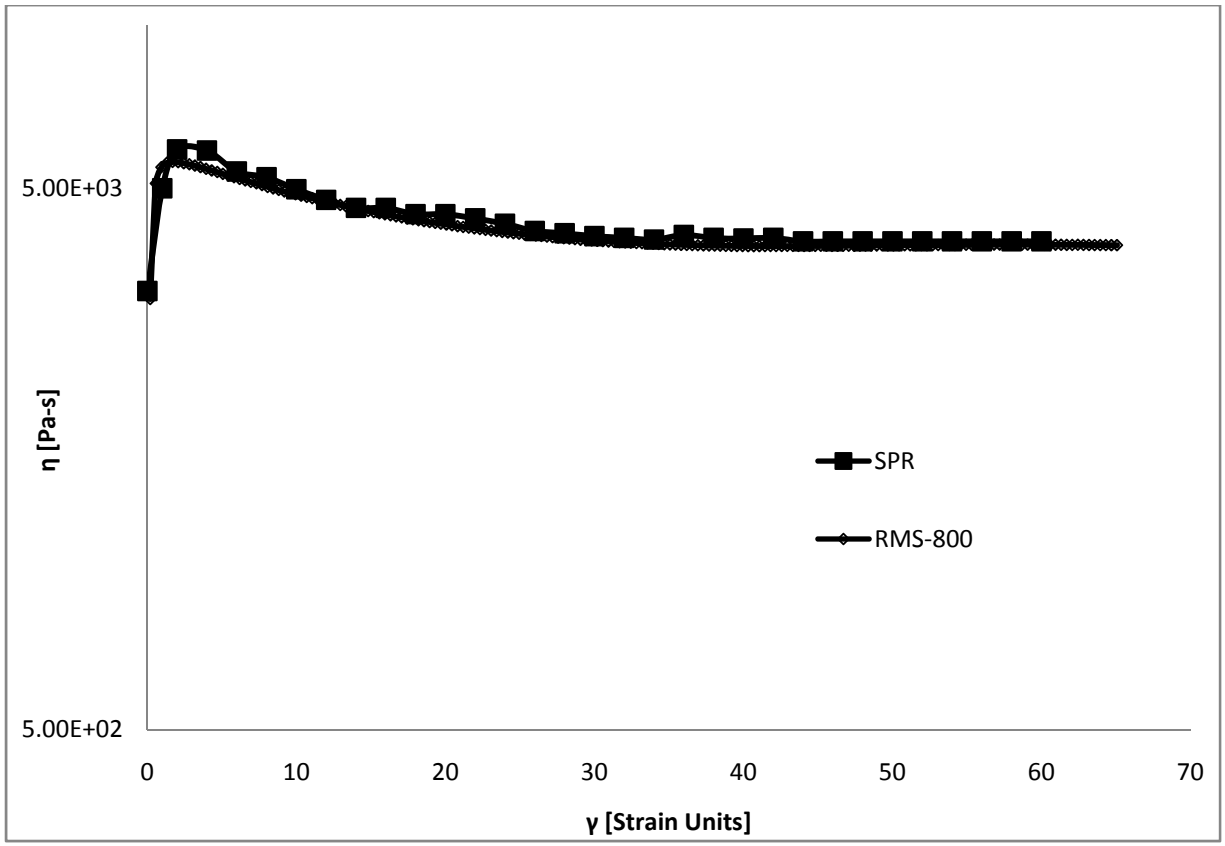

Figure 4.5. Comparison between shear viscosity growth curves obtained from the SPR and the RMS-800 for SGF-30, at a shear rate of 1.0 s^{-1}.

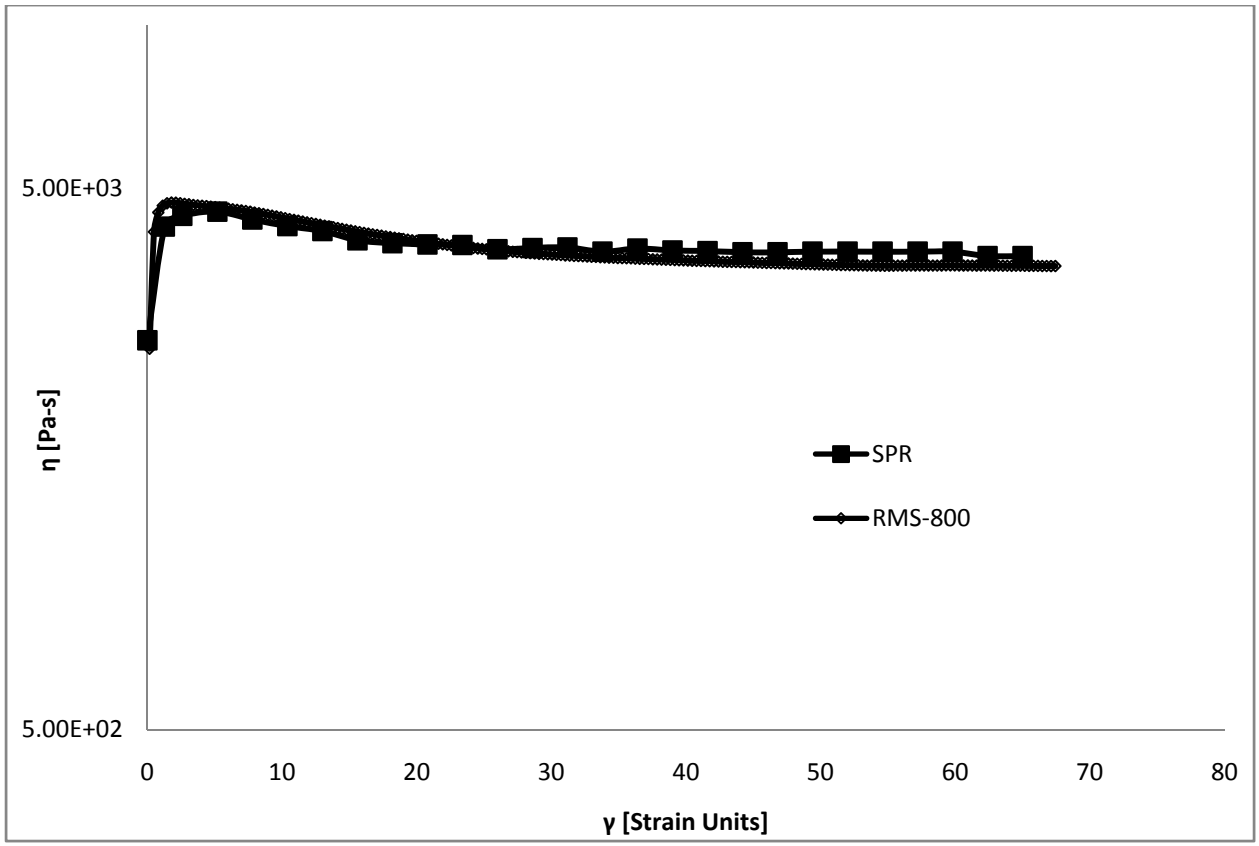

Figure 4.6. Comparison between shear viscosity growth curves obtained from the SPR and the RMS-800 for SGF-30, at a shear rate of 1.5 s^{-1}.

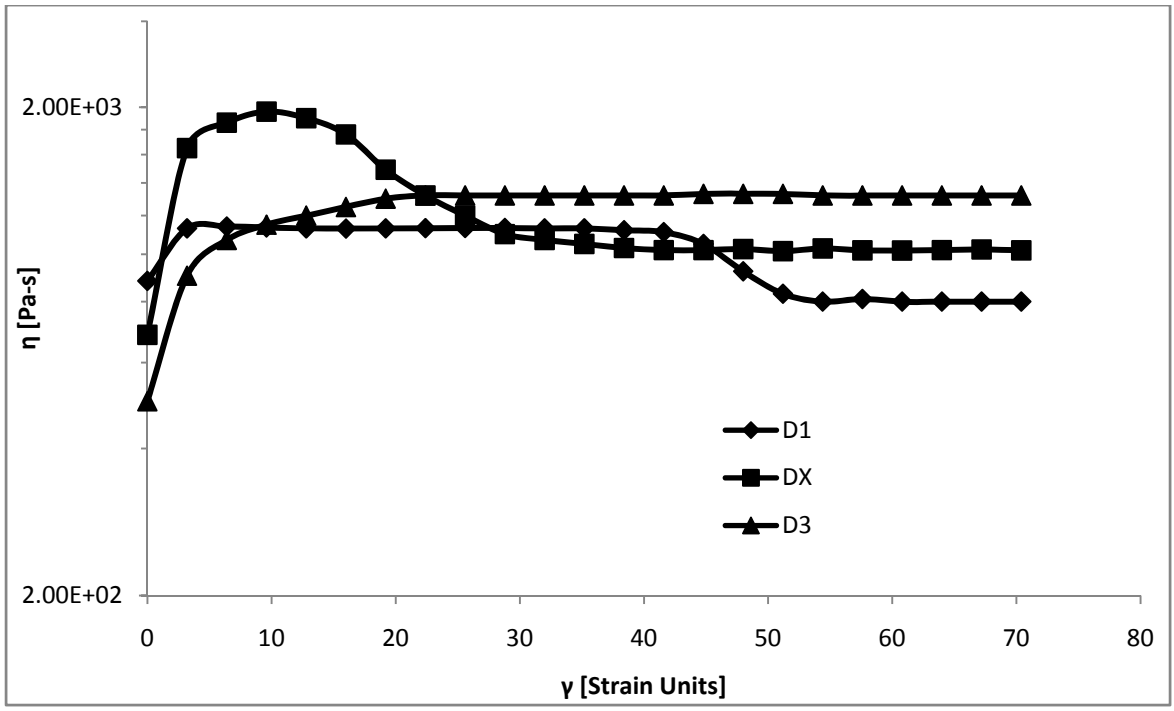

(a)

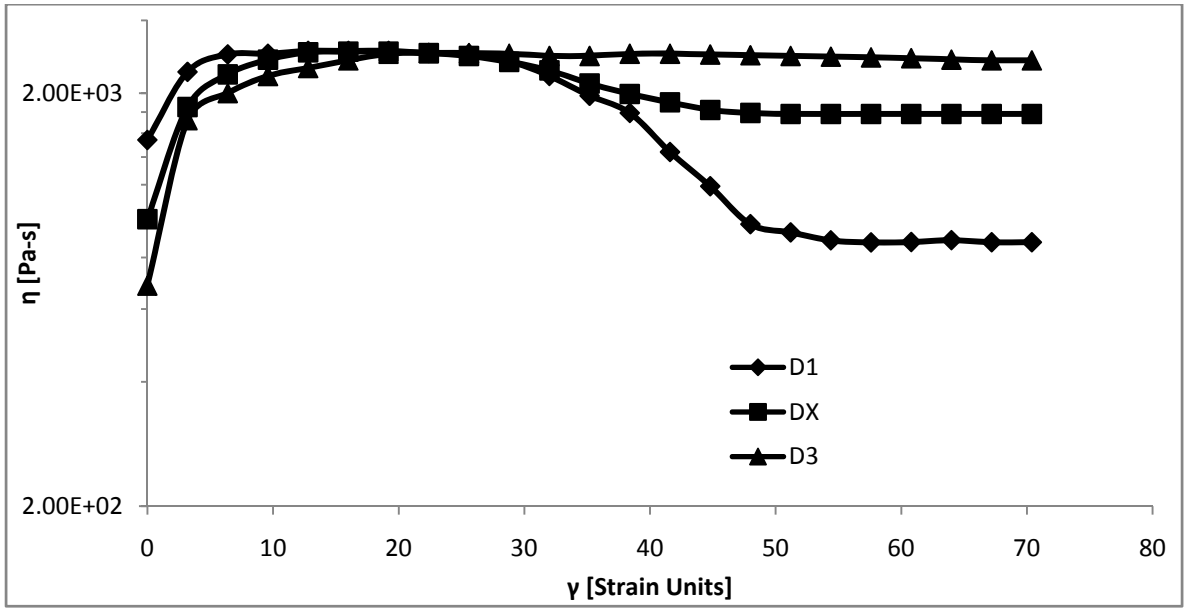

(b)

Figure 4.7. Shear viscosity growth behavior of (a) LGF13-10 and (b) LGF13-20 at a shear rate of 0.4 s^{-1}.

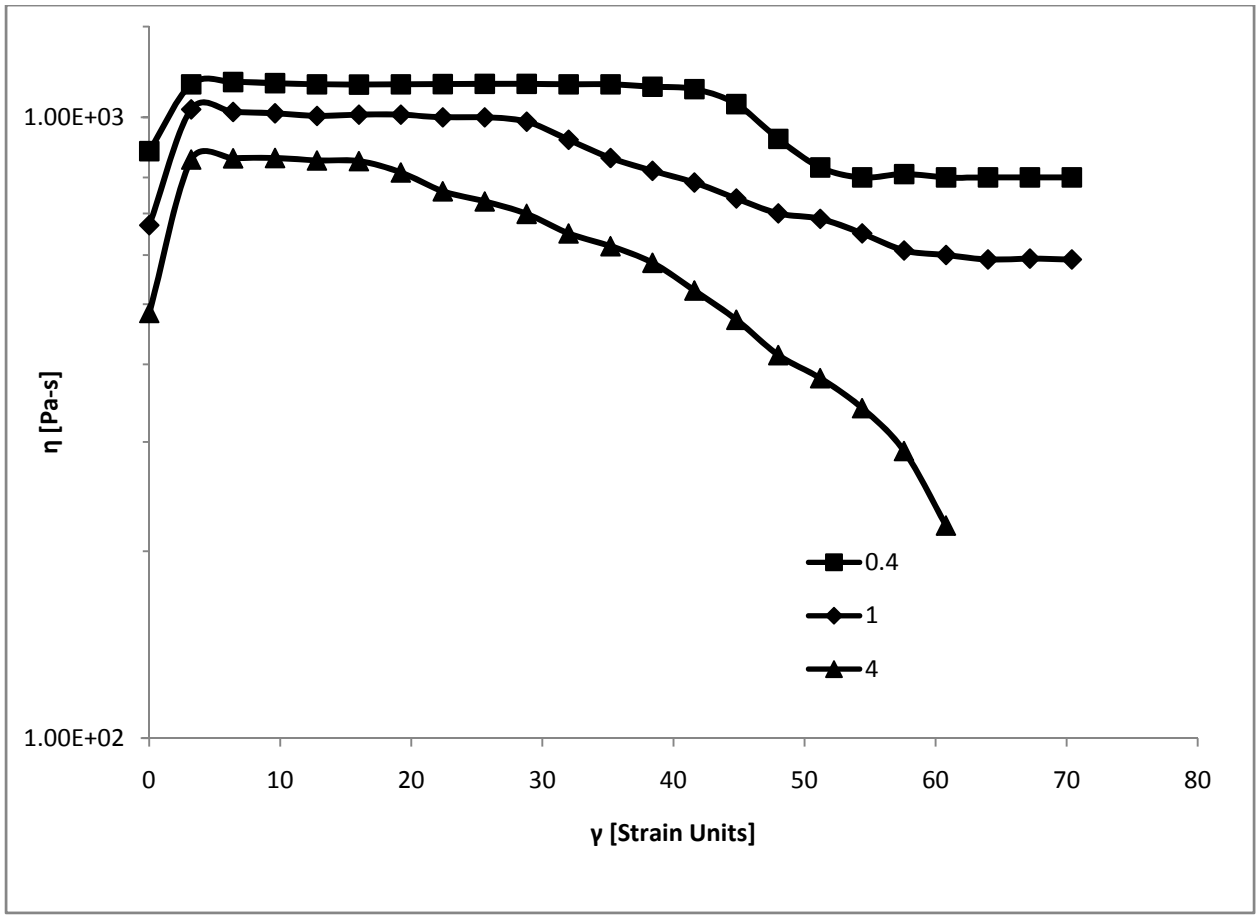

Figure 4.8. Shear viscosity growth behavior of LGF13-10 for D1 samples. The numbers in the legend relate to different shear rates (s^{-1}).

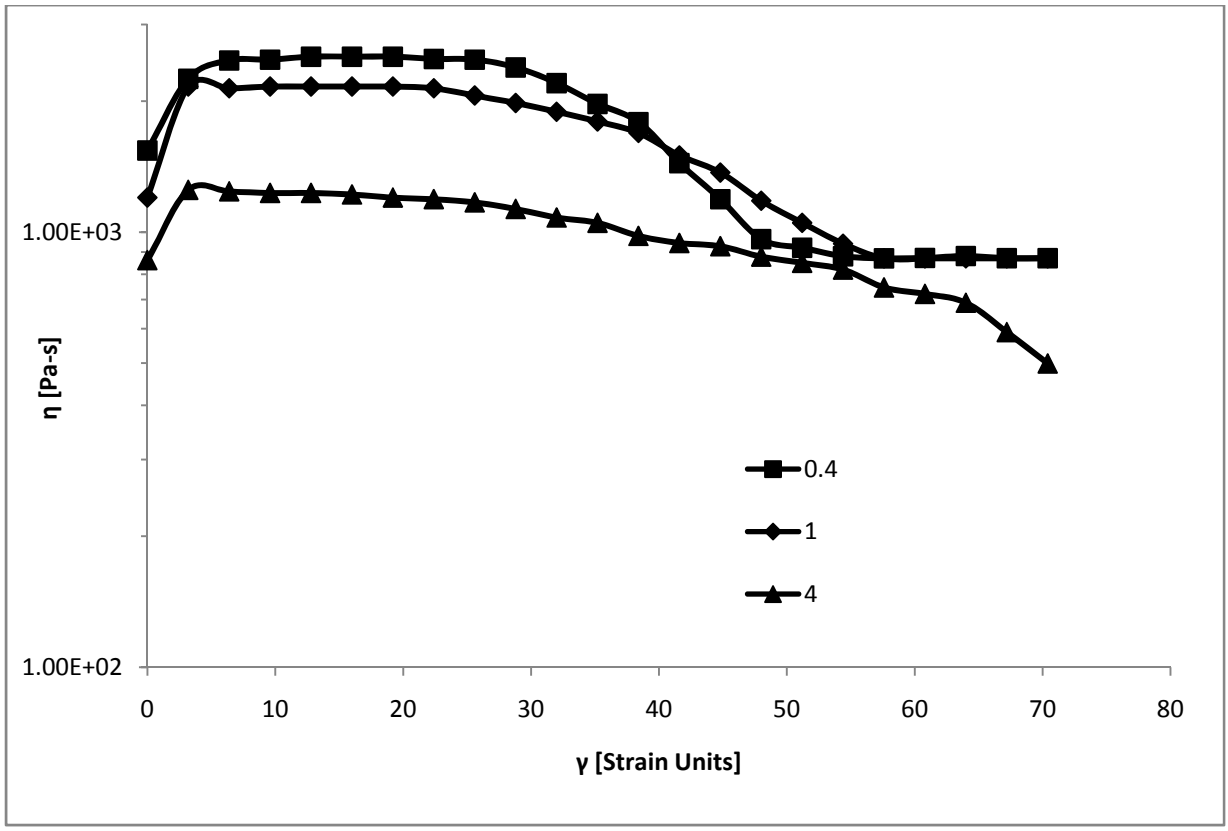

Figure 4.9. Shear viscosity growth behavior of LGF13-20 for D1 samples. The numbers in the legend relate to different shear rates (s^{-1}).

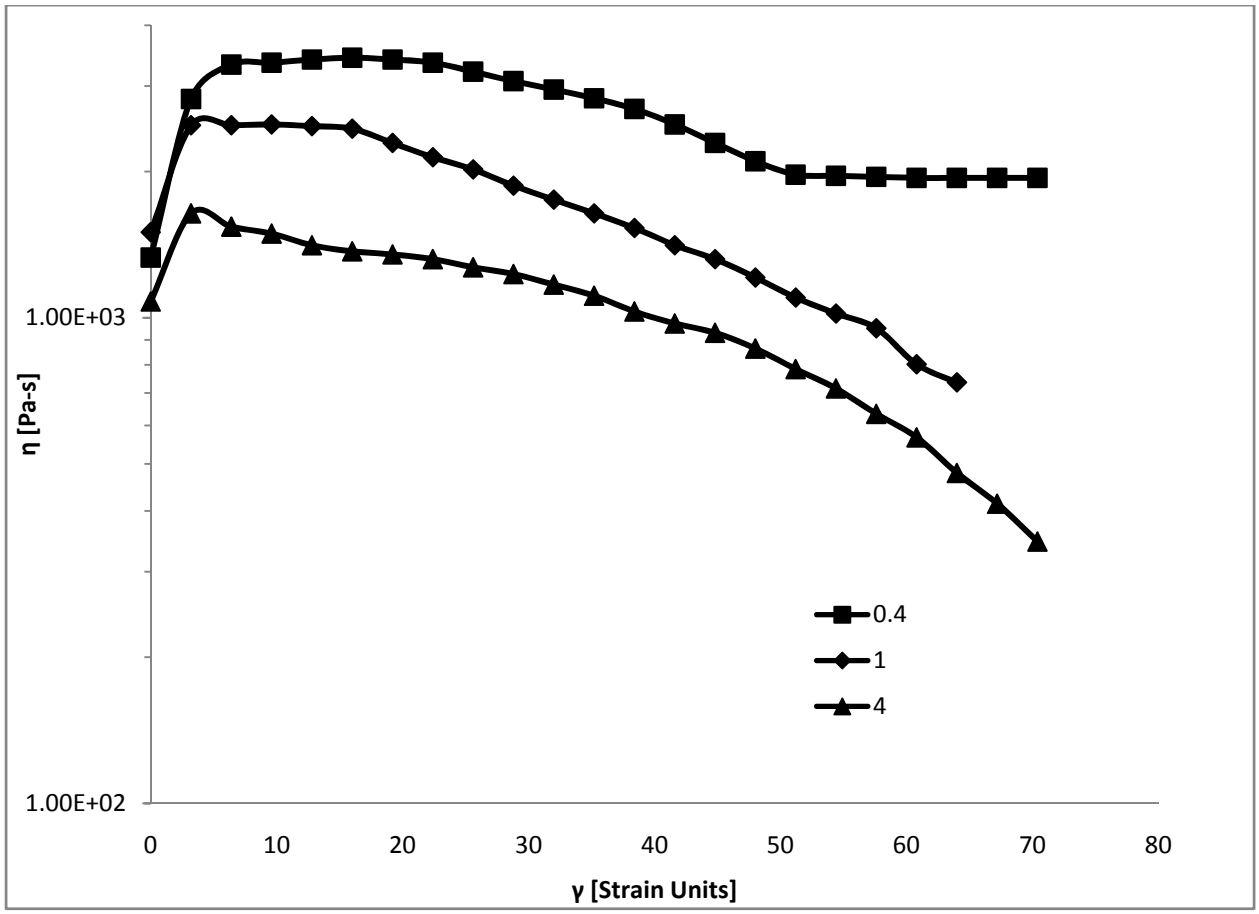

Figure 4.10. Shear viscosity growth behavior of LGF13-25 for D1 samples. The numbers in the legend relate to different shear rates (s^{-1}).

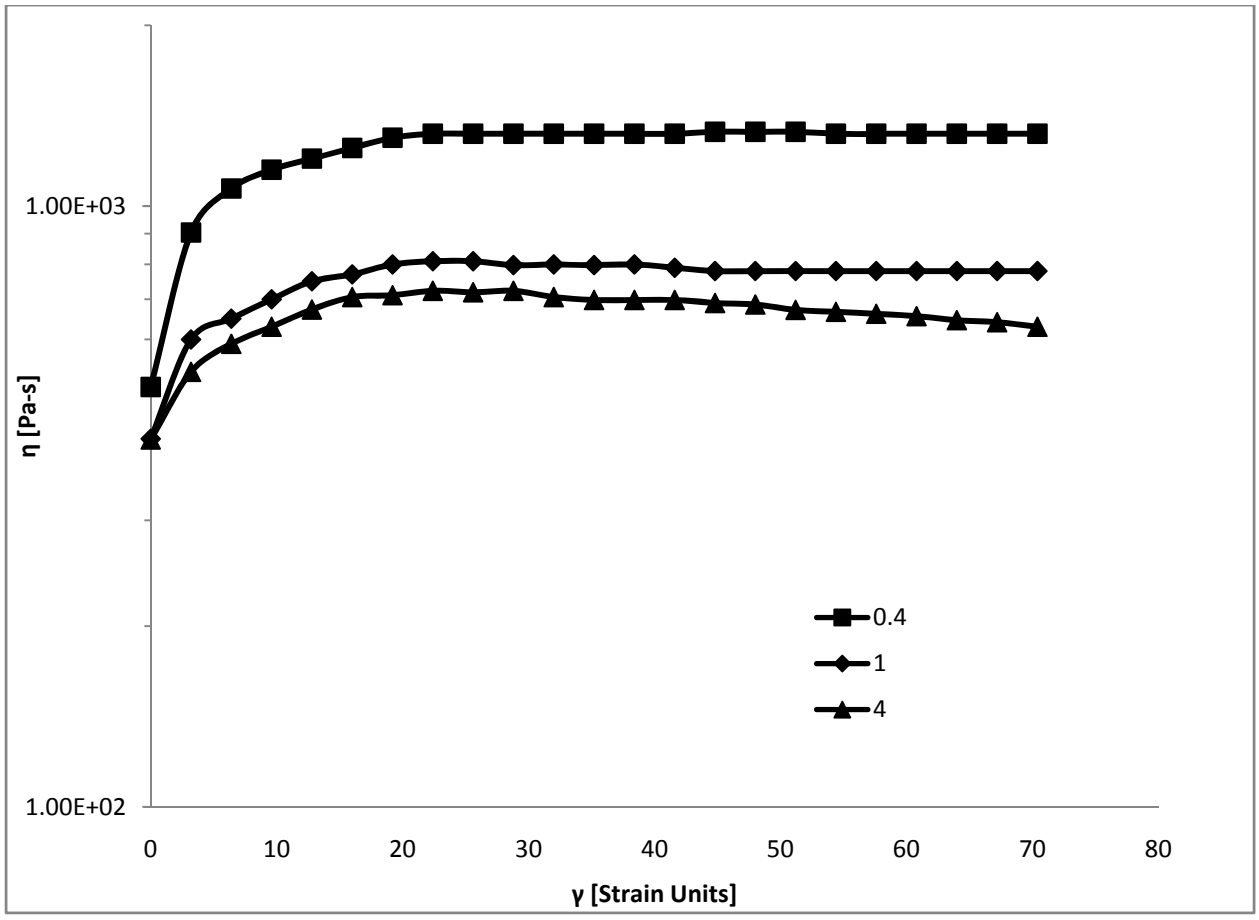

Figure 4.11. Shear viscosity growth behavior of LGF13-10 for D3 samples. The numbers in the legend relate to different shear rates (s^{-1}).

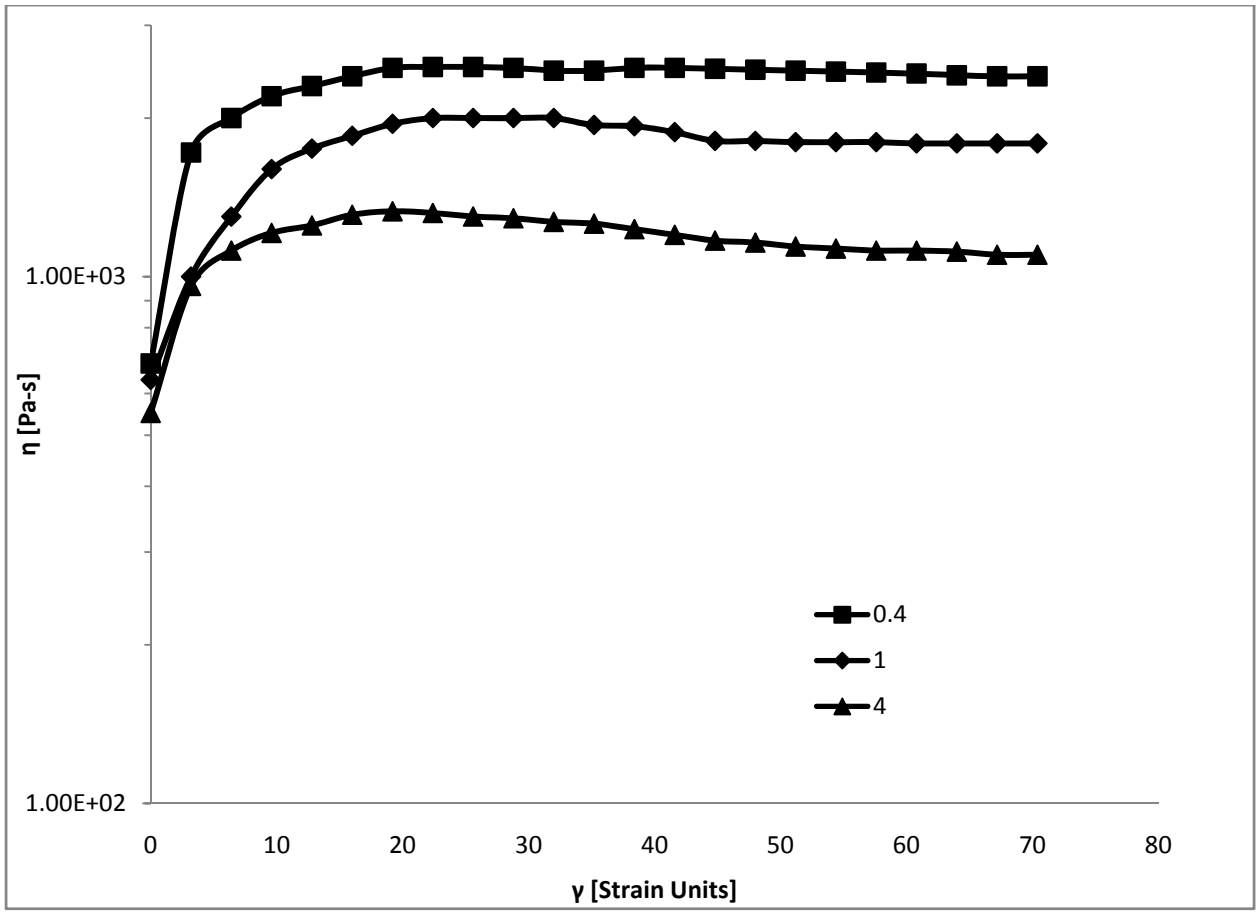

Figure 4.12. Shear viscosity growth behavior of LGF13-20 for D3 samples. The numbers in the legend relate to different shear rates (s^{-1}).

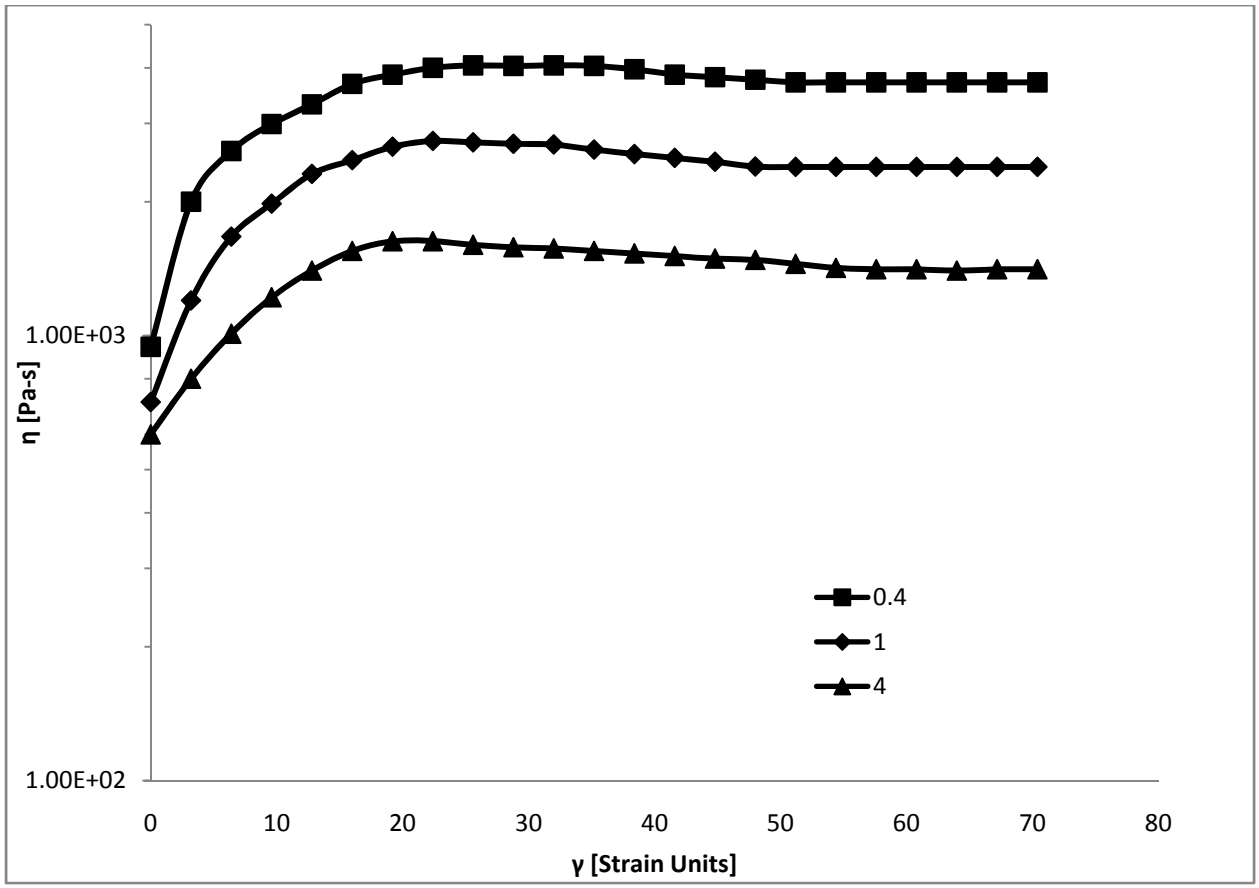

Figure 4.13. Shear viscosity growth behavior of LGF13-25 for D3 samples. The numbers in the legend relate to different shear rates (s^{-1}).

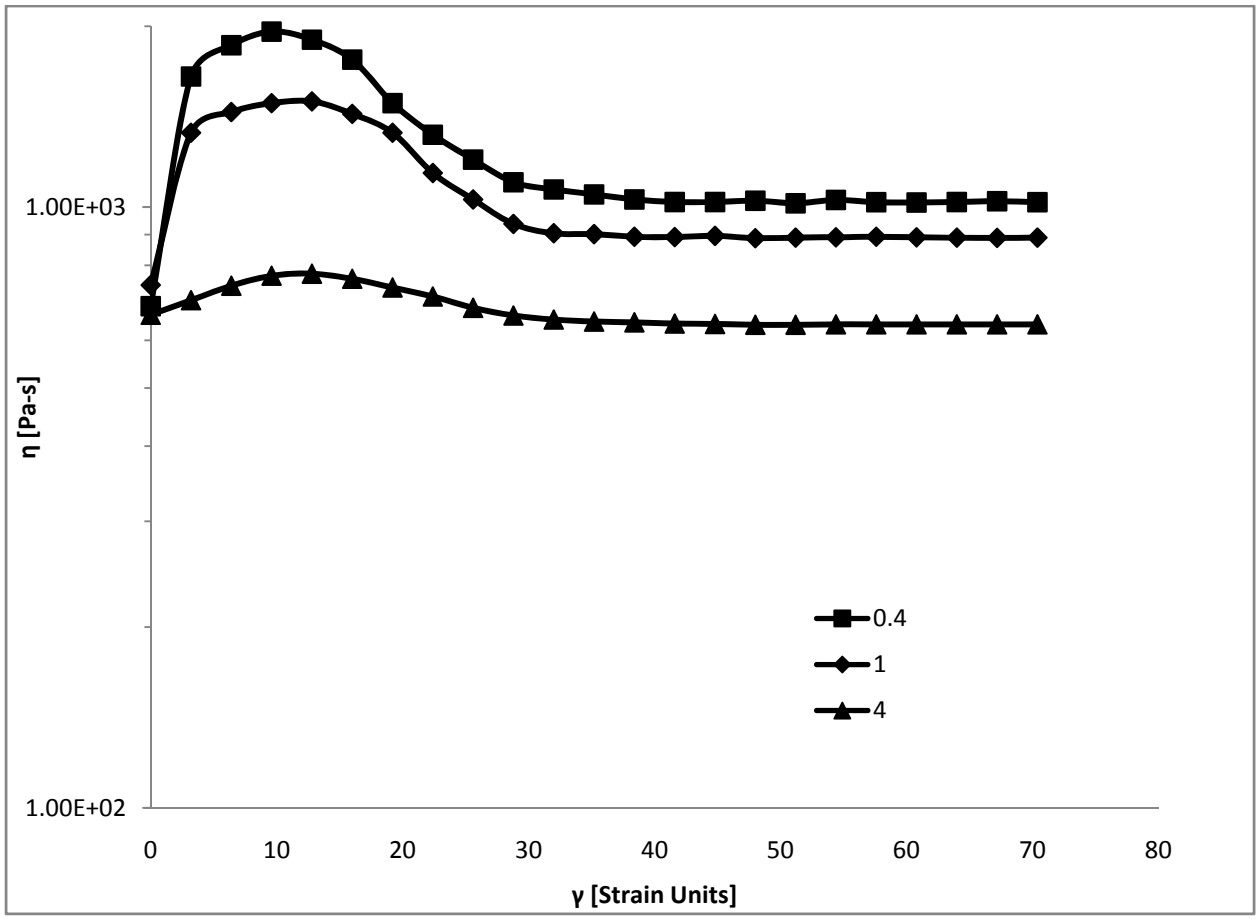

Figure 4.14. Shear viscosity growth behavior of LGF13-10 for DX samples. The numbers in the legend relate to different shear rates (s^{-1}).

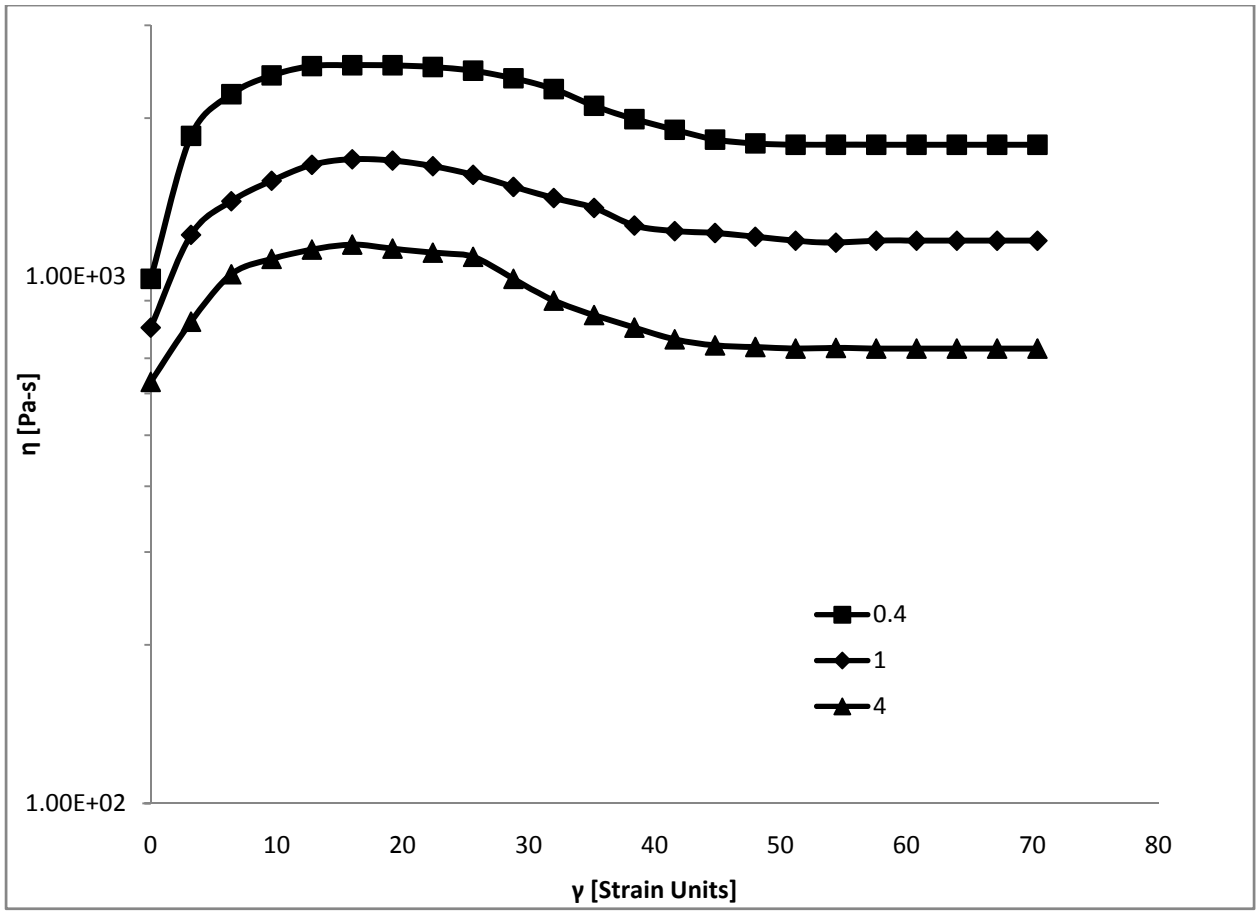

Figure 4.15. Shear viscosity growth behavior of LGF13-20 for DX samples. The numbers in the legend relate to different shear rates (s^{-1}).

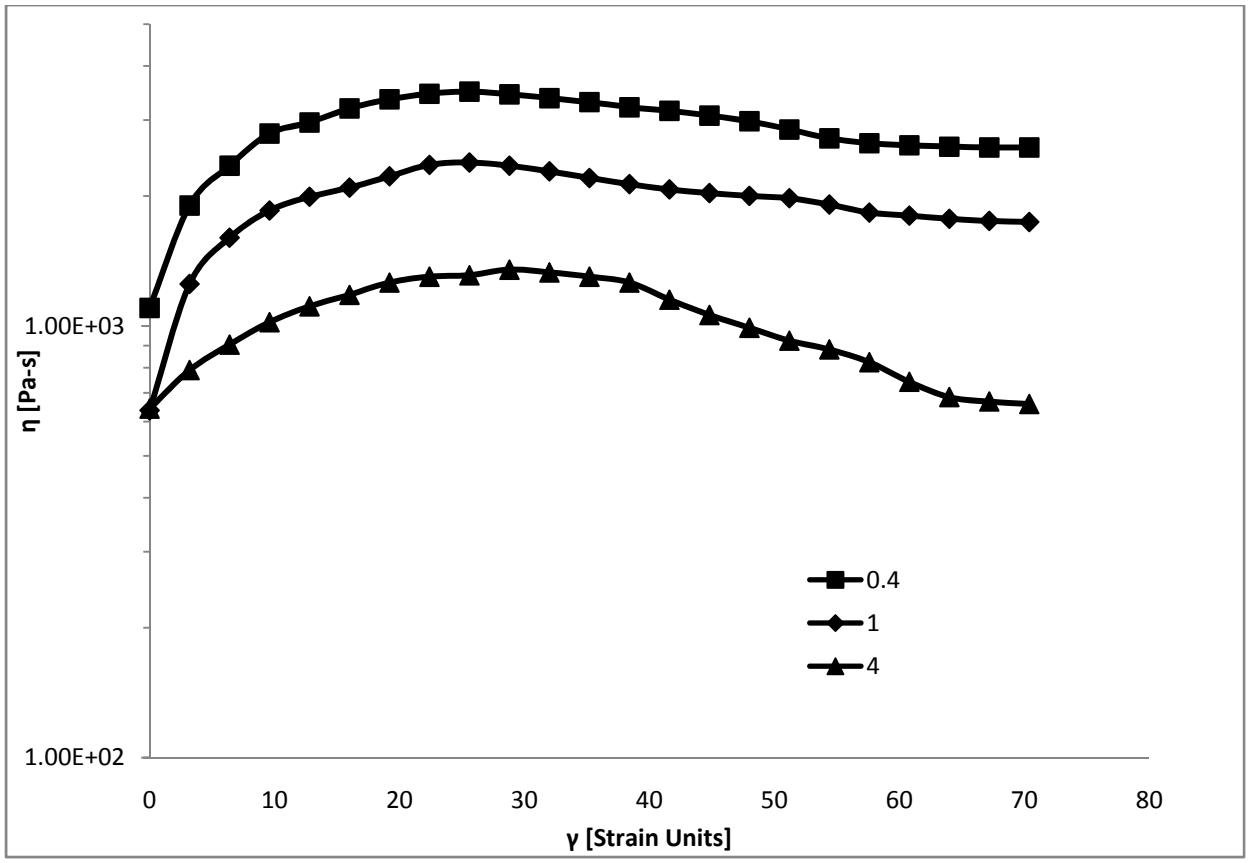

Figure 4.16. Shear viscosity growth behavior of LGF13-25 for DX samples. The numbers in the legend relate to different shear rates (s^{-1}).

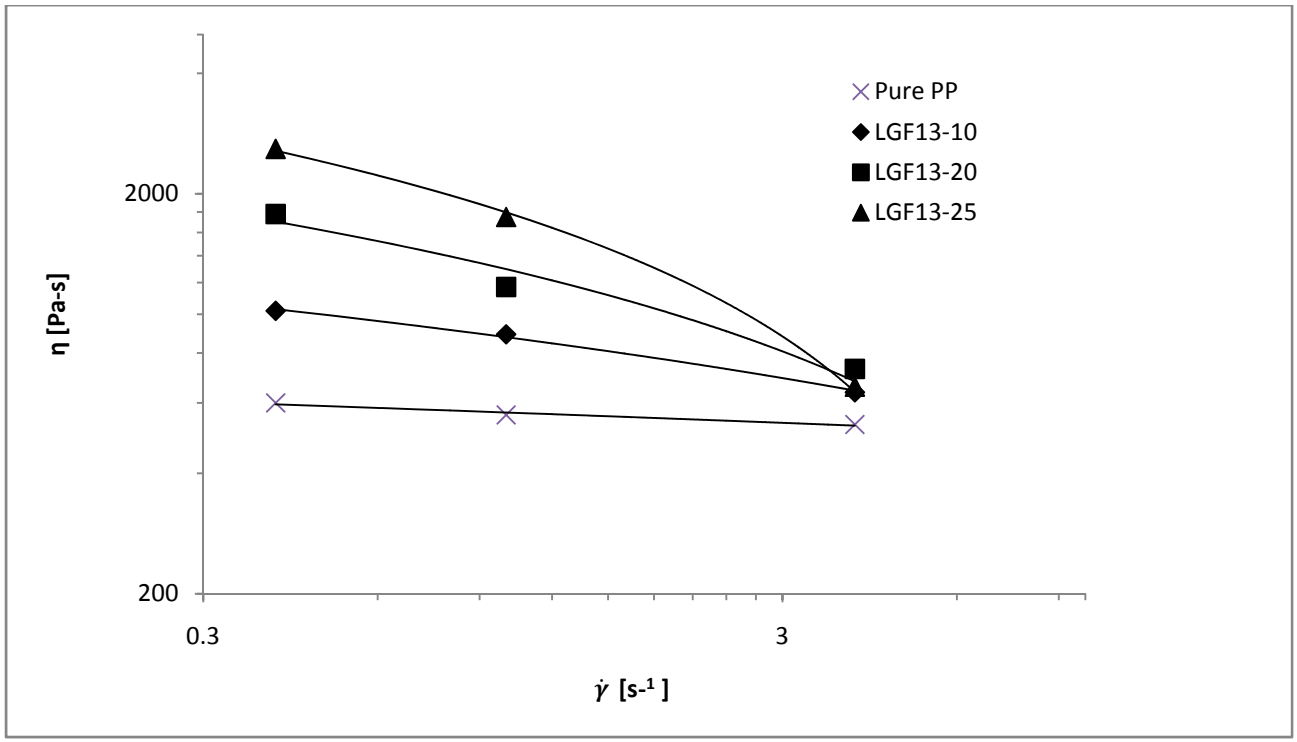

Figure 4.17. Shear thinning behavior for DX samples at fiber concentration of 0, 10, 20 and 25 wt. %.

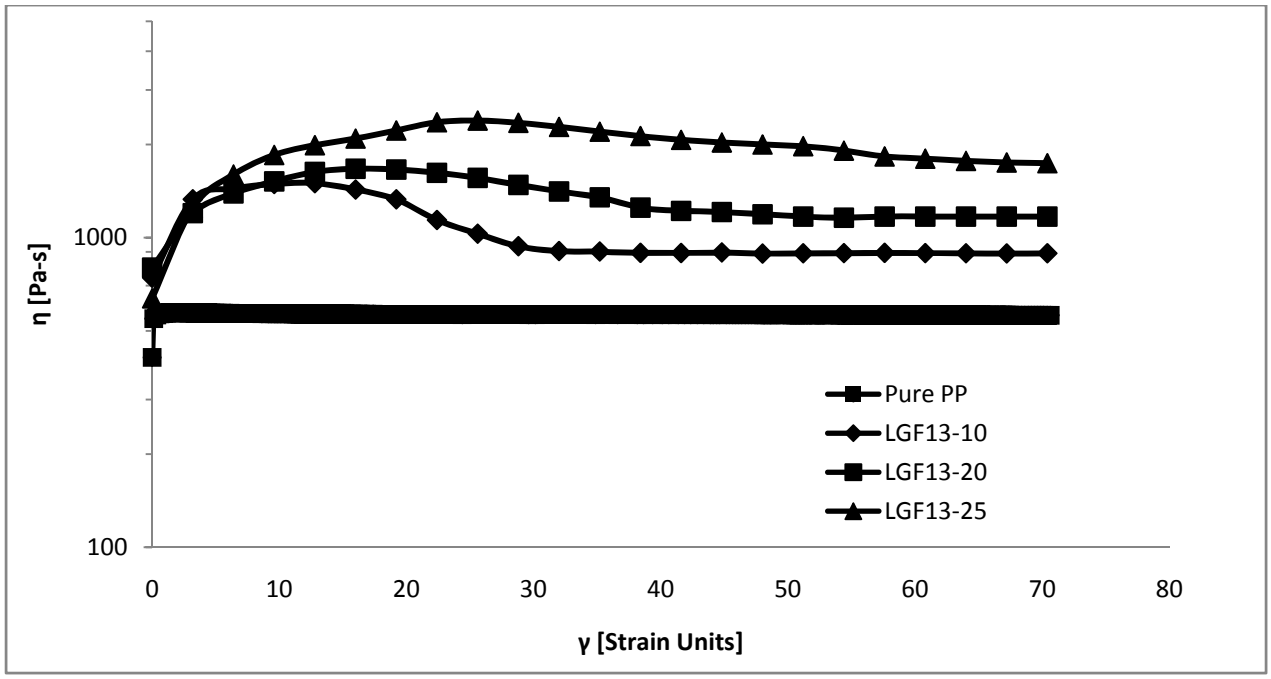

(a)

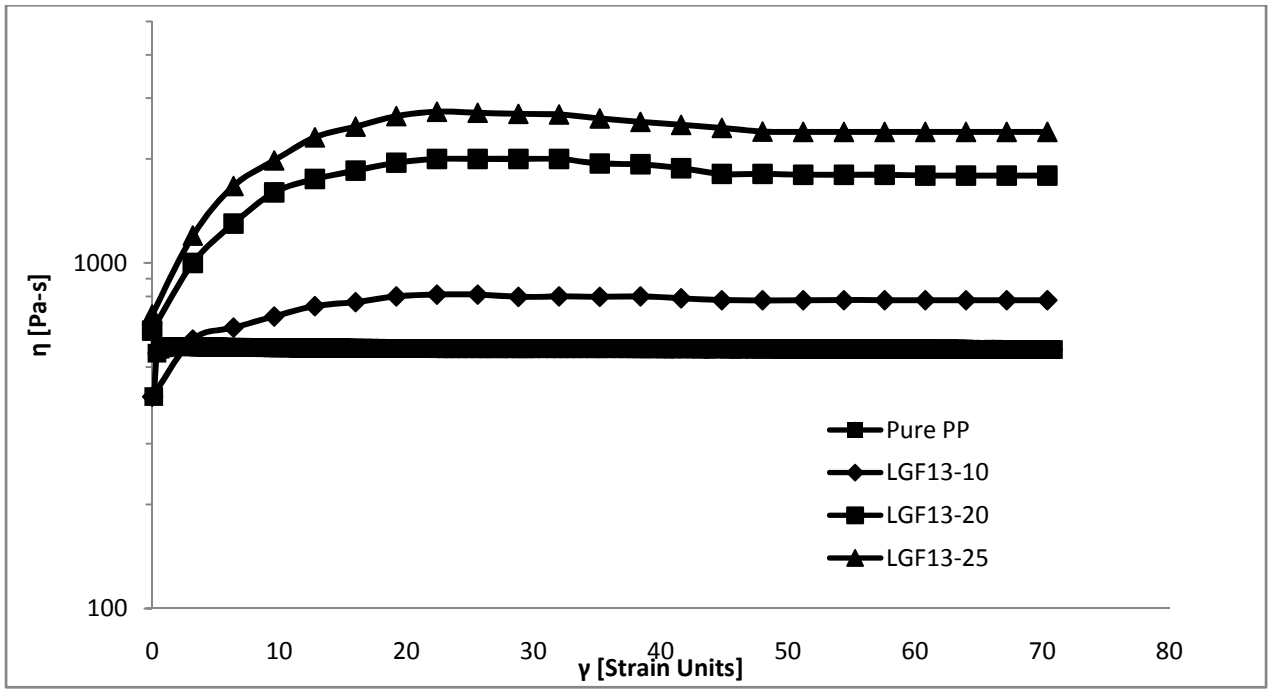

(b)

Figure 4.18. Shear viscosity growth behavior of (a) DX samples (b) D3 samples, at a shear rate of 1 s^{-1}.

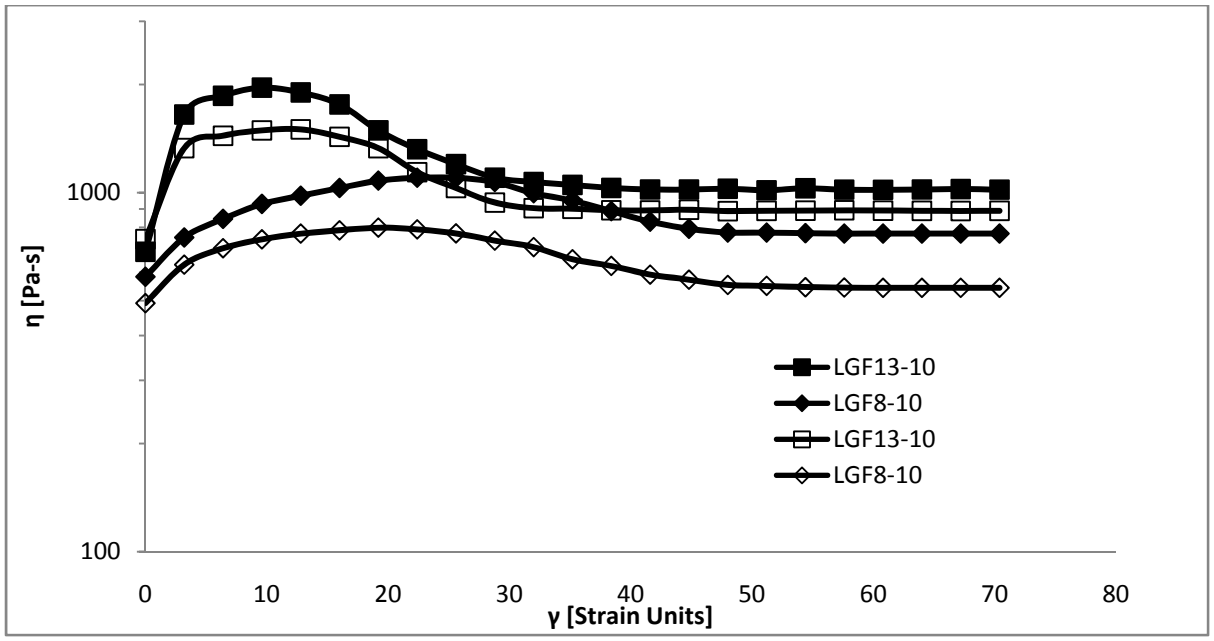

(a)

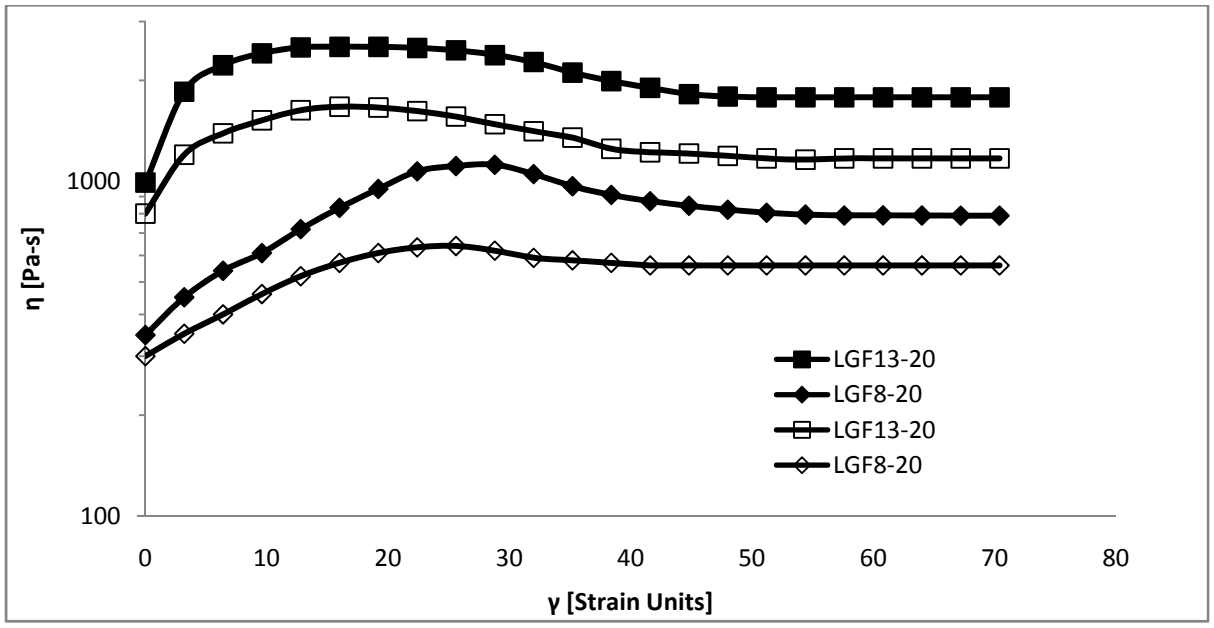

(b)

Figure 4.19. Comparison between viscosity growth behavior of DX samples for two different fiber aspect ratios at fiber concentration of (a) 10 wt. % (b) 20 wt. %. Filled and unfilled symbols represent that the samples are sheared at shear rate of 0.4 and 1.0 s^{-1}, respectively.

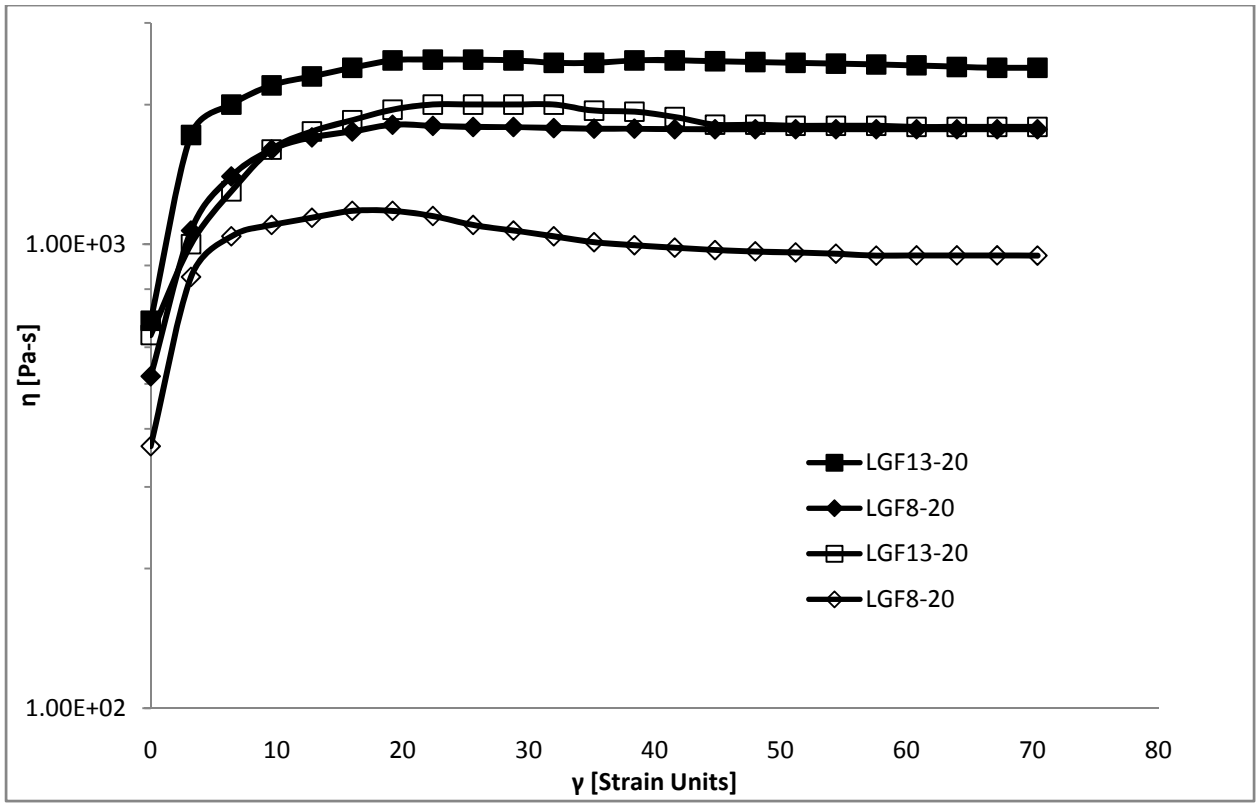

Figure 4.20. Viscosity growth behavior of D3 samples for two different fiber aspect ratios at fiber concentration of 20 wt. %. Filled and unfilled symbols represent that the samples are sheared at shear rate of 0.4 and 1.0 s^{-1}, respectively.

5.0 Recommendations for Future Work

1) The shear stress transducer used in this study made use of two transducers with different sensitivities in order to test a range of materials on the sliding plate rheometer. However, it was found that for the same material, the more sensitive transducer produced a little better results that the less sensitive tranducer. Therefore, construction of an even more sensitive transducer could help in minimizing the errors associated with the results produced in this study.
2) Transient behavior of pre-oriented samples has been explained by predicting how the fiber orientation evolves in simple shear flow. Hence, it would be useful to investigate the post structure of the fibers in the sheared samples. An agreement with the actual structure would prove the correctness of the suggested hypotheses.
3) For the experiments on long glass fiber suspensions, fibers were pre-oriented in the shear plane where there was no velocity gradient. However, it would be interesting to see how the transient rheological behavior of these samples changes if the fibers are oriented perpendicular to the shear plane. But, preparing such samples is a very difficult task and even if accomplished, gap effects would highly influence the shear viscosity growth behavior of such samples. In order to obtain a velocity gradient in the plane of the sample, a squeeze flow rheometer would be valuable. Due to the biaxial deformation, there are velocity gradients in the plane of the sample which may provide invaluable information regarding the fiber orientation evolution under certain velocity fields.

Appendix A. Fiber Length Distribution Data

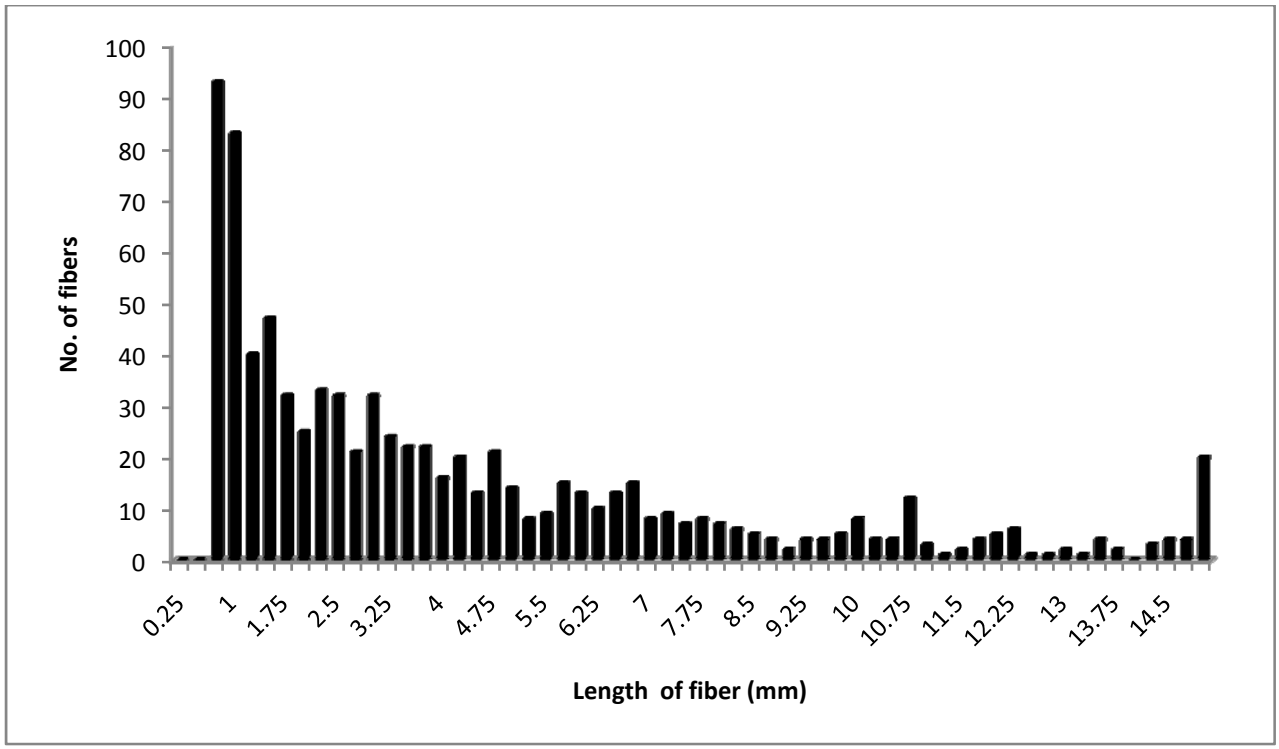

Figure A.1. Fiber length distribution after extrusion of 13 mm fiber pellets. The number average length (L_N) and the weight average length (L_W) are 4.22 and 7.48 mm, respectively.

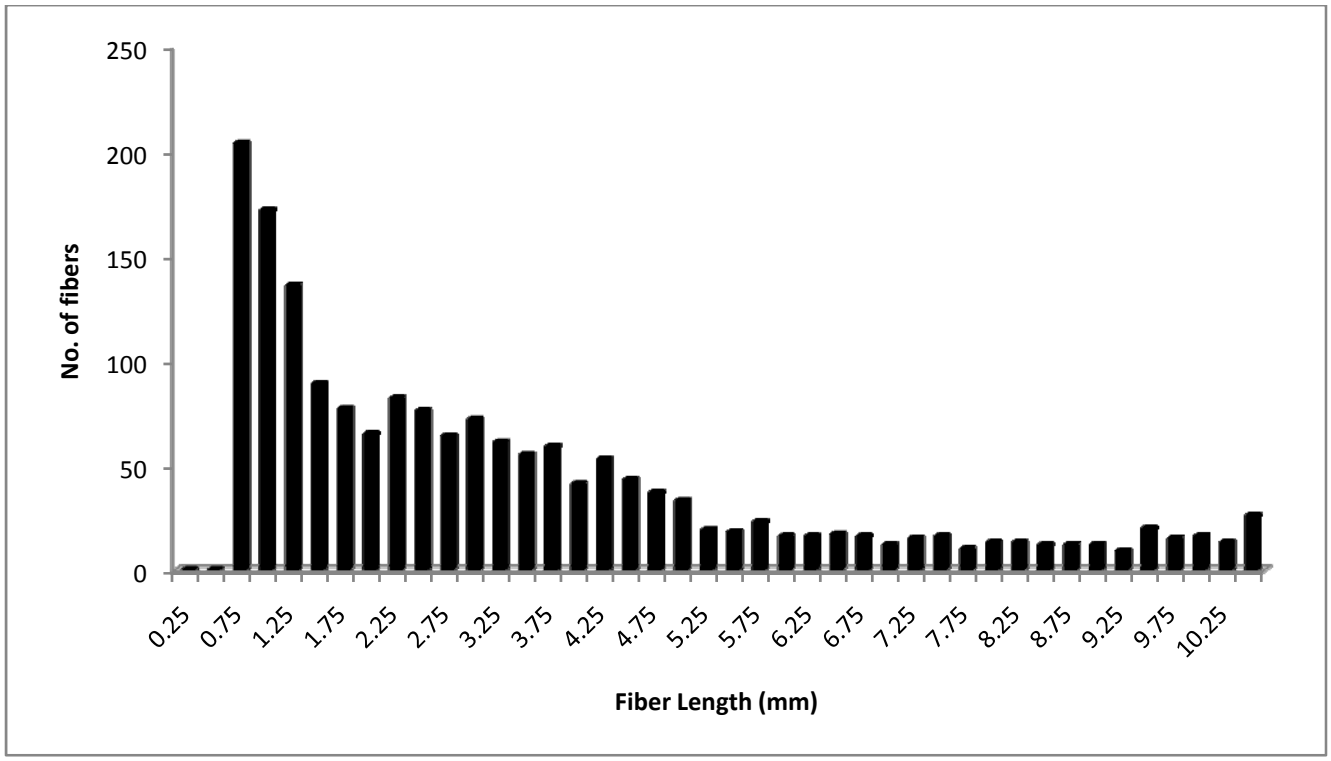

Figure A.2. Fiber length distribution after extrusion of 8 mm fiber pellets. The number average length (L_N) and the weight average length (L_W) are 3.32 and 5.33 mm, respectively.